

# **NEQAIR96, Nonequilibrium and Equilibrium Radiative Transport and Spectra Program: User's Manual**

Ellis E. Whiting, Chul Park, Yen Liu, James O. Arnold, and John A. Paterson

December 1996



National Aeronautics and  
Space Administration



# **NEQAIR96, Nonequilibrium and Equilibrium Radiative Transport and Spectra Program: User's Manual**

Ellis E. Whiting, Thermosciences Institute, NASA Ames Research Center,  
Moffett Field, CA 94035-1000

Chul Park, Department of Aeronautics and Space Engineering, Faculty of Engineering,  
Tohoku University, Aramaki, Aoba-Ku, Sendai, 980 Japan

Yen Liu, James O. Arnold, and John A. Paterson, NASA Ames Research Center,  
Moffett Field, CA 94035-1000

December 1996



National Aeronautics and  
Space Administration

**Ames Research Center**  
Moffett Field, California 94035-1000



# Table of Contents

	Page
List of Tables .....	v
List of Figures .....	v
Summary .....	1
Introduction .....	3
Overview .....	15
A. Radiation .....	20
B. Excitation .....	22
C. Options Available When Using NEQAIR96 .....	27
How to Use NEQAIR96 .....	31
A. Description of the <b>Input</b> File .....	40
B. Effect of Options and the <b>Output</b> File .....	62
Part 1. Effect of Options for Atomic Systems .....	64
Part 2. Effect of Options for Electronic Diatomic Systems .....	65
Part 3. Brief Statement About the <b>Output</b> File and Plot Files .....	71
Appendices .....	73
A. Radiation .....	73
Part 1. Bound-Bound Radiation .....	77
Part 2. Bound-Free Radiation .....	78
Part 3. Free-Free Radiation .....	79
Part 4. Nonequilibrium Absorption Coefficient .....	83
B. Einstein A Coefficients for Diatomic Rotational Lines .....	85
C. Wavelengths for Diatomic Rotational Lines .....	87
D. Atomic and Rotational Line Shapes .....	91
E. The Escape Factor .....	99
F. Diatomic Internal Partition Function .....	101
Part 1. Energy Levels and Vibrational-Rotational Dissociation .....	108
Part 2. Partition Functions for Single Electronic States .....	109
G. Nuclear Spin Multiplicities and Alternation of Line Intensities for Homonuclear Molecules .....	115
H. Scanning a Spectrum .....	119
I. The Three Data Base Files .....	123
J. Sample Cases .....	153
References .....	



## List of Tables

		Page
1.	Memory and time requirements for calculating the <b>EHL</b> files .....	10
2.	Number of electronic energy states used in the QSS method .....	25
3.	Tape unit number assignments .....	31
4.	Summary of four calculations for atomic systems to illustrate NEQAIR96 options .....	64
5.	Effect of options for electronic diatomic systems .....	66
G1.	Nuclear spin multiplicity .....	110

## List of Figures

1.	Comparison of calculated and experimental wavenumbers .....	6
2.	Comparison of calculated and experimental spectra for C <sub>2</sub> Swan (0,0) band .....	6
3.	Comparison of adjusted calculation and experimental spectra for C <sub>2</sub> Swan (0,0) band .....	7
4.	Portion of C <sub>2</sub> Swan (0,0) using spectroscopic constants from Huber and Herzberg (ref. 15) .....	8
5.	Comparison of spectroscopic constants from references 15 and 21 on the spectra of the C <sub>2</sub> Swan $\Delta v = 0$ sequence .....	8
6.	Calculated spectrum of low rotational lines of the C <sub>2</sub> Swan (0,0) band .....	9
7(a).	Functional flow chart of NEQAIR96 .....	16
7(b).	Input section of functional flow chart of NEQAIR96 .....	17
8.	Typical line-of-sight applications .....	18
9(a).	<b>Template.input</b> file .....	33
9(b).	<b>Template.input</b> file (concluded) .....	34
10.	<b>Template.region</b> file .....	36
11.	<b>Template.los</b> file .....	37
12.	<b>Template.scan</b> file .....	38
13.	Model flow field geometries used in NEQAIR96 .....	39
14.	<b>Los.data</b> file for evaluating the effects of NEQAIR96 options .....	63

15.	Effect of the IPEAK option on the time to calculate and spread the rotational lines .....	68
16.	Electronic diatomic spectra for testing effect of IPEAK and Nmax options .....	68
17.	Electronic diatomic spectra for testing effect of rectangular line shape option .....	70
E1.	Effect of line shape on the escape factor .....	95
E2.	Effect of optical density at the line center, $\tau_0$ on the absorption in Gaussian profile lines with $d = 1.0$ cm .....	96
E3.	Effect of approximate Gaussian profiles on escape factor .....	98
F1.	Potential curves of $N_2$ ground state .....	101
G1.	Spectrum of $N_2^+(1-)$ (0,0) band showing line alternation. Dotted curve is without alternation .....	112
G2.	Spectrum of $O_2$ SR (0,0) band showing line alternation. Dotted curve is without line alternation .....	112
I1.	A portion of the <b>spectroscopic.data</b> file for NEQAIR96 .....	120
I2.	A portion of the <b>excitation.data</b> file for NEQAIR96 .....	121
I3.	A portion of the <b>radiation.data</b> file for NEQAIR96 .....	122
J1(a).	<b>Input</b> file for sample case 1 .....	125
J1(b).	<b>Input</b> file for sample case 1 (continued) .....	126
J1(c).	<b>Input</b> file for sample case 1 (concluded) .....	127
J2.	<b>Los.data</b> file for sample cases 1 and 2 .....	128
J3.	<b>Scan.data</b> file for sample case 1 .....	129
J4(a).	<b>Output</b> file for sample case 1 .....	130
J4(b).	<b>Output</b> file for sample case 1 (continued) .....	131
J4(c).	<b>Output</b> file for sample case 1 (concluded) .....	132
J5.	Calculated and scanned spectra from sample case 1 .....	133
J6.	Calculated and scanned spectra of the $\Delta v = 1$ sequence of $N_2^+(1-)$ from sample case 1 .....	133
J7.	Calculated and scanned spectra of atomic N lines from sample case 1 .....	134
J8(a).	<b>Input</b> file for sample case 2 .....	135
J8(b).	<b>Input</b> file for sample case 2 (continued) .....	136
J8(c).	<b>Input</b> file for sample case 2 (concluded) .....	137
J9(a).	<b>Output</b> file for sample case 2 .....	138

J9(b).	<b>Output</b> file for sample case 2 (continued).....	139
J9(c).	<b>Output</b> file for sample case 2 (concluded) .....	140
J10.	Calculated spectra of atomic O lines and background radiation, with and without absorption, from sample case 2.....	141
J11.	Calculated spectrum of atomic O lines and background radiation, with absorption, vs. wavenumbers, from sample case 2 .....	141
J12.	Calculated spectra of the 3 atomic O lines and background radiation near 777 nm, with and without absorption, from sample case 2.....	142
J13(a).	<b>Input</b> file for sample case 3 .....	143
J13(b).	<b>Input</b> file for sample case 3 (concluded).....	144
J14.	Region.data file for sample case 3 .....	145
J15(a).	<b>Output</b> file for sample case 3 .....	146
J15(b).	<b>Output</b> file for sample case 3 (continued).....	147
J15(c).	<b>Output</b> file for sample case 3 (concluded) .....	148
J16.	One layer equilibrium <b>los.data</b> file produced by sample case 3.....	149
J17.	Region 1 spectra for sample case 3 .....	150
J18.	Region 1 detail spectra for sample case 3 .....	150
J19.	Region 2 spectra for sample case 3 .....	151
J20.	Region 2 detail spectra for sample case 3 .....	151



# **NEQAIR96, Nonequilibrium and Equilibrium Radiative Transport and Spectra Program: User's Manual**

Ellis E. Whiting,\* Chul Park,<sup>†</sup> Yen Liu, James O. Arnold, and John A. Paterson

Ames Research Center

## **Summary**

This document is the User's Manual for a new version of the NEQAIR computer program, NEQAIR96. The program is a line-by-line and a line-of-sight code. It calculates the emission and absorption spectra for atomic and diatomic molecules and the transport of radiation through a nonuniform gas mixture to a surface. The program has been rewritten to make it easy to use, run faster, and include many run-time options that tailor a calculation to the User's requirements. The accuracy and capability have also been improved by including the rotational Hamiltonian matrix formalism for calculating rotational energy levels and Hönl-London factors for dipole and spin-allowed singlet, doublet, triplet, and quartet transitions.

Three sample cases are also included to help the User become familiar with the steps taken to produce a spectrum. A new input format is included that uses check locations, to select run-time options and to enter selected run data, making NEQAIR96 easier to use than the older versions of the code. The ease of its use and the speed of its algorithms make NEQAIR96 a valuable educational code as well as a practical spectroscopic prediction and diagnostic code.

---

\*Thermosciences Institute, NASA Ames Research Center, Moffett Field, CA 94035-1000.

<sup>†</sup>Dept. of Aeronautics and Space Engineering, Faculty of Engineering, Tohoku University, Aramaki, Aoba-Ku, Sendai, 980 Japan.



## Introduction

The primary purpose of this manual is to describe how to use the present version of the NEQAIR Program, NEQAIR96, but it has other goals as well. Our experience with the original manual showed that many Users want to know more about NEQAIR. They want to know its basic structure: what equations are used, what assumptions are made, where its weaknesses are, etc., so that they can use it with confidence and change it when necessary. This manual attempts to meet many of these needs. There are also comment lines in most of the subroutines that describe, or at least indicate, the steps that are programmed.

Computer time and memory management are always practical concerns for Users. These issues are not dealt with in a comprehensive manner, but information is presented and options are discussed that may enable the User to have better control over the use of resources. The authors have optimized the code in many places to run quickly on a CRAY C-90 computer. The results of this effort have been very fruitful. But they may be of little help or even a handicap on nonvector computers.

Copies of NEQAIR96, its data base files and the three sample cases discussed herein are available to U.S. citizens upon request from the Reacting Flow Environments Branch at Ames Research Center. This computer code is available to Users for their use only, and Users must agree that they will not distribute the code to others within or outside the United States. Note that NEQAIR96 and its data base and input files are NOT compatible with the older versions of the code and should not be placed in a common directory with the old files.

NEQAIR96 is a line-by-line and line-of-sight computer program. It is designed to calculate, line by line, the optical radiation emitted and absorbed by atomic and rotational lines along a line-of-sight in a gas mixture or flow field. It also calculates bound-free and free-free continua caused by the interaction of free electrons with neutral and ionized atoms. It is a fairly comprehensive program in that it includes options for duplicating the flow environments in shock layers and shock tubes, calculating an equilibrium gas mixture at selected conditions, estimating signals from radiometers and spectrometers, mimicking operations performed by spectroscopists, and enabling Users to select, visually, run-time options that tailor a calculation to their needs.

The code was developed to help scientists and engineers estimate and interpret spectra emitted by radiating species in high temperature gas environments. Having successfully achieved this purpose, its ease of use also makes it an effective educational and training package for understanding the complex, nonlinear effects of absorption and line shape in the transport of radiation.

The thermodynamic and chemical properties of the gas along the line-of-sight must be provided from an external calculation, except when the equilibrium flow option is specified. In the equilibrium option, the code calculates the properties of the gas at conditions specified by the User and saves the solution as a one layer line-of-sight data (**los.data**) file that can be used in other calculations. The energy lost from the flow field by radiation is not considered in the calculations. The calculated spectra can, of course, be used to adjust the fluid dynamic flow solutions that are used to produce the **los.data** file, if they contain radiative cooling terms. Our experience indicates that radiative cooling is usually small compared to the total energy in the flow field.

In this manual, the terms “atomic lines” and “rotational lines” are used to designate the spectral lines produced by transitions in atoms and diatomic molecules, although physically they are identical. The term “lines” by itself is used when referring to both atomic and rotational lines. Note: In NEQAIR96 and in this manual, the line width is ALWAYS the **full width at half maximum** (FWHM). Also, in this manual, bold face type is used when referring to the names of subroutines, data base files, and input files.

Two kinds of diatomic transitions are included: those between different electronic states (electronic band systems) and those between vibrational levels within a single electronic state (infrared (IR) band systems). Pure rotational transitions in the far infrared and microwave regions of the spectrum are not included.

NEQAIR (refs. 1 and 2) was developed to produce reasonably realistic estimates of spectra emitted under equilibrium or nonequilibrium conditions encountered:

1. Within the shock layer that forms ahead of vehicles entering planetary atmospheres.
2. Behind the shock wave in shock tubes.
3. In arcjet facilities.
4. In the base flow region around rockets.

It has been used to estimate the signal strengths for radiometers (ref. 3), identify atomic and diatomic spectral features (ref. 4), predict the radiative heating rate at the stagnation point of entry vehicles (ref. 5), help interpret spectral data (refs. 6–8) and determine species concentrations and temperatures within radiating gas flows (refs. 7 and 9).

The production of a spectrum begins by calculating the integrated emission and absorption coefficients of the atomic and rotational lines included in a run. A single calculation can contain anywhere from one line to several million lines. A spectrum is produced from the integrated line emission values by spreading them spectrally using a line shape function. Spectral features are calculated to high resolution if the spectroscopic data entered are of high quality.

The wavelengths of atomic lines are entered directly in the **radiation.data** file. Shifting of the line wavelengths by collisions, or any other means, is not considered. The wavelengths of individual diatomic or polyatomic rotational lines can be entered in the same manner as atomic lines, when the highest possible resolution is needed. This is a very tedious task for the large numbers of lines in such systems. For example, reference 10 lists over 307 million lines for H<sub>2</sub>O that could be entered into NEQAIR96. Fortunately, high resolution studies often involve only a few lines. In practice, rotational lines are not normally entered as individual lines. Rather, the wavelengths and Hönl-London factors of rotational lines are calculated from known formulae or from quantum matrix methods (refs. 11–13) using a few appropriate spectroscopic constants (refs. 14 and 15). Note, the energy levels of H<sub>2</sub>, which are used to calculate the wavelengths, cannot be easily expressed with the usual spectroscopic constants. Thus, for this one molecule, the energy levels for the X, B, C, and B' states are entered directly in the code, rather than calculated by the Dunham (ref. 16) expansion.

NEQAIR96 uses the matrix method for calculating the rotational line wavelengths and Hönl-London factors because of its greater accuracy for higher spin multiplicities. Also, the matrix method is closely related to the fundamental theory of quantum mechanics and offers a more rigorous approach to spectral results. This is a departure from the older versions of the code, which used the Dunham expansion (ref. 16) and Hönl-London formulae (refs. 13, 14, and 17). Further, the older versions only included equations for singlet transitions and one doublet transition, doublet  $\Pi$  to doublet  $\Sigma$ . These few formulae were applied to all higher spin multiplicities, as a convenient and often reasonable approximation. Unfortunately, such approximation can lead to poor results when high resolution is needed, or significant absorption occurs in the flow field.

The initial energy matrix elements are calculated using the Hund's case-a equations on pages 54 and 55 of reference 13, except that lambda doubling terms are not included. The inclusion of lambda doubling terms in a general code, such as NEQAIR96, would at least double the computer time and memory requirements, and would seldom add to the value of the results. The effect of this omission is that the closely spaced rotational line doublets that occur in non $\Sigma$  to non $\Sigma$  transitions are treated as a single line. The lambda splitting is usually much less than the spectral resolution in most spectra, and is often less than the width of the lines themselves. This is particularly true at high temperatures where thermal and sometimes Stark broadening are dominant broadening mechanisms. Some additional comments about the effects of lambda doubling are presented in the last two paragraphs of Appendix G.

The matrix operations used to produce the rotational energies and Hönl-London factors are discussed in references 18, 19, and 20, and the code described in reference 19 is now a part of NEQAIR96. This code appears in subroutines **Hönl**, **solve**, and **diag**, and has the potential to calculate the wavelengths and Hönl-London factors of all spin-allowed and spin-forbidden dipole transitions. However, NEQAIR96 is structured and dimensioned only to calculate the spin-allowed singlet, doublet, triplet, and quartet transitions. This is a major advance over the old code, in providing realistic band structures when high resolution is necessary. The potential exists to incorporate other kinds of band structures with modest program changes.

The accuracy of the matrix method is demonstrated in figure 1 by showing a comparison of line positions, in wavenumbers, for a portion of the C<sub>2</sub> Swan (0,0) vibrational band. These calculations were made using spectroscopic constants determined in reference 21 from high resolution data. The calculated results are shown by the solid curves and the data are shown by the circular symbols. Only the R<sub>1</sub> and P<sub>1</sub> branch lines are shown but all six major branches show the same level of excellent agreement.

The calculated spectrum for a small region of the C<sub>2</sub> Swan (0,0) vibrational band is shown in figure 2. The calculated spectrum for this region is shown by the spectral curve and the measured locations of the lines (ref. 21) are shown by the "+" and "v" symbols. The "+" symbols locate R branch lines and the "v" symbols P branch lines. The agreement between the calculated and measured wavelengths is quite good. However, on closer inspection a small bias to longer wavelengths is evident in the calculations. Shifting the calculated spectrum by 0.04 Angstrom toward shorter wavelengths gives better agreement between the measured and calculated wavelengths, as shown in figure 3. Such a shift of the entire spectrum indicates a slight difference in the location of the calculated band origin from the correct value. A universally accepted method for determining

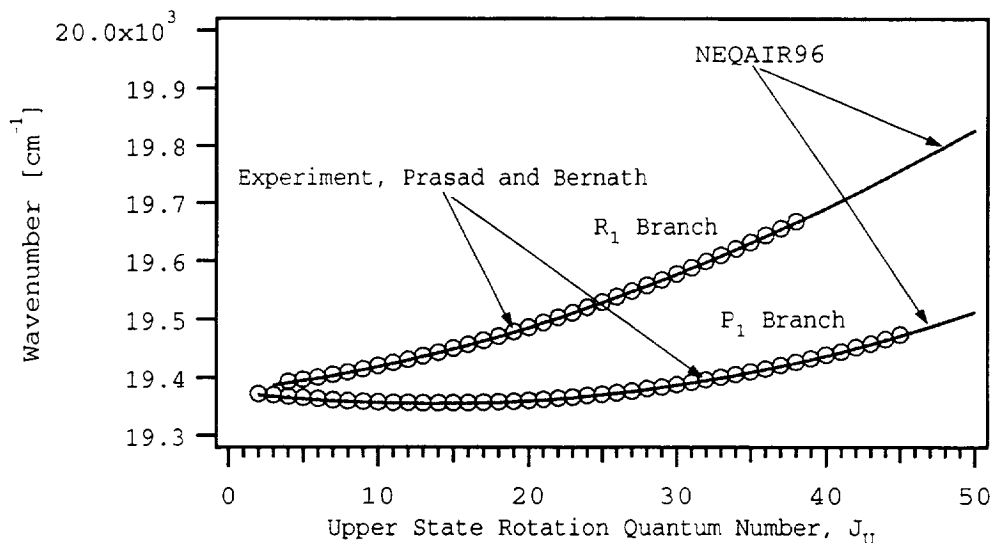


Figure 1. Comparison of calculated and experimental wavenumbers.

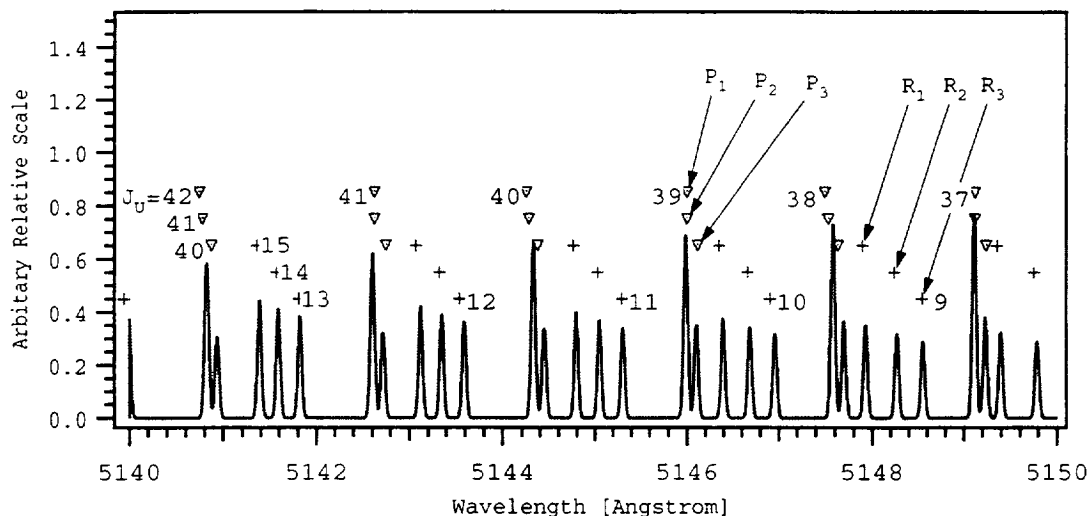


Figure 2. Comparison of calculated and experimental spectra for  $C_2$  Swan (0,0) band.

band origins does not exist, and is a source of uncertainty in such calculations (see refs. 22 and 23 for discussions of this problem).

The remaining differences between the calculated and experimental wavelengths in figure 3 are due to the staggering of the experimental line positions caused by lambda doubling. The rotational lines in this case are not lambda doubled even though two  $\Pi$  states are involved. This occurs because  $C_2$  is a homonuclear molecule, and the nuclear spin of the C atom is 0.0. These conditions allow only one of the lambda substates to exist for each rotational level. The existing sublevel is alternately the higher and then the lower one, as the rotational number changes (see Appendix G).

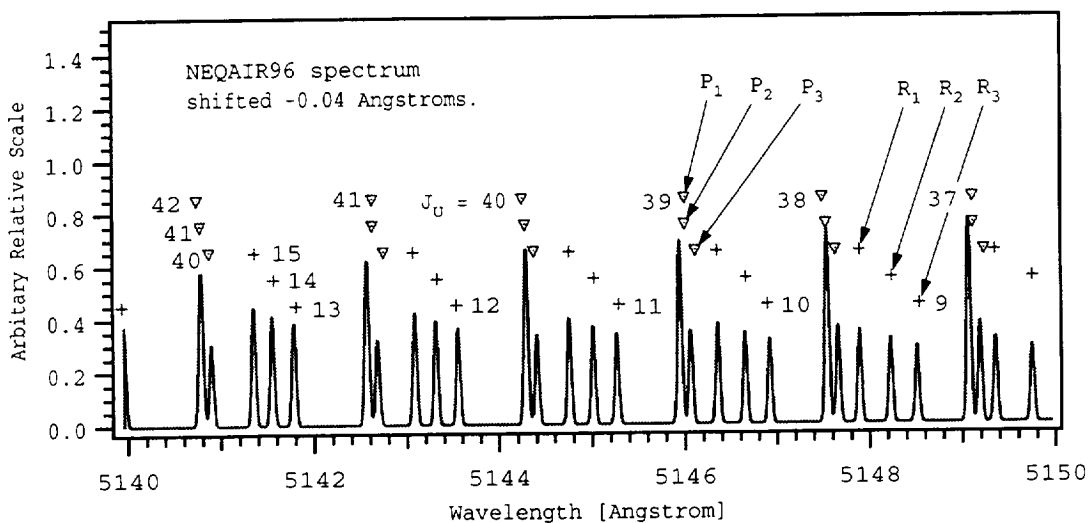


Figure 3. Comparison of adjusted calculation and experimental spectra for  $C_2$  Swan (0,0) band.

The “v” symbols for the P branches in figure 3 show this small staggering effect. It is not apparent in the R branch lines, because lambda splitting is very small for low rotational quantum numbers. The staggering of the lines does not appear in the calculated line positions, because lambda doubling terms are not included in the energy matrices. This is a good example of the normally small effect of lambda doubling, and illustrates why lambda doubling is not included in NEQAIR96.

The accuracy of a calculation is obviously dependent on the accuracy of the spectroscopic constants used. Reference 23 contains a thorough discussion of how to determine the most reliable and physically realistic constants. This reference refers to a matrix method that can involve several bands or band systems simultaneously. As a demonstration of the effect of different spectroscopic constants, an identical calculation to that shown in figure 2 is shown in figure 4, but using the less accurate spectroscopic constants from reference 15. A comparison of these figures shows some obvious differences. However, the integrals of the areas under the two spectra are the same.

The effects of the spectroscopic constants on lower resolution spectra are shown in figure 5. The spectroscopic constants are identical to those used in figures 3 and 4 but using a resolution of 2.5 Angstrom and showing the entire (0,0) vibrational band. The spectra appear to be identically overlapped at this resolution, which is actually a fairly high resolution for many cases, and the figure appears to display a single spectrum. Thus, for many practical applications the spectroscopic constants in reference 15 are adequate.

Another advantage of the matrix method is that all of the rotational lines are calculated correctly, even the first few lines that occur before the multiplicity is fully developed (ref. 24). These initial or low-J rotational lines are quite weak and unlikely to make an important contribution to the radiative heating. However, they can be very important at low temperatures where they may be the only lines present for analysis. One application where these lines are important is in the study of the molecular radiation emitted by molecules in interstellar space.

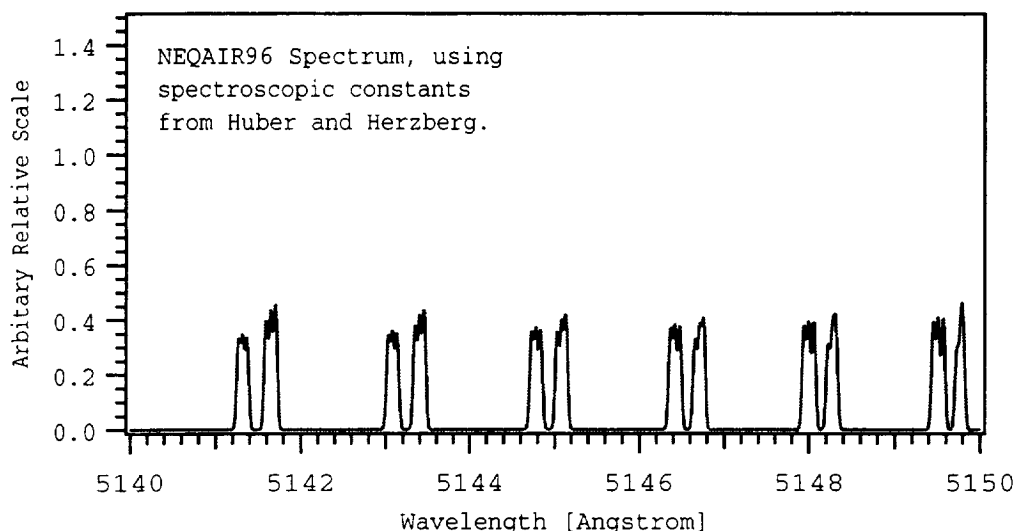


Figure 4. Portion of  $C_2$  Swan (0,0) using spectroscopic constants from Huber and Herzberg (ref. 15).

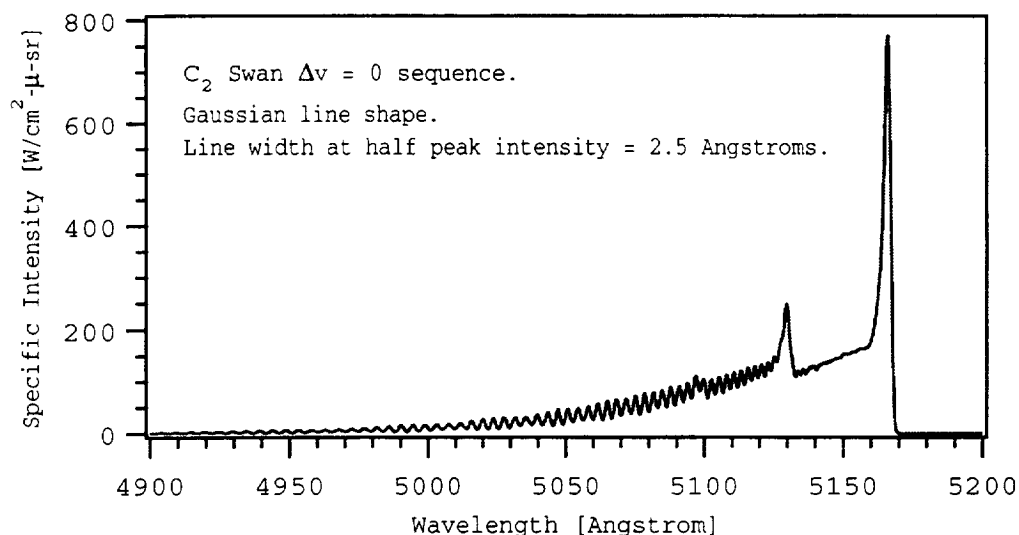


Figure 5. Comparison of spectroscopic constants from references 15 and 21 on the spectra of the  $C_2$  Swan  $\Delta v = 0$  sequence.

The capability of the code to include the first rotational lines correctly is demonstrated in figure 6, where the first few lines of the  $C_2$  Swan (0,0) band are shown. Only the  $P_3$  branch has a line associated with a transition from the upper rotational level with  $J_U = 0$ ; three are from  $J_U = 1$ , five from  $J_U = 2$  and finally all six of the major branches appear for  $J_U = 3$  and above. The  $P_3(3)$  line is off the edge of the figure. Had these lines been calculated with the analytic Dunham and Hönl-London expressions normally used, fictitious lines would have appeared and the intensities of some lines would not have been calculated correctly.

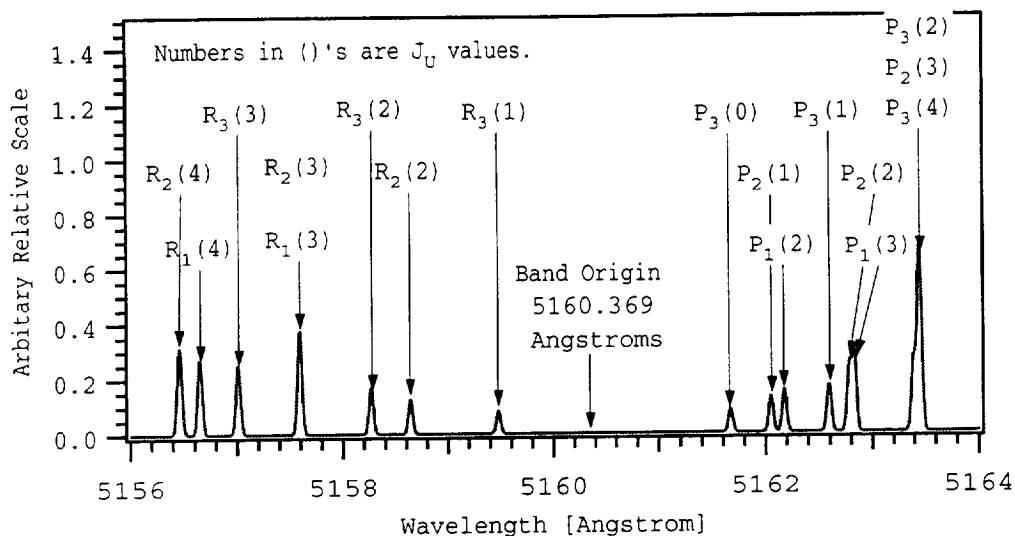


Figure 6. Calculated spectrum of low rotational lines of the  $C_2$  Swan (0,0) band.

The improved accuracy of the spectral wavelengths given by the matrix method is not entirely free. The energy and Hönl-London factor (**EHL**) file generated for each diatomic band system is quite large and requires a few seconds of computer time for its calculation. The information in table 1 illustrates these points. Here 19 band systems in the **radiation.data** file are shown, and the size of their **EHL** files (the CRAY C-90 word size is 8 bytes) and the clock time required to generate them, in seconds, are listed for two spin conditions. The column headed "Singlet Multiplicity" gives the memory and run time values calculated as if all bands have a spin multiplicity of 1. The results in the column headed "Correct Multiplicity" are for the correct spin multiplicities, which are shown in column 5. The reason for allowing the spin multiplicity to be selected is discussed in the "How to Use NEQAIR96" section of this manual.

An **EHL** file is generated during a calculation if the file does not already exist. Once generated a file can be used repeatedly with very little or no time penalty. Tape, or file, unit 7 is used for reading and writing these files. The User has the option to save or delete the **EHL** files. Saving them reduces the computer time for later runs, but requires significant memory and at least some effort to manage them. The risk in saving them is that they might not be deleted when appropriate. The values in these files are a function of the constants in the **spectroscopic.data** file and of the number of vibrational bands in the **radiation.data** file. Whenever these data are changed, the appropriate existing **EHL** files **MUST** be deleted so that new ones can be generated. Otherwise the code will continue to use the files calculated with the older data. This point is discussed again in the section of the manual that explains how to use the program.

Table 1. Memory and time requirements for calculating the **EHL** files

Band system		Singlet multiplicity		Correct multiplicity	
		Size [MBytes]	Time [s]	Size [MBytes]	Time [s]
1	N <sub>2</sub> <sup>+</sup> 1-	2.1	3.7	2	8.5
2	N <sub>2</sub> 1+	2.0	3.6	3	17.5
3	N <sub>2</sub> 2+	0.9	1.5	3	7.8
4	N <sub>2</sub> BH2	2.7	4.7	1	2.7
5	NO $\beta$	3.9	6.7	2	15.3
6	NO $\gamma$	1.3	2.5	2	5.3
7	NO $\delta$	0.5	0.9	2	1.9
8	NO $\epsilon$	0.5	1.0	2	2.1
9	NO $\beta'$	0.8	1.4	2	3.1
10	NO $\gamma'$	0.3	0.6	2	1.2
11	O <sub>2</sub> SR	2.0	3.5	3	17.4
12	CN v	0.7	1.2	2	2.9
13	CN Red	2.5	4.5	2	9.9
14	CO 4+	1.5	2.7	1	1.5
15	C <sub>2</sub> Swan	0.5	0.9	3	4.4
16	OH A-X	0.04	0.08	2	0.2
17	H <sub>2</sub> B-X	0.9	1.4	1	0.9
18	H <sub>2</sub> C-X	0.4	0.6	1	0.4
19	H <sub>2</sub> B'-X	0.1	0.2	1	0.1

The line shapes used in NEQAIR96 are of two basic kinds, Voigt profiles and rectangles. The Voigt profile provides a reasonably accurate description of atomic and rotational lines, but requires more computer time for spreading the lines into the spectrum than does the rectangular shape. A rectangular line is spread uniformly over four spectral intervals and provides a higher speed option for the early stages of an investigation. The rectangular line shape can produce quite acceptable spectra for low resolution studies in an optically thin gas.

Line shapes have a pronounced effect on a spectrum if high resolution is needed and/or significant optical absorption occurs in the flow field. For these cases, an accurate line shape is essential and the most realistic approximation used in the code is the Voigt profile. The Voigt line shape is formed from the full line widths at the half height, of its Gaussian and Lorentzian line components. Thus, either a pure Gaussian or Lorentzian line is specified by entering a zero value for the unwanted component. The shapes of individual atomic lines, and all rotational lines in a vibrational band, can be calculated by NEQAIR96, but this step is not necessary. The User can also enter a single Voigt shape to be used for all atomic and rotational lines.

The use of realistic line shapes requires a fine mesh of spectral grid points because the actual widths of lines in the flow field are quite narrow, often less than 0.1 Angstrom. This can result in an extensive calculation if a large spectral range is specified. Currently the maximum number of spectral grid points allowed by the dimensioning statements is 50,000. Thus, the maximum possible spectral range, for lines that are 0.1 Angstrom wide and described by 10 points per line width, is 500 Angstroms. Such a calculation can be made but its usefulness is questionable. High resolution research is usually focused on the effects in a much smaller region of the spectrum. For a spectral region of 10 Angstroms, the above conditions would only involve 1000 spectral points.

Detailed and time consuming calculations are not always necessary. Frequently the resolution needed is far greater than the line width, and the gas is nearly optically thin. In these cases a broad line width that approximates the spectral resolution of the data rather than the actual line width gives good results and costs far less. A further advantage of using a broad line width is the appearance of the resultant spectrum. Even familiar spectral patterns are difficult to recognize in the picket fence pattern of individual lines at high resolution.

An alternative to the line-by-line approach to producing optical spectra is to use Band model codes. Band model codes, in contrast to line-by-line codes, approximate the line patterns by grouping many lines into composite lines and continuous bands of radiation. One such code is the LORAN (ref. 25) program developed by researchers at Langley Research Center. It runs faster than NEQAIR96 and can be used with good advantage when the spectral resolution is not critically important. Further, it has the potential to couple the radiation processes to the thermodynamic and chemical processes occurring in the flow field. Thus, NEQAIR96 and LORAN are complementary and together provide a powerful approach to solving the problems of radiative heating and of characterizing high energy gas dynamic flows.

The first version of NEQAIR (ref. 1) was developed by combining the quasi-steady-state (QSS) nonequilibrium excitation code discussed in reference 26 with the radiation code described in reference 2. The QSS code is a practical method for calculating nonequilibrium excited state populations under appropriate conditions. Spectra calculated using the QSS code, when compared to experimental data, provide critical information about the physical and chemical state of a non-equilibrium gas—such as the electronic, vibrational and rotational populations or temperatures, and their distributions from band to band and line to line (ref. 9). NEQAIR96 continues this development by:

1. Making the code easier to use.
2. Providing a wide range of run-time options.
3. Enabling greater accuracy in the spectral portions of the code.
4. Eliminating redundant data in the input files.
5. Specifying all array dimensions with variables.

The last two items simplify the process of entering new species or band systems.

This manual includes an “Overview” section and a “How to Use NEQAIR96” section, in addition to this Introduction, and 10 appendices.

The Overview section:

1. Provides a perspective of what the code does.
2. Discusses key assumptions.
3. Mentions some of its limitations.
4. Summarizes its important options.

The How to Use NEQAIR96 section discusses the data entry process in detail.

The appendices contain:

1. Important equations, derivations, concepts and assumptions.
2. Partial listings of the three data files provided with the code.
3. Three sample cases including **Input** and **Output** files. Test case 2 calculates nearly 1.5 million lines, and spreads 1.0 million of these into a spectrum, in about 25 seconds on the CRAY C-90 computer.

The new code evolved from comments and suggestions made by many Users and differs from the original code in several ways. Some of these are:

1. New functions. Radiative transport, shock tube flow, equilibrium calculations, diatomic IR bands, incident spectra, and slit and instrument functions.
2. Substantial upgrades. A new simplified input format, an improved escape factor code, new method of calculating the partitions functions of diatomic molecules, the addition of the matrix method for finding rotational energy levels and rotational line Hönl-London factors, and the inclusion of all spin-allowed singlet, doublet, triplet, and quartet transitions.
3. The use of either one or two alphabetic characters to identify an atom. The first character must be a capital letter and the second character, if there is a second one, must be a lowercase letter. The older versions of NEQAIR used only a single capital letter to identify each atom. This was adequate for air, which includes N<sub>2</sub>, O<sub>2</sub>, CO<sub>2</sub>, and argon, but required argon to be identified by the capital letter A, rather than by Ar. The enhancement to two character designations allows the correct chemical symbols to be used, and makes it much easier to add new species to the code.
4. Extensions to the **spectroscopic.data** file. Particular thanks are due Christophe Laux of Stanford University for his many contributions (refs. 27–31), especially for showing the need

to include higher order vibrational spectroscopic terms when calculating NO band systems, for entering improved data in the **spectroscopic.data** and **radiation.data** file, and for entering the NO $\delta, \epsilon, \gamma$ , &  $\beta$  band systems.

5. Corrections of errors. Special thanks are due:

- a. Debbie Levin of the Institute for Defense Analysis for her critical review and perceptive use of the QSS code in a low temperature regime where heavy particle excitation of atomic oxygen is important (refs. 32 and 33). Unfortunately, the inclusion of a general treatment for heavy particle excitation of atoms has not been possible because of the lack of adequate excitation rate coefficients.
- b. Lin Hartung-Chambers of Langley Research Center for her careful and thoughtful study of the original code (refs. 25 and 34).
- c. Scott Meyer (refs. 35 and 36) for his critical reading of the equilibrium code and for showing that the Lorentzian line shape is valid for resonance broadening of atomic oxygen lines at 130 nm, for over a thousand line widths into the wings. His work also shows that the resonance or self broadening of oxygen lines by collisions between oxygen atoms is not correctly handled in the code. A general solution of this problem has not yet been found.
- d. Chung Park (ref. 37) and Dinesh Prabhu (ref. 38) of Ames Research Center; Chris Parigger and James Hornkohl (refs. 39–41) of the University of Tennessee Space Institute; Bill Rochelle (ref. 42) of Johnson Space Center; and former colleagues at Ames Research Center Dikran Babikian (ref. 4) and Stephan Moreau (ref. 27), all of whom found errors in, and suggested improvements to, the code.
- e. Tobin Munsat of Princeton Plasma Laboratory, a Princeton University graduate student, for correcting errors in ionization energies in the **spectroscopic.data** file, and for entering atomic hydrogen and helium, and H<sub>2</sub> band systems in the **spectroscopic.data** and **radiation.data** files. The excitation rate data for these systems have not yet been entered into the **excitation.data** file, and thus these systems cannot be included in nonequilibrium studies. Also, the Stark line broadening data for H and He have not been entered in the **radiation.data** file.

With all of the changes made to NEQAIR, the original structure of NEQAIR described in references 1 and 2 is, in many ways, still intact; although nearly all of the algorithms have been rewritten to increase accuracy and speed of computation, when run on the CRAY C-90 computer.

The work reported herein needs to be continued. Several portions of the code must be improved, if it is to be a truly comprehensive spectroscopic capability. Clearly, the nonequilibrium, or QSS, portion of the code needs to be improved in many ways. Some of these are:

1. Expand the **excitation.data** file to include new species and more energy levels.
2. Extend the QSS concept into the vibrational and rotational regimes, or find realistic models for nonequilibrium vibrational and rotational population distributions.
3. Determine better criteria and models for the escape factor and/or the escape distance.
4. Derive a more precise method for defining the effective absorption coefficient when several lines are overlapped, and whose upper to lower level population ratios are not the same.

The line shape function also needs to be improved for high resolution studies, or whenever absorption is important. Some of the improvements needed are:

1. Variable rotational line width across vibrational bands.
2. A more accurate Voigt profile expression that retains the correct Gaussian and Lorentzian shapes at both limits.
3. A line shape function that allows for the shifting of the line wavelength, and for asymmetric line shapes due to collisions.

The code should also be changed to permit spin-forbidden, but still-dipole allowed, rotational transitions to be calculated, as that potential capability exists in the present code. Further changes to include other multipole transitions would be appreciated by several Users, and the incorporation of rotational level perturbations schemes, hopefully in a general way, would be useful for high resolution studies.

The changes that are made will be driven by, and very likely done by, the Users as they solve the problems related to their research. All Users are urged to keep the caretakers of NEQAIR apprised of errors found and of changes made to the code. Hopefully, this effort will continue to be supported and NEQAIR will continue to evolve.

## Overview

NEQAIR96 is a comprehensive line-of-sight, line-by-line computer program. It is used to calculate the optical spectrum emitted along a line-of-sight within a gas and the transport of optical radiation to, or through, a surface. An overall perspective of the program is provided by the functional flow chart shown in figures 7(a) and 7(b).

The title at the top of each box in the diagram indicates the function performed in that portion of the code. If the function is performed or controlled by subroutines, the names of the principal subroutines are noted in parentheses just below the title. If a file is read from, or written to, a particular tape unit, the tape unit numbers are also noted in the box as fort.N, where N is the tape unit number. The **Input** file (standard tape unit 5) is read, principally, in subroutine **input** and most of the **Output** file (standard tape unit 6) is written in subroutines **accontrol**, **input**, **planck**, **eqgas**, **eqTrho**, **shockjump**, **transport**, **bandpass**, **voigtscan**, and **linearscan**, which are shown within dashed boxes on the flowchart. The name of the main program, **aaMain**, was chosen to ensure that it would be listed first in an alphabetical listing of subroutines and functions, and the name of **accontrol** was chosen so that it would be listed second.

The five major functions of the code are shown in the first row of boxes below the subroutine **accontrol** box. Generally, the program proceeds from the functions on the left toward those on the right, although not all functions are used in every calculation. The input section of the flow chart is shown in figure 7(b); it illustrates the large number of run-time options available to the User, and the **spectroscopic.data**, **excitation.data**, and **radiation.data** files that are needed to run the program. These options and data are discussed in the "How to Use NEQAIR96" section of the manual. The excitation portion of the code is only used when the nonBoltzmann option is selected in the **Input** file. The principal results from the code are printed in the **Output** file (standard tape unit 6), and the plot files. The flow chart shows, near its right hand side, that the basic calculated spectra are printed on tape units 21 to 30 and the scanned spectra on tape units 31 to 40.

A few possible lines-of-sight, along which one might want to estimate the emitted radiation and its transport, are indicated in figure 8. The line-of-sight can be directed toward a vehicle surface, away from a surface, or across a flow field. The species number densities [ $\text{cm}^{-3}$ ] and temperatures [K] along a line-of-sight from the base to the head of the arrows must be provided from an external source, except when the equilibrium option is selected in the **Input** file. For the equilibrium option, the code calculates the gas properties and species number densities for a single layer, line-of-sight from flow parameters provided by the User. This calculated single layer **los.data** file is used in the radiation calculations and then saved on tape unit 20.

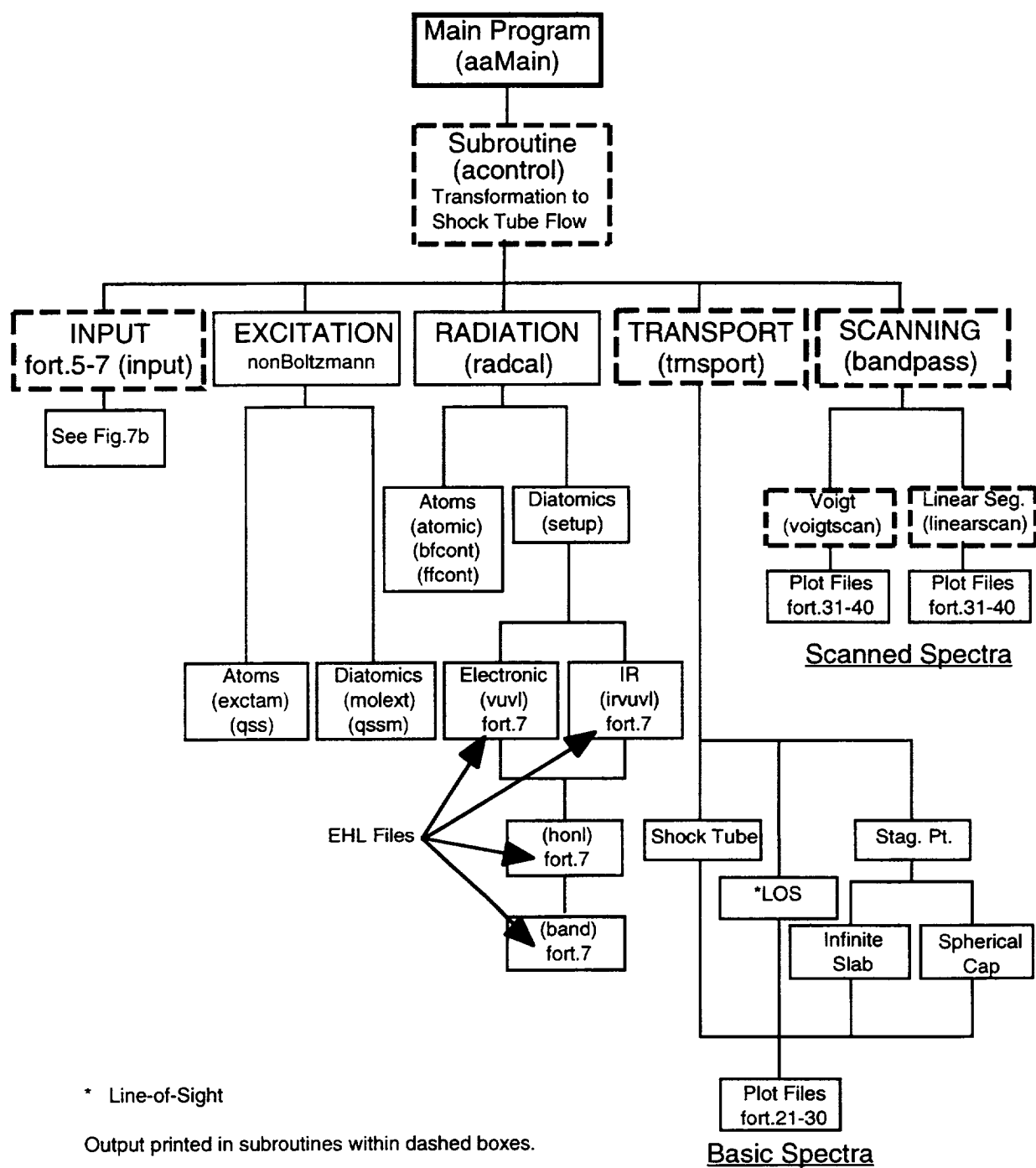


Figure 7(a). Functional flow chart of NEQAIR96.

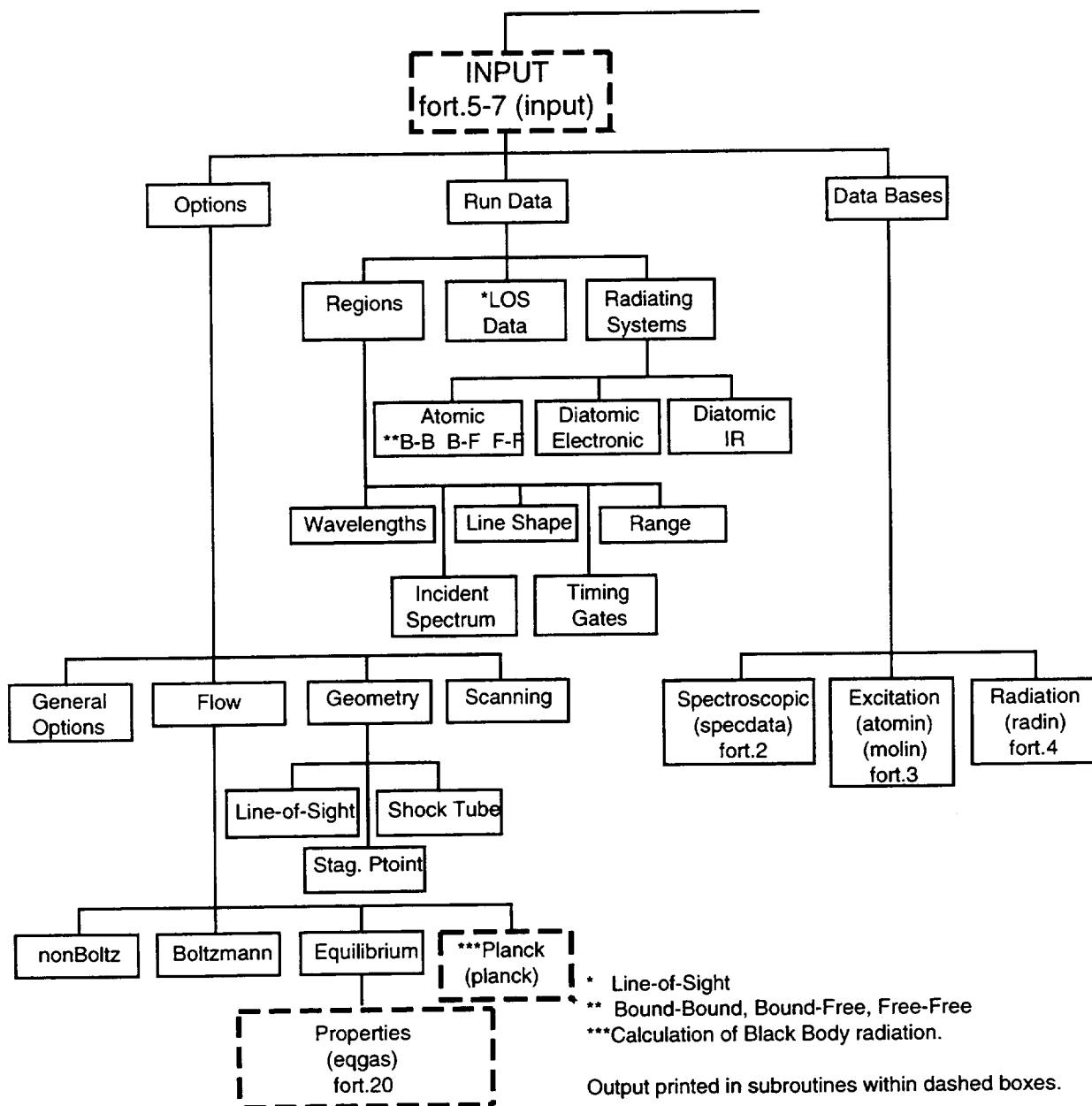


Figure 7(b). Input section of functional flow chart of NEQAIR96.

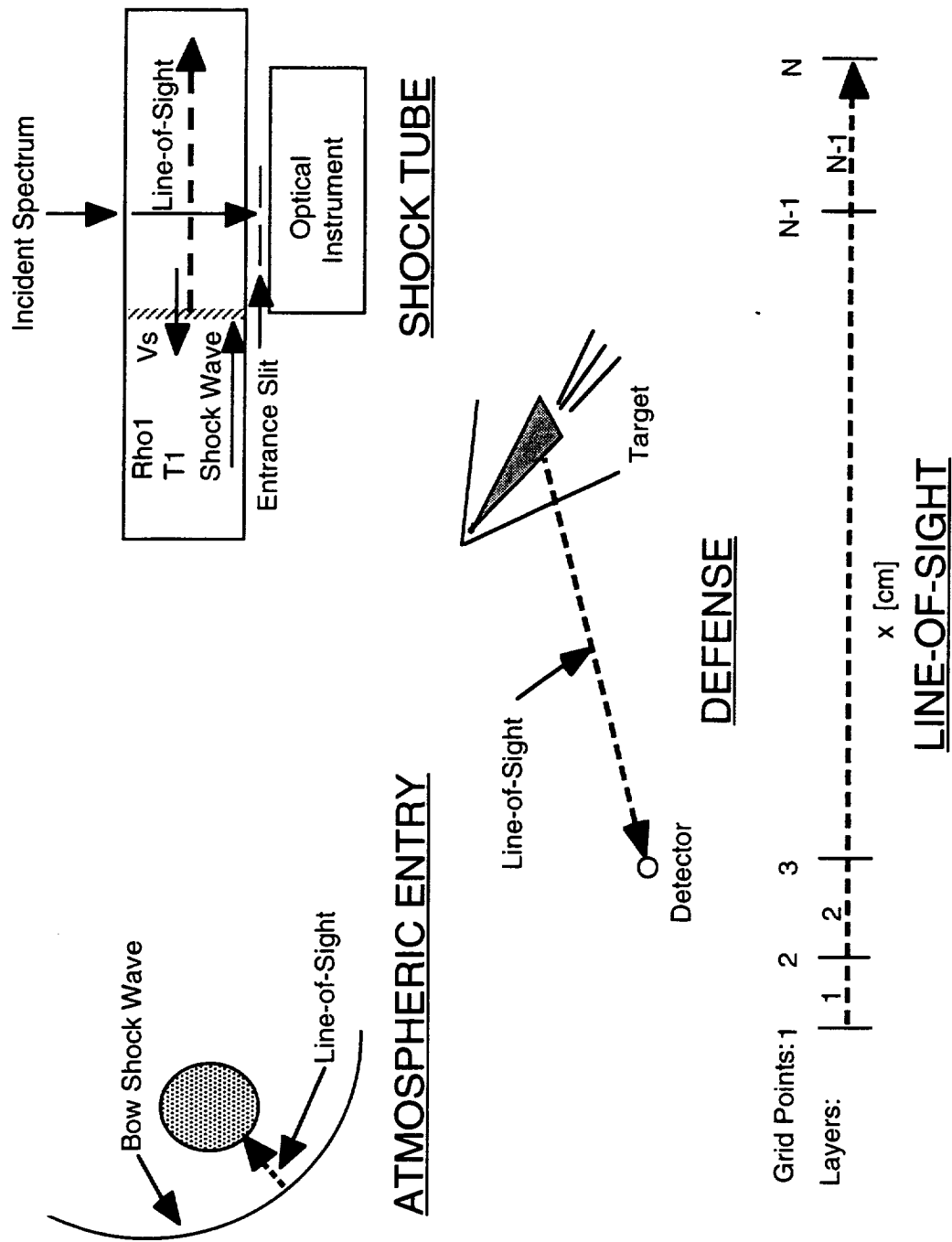


Figure 8. Typical line-of-sight applications.

A typical line-of-sight and its grid coordinates are illustrated by the sketch near the bottom of figure 8. The first grid point,  $x_1$ , is used to establish the initial point for the calculation. The species concentrations and temperatures at this point are not used. The distance between the first and second grid points defines the first radiating layer of gas and its width  $(x_2 - x_1)$  [cm]. The species concentrations and temperatures are constant within each layer and the values for the first layer are specified at the second grid point. An external spectrum, incident on the line-of-sight at  $x_1$ , can also be entered. The line-of-sight data and the incident spectrum values are used to calculate the emission and absorption within a layer, and the resultant spectrum leaving the layer. This process is repeated layer by layer along the line-of-sight until the last grid point is reached, always using the resultant spectrum from the previous layer as the current incident spectrum.

The calculation for the shock tube option, where one looks across the line-of-sight, is done differently. Here the radiating gas seen by the instrument is nearly uniform but changes with time as the gas flows past the entrance slit of the instrument. The width of the radiating gas layer is equal to the shock tube diameter, and the incident spectrum is constant for all layers along the line-of-sight. The distance along the line-of-sight is transformed to the time a gas particle crosses the centerline of the entrance slit, from the time the shock wave passed the entrance slit. This transformation is performed in subroutine **acntrol**. The User must enter the time that the instrument is "gated" to start taking data and the time the gate remains open. The code integrates the spectral signal during the time the gate is open.

The line-by-line feature of the code means that all of the atomic and rotational lines included in a run, often millions, are calculated individually and added into the spectrum. The major factors in developing a specific spectrum, and the run-time options available to a User, are discussed in the remainder of this section. The discussion is divided into three subsections as follows:

- A. Radiation. Summarizes the emission and absorption expressions used to calculate an optical spectrum.
- B. Excitation. Summarizes the expressions used to calculate the upper state populations.
- C. Options. Summarizes the User run-time options available.

Physical units are shown liberally throughout the manual whenever it seems appropriate. They are shown in square brackets such as [cm] and are often redundant but are included for clarity. When units are separated by dashes, as in the group of units " $\text{cm}^2\text{-}\mu\text{-sr}$ ," the entire group is used as a whole, in either the numerator or the denominator of an expression. The primary wavelength unit for input into, and for operations within, the code is Angstroms. When other units such as cm, nm, or  $\text{cm}^{-1}$  are used they are usually noted. The User can elect to print the spectra in terms of wavelength in Angstrom and/or nm, and/or in terms of wavenumber [ $\text{cm}^{-1}$ ]. The units used are a mixture of the cgs and MKSA systems. The cgs system is used because species concentrations are usually given in particles/ $\text{cm}^3$  and wavenumbers [ $\text{cm}^{-1}$ ] are nearly inescapable in spectroscopy, and yet the MKSA system is usually used to specify energy and power in Joules and Watts.

## A. Radiation

The spontaneous emission intensity of each atomic and rotational line in a layer of gas with uniform properties is calculated using the following phenomenological equation expressed by Einstein (ref. 41), but here divided by  $4\pi$  to restrict the emission to that within a small cone in a definite direction.

$$E = E'/4\pi = g_U N_U A_{UL} hc \bar{\nu}_{UL}/4\pi \quad [\text{W/cm}^3\text{-sr}] \quad (1)$$

Here  $E'$  is the radiant power density emitted by a line into  $4\pi$  steradians,  $g_U$  is the degeneracy of the upper state,  $N_U [\text{cm}^{-3}]$  is the population of a nondegenerate level in the upper state,  $A_{UL} [\text{s}^{-1}]$  is the Einstein spontaneous emission transition probability per particle,  $\bar{\nu}_{UL} [\text{cm}^{-1}]$  is the energy separation between the upper and lower states in wavenumbers (and also the energy of the photons emitted),  $h [\text{J s}]$  is Planck's constant,  $c [\text{cm/s}]$  is the speed of light, and  $hc \bar{\nu}_{UL} [\text{J}]$  is also the energy of an emitted photon in more usual units. The wavelength of an emitted photon is given by

$$\lambda = 10^8/\bar{\nu}_{UL} \quad [\text{Angstrom}] \quad (2)$$

Because the units of  $E$  are in terms of the radiant power density, it might seem more appropriate to use the symbol "P" rather than "E." However, the symbol used for this parameter in the NEQAIR96 code is "E," and for this reason it is also used herein.

The parameters shown in equation 1 for atomic lines, except for the population of the upper state, are entered directly in the **radiation.data** file and used in subroutine **atomic** for calculating the emission from atomic lines. In the case of diatomic rotational lines the quantities  $A_{UL}$  and  $\lambda$  are expressed as functions of electronic, vibrational and rotational components (see Appendices B and C). The spectroscopic constants used to find these components are entered in the **spectroscopic.data** and **radiation.data** files. The parameters used in equation 1 are calculated in subroutines **setup**, **vuvl**, **irvuvl**, and **band**. The expressions used to determine the populations of the excited states are described in the following subsection.

The emitted power density given by equation 1 is spread over a spectral range by multiplying by the line shape function,  $\phi_\lambda [\mu^{-1}]$ . That is,

$$E_\lambda = E \phi_\lambda \quad [\text{W/cm}^3\text{-}\mu\text{-sr}] \quad (3)$$

The line shape function (see Appendix D) is normalized by setting its integral over wavelength equal to 1.0, and is calculated in subroutine **lineshape**.

The total emission spectrum for a uniform layer of gas is found by summing all  $E_\lambda$  spectra from the atomic and rotational lines (calculated in subroutines **atomic** and **band**) plus the bound-free and free-free continua spectra (calculated in subroutines **bfcont** and **ffcont**).

The specific intensity [W/cm<sup>2</sup>-μ-sr] of the radiation passing through or striking a surface is found using the radiative transport equation (ref. 42) in subroutine **transport**. This equation is written for each layer along the line-of-sight in the form (see eqs. A15 and A16 in Appendix A)

$$I_{\lambda} = I_{\lambda}^0 e^{-\alpha_{\lambda} w} + B_{\lambda}(1 - e^{-\alpha_{\lambda} w}) \quad [\text{W/cm}^2\text{-}\mu\text{-sr}] \quad (4)$$

where  $I_{\lambda}$  is the specific intensity at the exit of each layer,  $I_{\lambda}^0$  is the incident spectrum coming from the previous layer or the incident spectrum entered by the User for the first layer,  $B_{\lambda}$  [W/cm<sup>2</sup>-μ-sr] is the effective or piecewise Black Body spectrum in the wavelength region near each line,  $\alpha_{\lambda}$  [cm<sup>-1</sup>] is the effective volumetric absorption coefficient within the layer, and  $w$  [cm] is the layer width. The flow and thermodynamic properties within each layer are assumed to be uniform throughout the layer. The specific intensity is also referred to in the literature as the radiative heating rate spectrum [(J/cm<sup>2</sup>-μ-sr)/s], the radiative power flux spectrum, and the spectral radiance.

The total radiative heating rate [W/cm<sup>2</sup>] or [J/cm<sup>2</sup>-s] is calculated by finding the specific intensity,  $I_{\lambda}$ , along several lines-of-sight to the same surface point, and then integrating over wavelength and solid angle. These integrations are done in the code for the stagnation point option only, and are performed in subroutine **transport**.

The effective volumetric absorption coefficient is referred to herein as just the absorption coefficient, except where it seems necessary to use the complete phrase. The total absorption coefficient in a layer,  $\alpha_{\lambda}$ , is the sum of the spectral absorption coefficients for all atomic and rotational lines and the bound-free and free-free continua. The individual line and total absorption coefficients are calculated in subroutines **atomic**, **band**, **bfcont**, and **ffcont**.

The absorption coefficients for the continua are specified in the literature (ref. 38) in terms of cross sections per particle,  $\sigma_{\lambda}$  [cm<sup>2</sup>]. These particle cross sections are converted to volumetric absorption coefficients,  $\alpha_{\lambda}$  [cm<sup>-1</sup>], by multiplying by the appropriate number densities [cm<sup>-3</sup>].

The absorption coefficient for a line in NEQAIR96 is expressed as (see eq. A18 in Appendix A)

$$\alpha_{\lambda} = E_{\lambda}/B_{\lambda} \quad (5)$$

The appropriate temperature used to calculate  $B_{\lambda}$  for each line, is determined by the ratio of the population number densities of the lower to the upper state. That is (see eqs. A6–A8 in Appendix A),

$$B_{\lambda} = 2hc^2 \lambda^{-5} 10^{-4}/(e^{hc\bar{\nu}/kT} - 1) \quad [\text{W/cm}^2\text{-}\mu\text{-sr}] \quad (6)$$

or (see Appendix A, eq. A11)

$$B_{\lambda} = 2hc^2 \lambda^{-5} 10^{-4}/(N_L/N_U - 1) \quad [\text{W/cm}^2\text{-}\mu\text{-sr}] \quad (7)$$

The wavelength  $\lambda$ , in this case, is expressed in cm and the factor of  $10^{-4}$  converts one of the cm's to μ's to give the spectral power per micron.

Note from the transport equation, equation 4, that when  $(\alpha_\lambda w)$  is very small the exponential factor is nearly 1.0 and the second term can be approximated by  $B_\lambda(1 - 1 + \alpha_\lambda w)$ , giving  $I_\lambda \approx I_\lambda^0 + E_\lambda w$ , which is the normal expression used for an optically thin medium or flow. Also, when  $(\alpha_\lambda w)$  is very large the exponential factor is nearly 0.0 and  $I_\lambda \approx B_\lambda$ , which gives the optically thick or Black Body spectrum at  $\lambda$ . The product  $(\alpha_\lambda w)$  is also known as the optical depth,  $\tau_\lambda$  [Dimensionless].

The equations given above are used to calculate optical spectra. The line shape functions are either specified at data entry or calculated from expressions in the code (see Appendix D). The populations of the energy states  $N_U$  and  $N_L$  are discussed in the following subsection.

## B. Excitation

The populations of the electronic energy states within atoms and diatomic molecules are found either by using the Boltzmann function or the QSS approximation (ref. 26), which is programmed in subroutines **qss** and **qssm**. The Boltzmann function is appropriate for equilibrium conditions and expresses the population of a nondegenerate energy level within an energy state as

$$N_i = (N_t/Q)e^{-c_2 E_i/T} \quad (8)$$

where  $N_t$  is the total species number density [ $\text{cm}^{-3}$ ],  $c_2 = hc/k = 1.43879$  [ $\text{cm K}$ ] is the second radiation constant,  $E_i$  [ $\text{cm}^{-1}$ ] is the energy of the  $i^{\text{th}}$  state,  $T$  [ $\text{K}$ ] is the temperature, and  $Q$  is the partition function (see Appendix F) given by

$$Q = \sum g_i e^{-c_2 E_i/T} \quad (9)$$

where  $g_i$  is the degeneracy of the  $i^{\text{th}}$  state. Equations 8 and 9 are valid for both atoms and diatomic molecules, but the energy values,  $E_i$ , for diatomic states are usually expressed as a sum of the electronic, vibrational, and rotational components, i.e.,  $E_i = E_e + G_v + F_J$  (see Appendix C).

The Boltzmann function is also used in a modified form for nonequilibrium conditions that are described by separate temperatures in each of the electronic, vibrational, and rotational energy modes. The modified expression is given by

$$N_i = (N_t/Q)e^{-c_2(E_e/T_e + G_v/T_v + F_J/T_J)} \quad (10)$$

The “nonequilibrium” partition function,  $Q$ , is then expressed using the exponential factor shown here rather than the one in equation 9. These three temperatures and the translational temperature are equal under equilibrium conditions.

Notice from equation 8 that the ratio of the population of any two nondegenerate energy levels can be expressed as

$$N_L/N_U = e^{-c_2(EL-EU)/T} = e^{c_2(EU-EL)/T} \quad (11)$$

The expression on the right side of this equation is identical to the exponential term in the denominator of the Planck or Black Body function, shown in equation 6, at the spectral location  $\bar{\nu} = (E_U - E_L) [\text{cm}^{-1}]$ , and noting that  $c_2 = hc/k [\text{cm-K}]$ . Equation 11 is the basis for expressing the Planck function ( $B_\lambda$ ) in terms of  $N_L/N_U$  in equation 7.

Equation 11 illustrates that under nonequilibrium conditions the “temperature” is only a parameter that relates population ratios. There can be an enormous number of such temperatures in a gas, one for each pair of energy states. This implies that each energy level can be associated with a large number of temperatures, but very few of these temperatures have any descriptive value in describing the thermal state of the gas as a whole. Thus, using population ratios to describe the thermal state of a gas under nonequilibrium conditions is simpler and less confusing than using temperatures. However, the intuitive feel of temperature is deeply embedded in our way of thinking and its use is often invaluable. Thus, the use of temperatures will always be with us, but their use for describing nonequilibrium environments needs to be expressed in clear and limited ways.

Using different electronic, vibrational, and rotational temperatures to calculate level populations in nonequilibrium flow certainly simplifies that task, but leaves much to be desired in many cases. For example, the electronic temperature determined in a chemically reacting fluid flow solution is an approximation to the electronic portion of the internal energy of the gas. However, most of the internal energy comes from the two or three lowest energy states. Thus, the electronic temperature found in this way may not adequately describe the populations of the high electronic energy states, which must be known to calculate the radiation emitted by transitions from these states.

The QSS method (ref. 26) overcomes this difficulty by using a “first principles” method to calculate the populations of the excited electronic states under thermal nonequilibrium conditions. This method is discussed thoroughly in reference 26, so it is only briefly summarized here. The QSS code in NEQAIR96 and the old NEQAIR of reference 1 differ in a few ways. The most significant of these are:

1. The populations of the nondegenerate electronic states are calculated in the new code rather than effective temperatures. The effective temperatures in the old code were converted to populations, as needed. The new code also uses population ratios to calculate the Planck function instead of the effective temperatures.
2. The average transition probabilities for atomic transitions from composite energy states are now calculated in subroutine **qss** from data in the **radiation.data** file. The old code required that these data be entered in the **excitation.data** file.
3. The atomic bound-free, optical recombination rate coefficients are now calculated using the bound-free absorption cross sections from reference 38, which are entered in the **radiation.data** file, rather than entering similar data from reference 43 in the **excitation.data** file. The redundant entry of these data is avoided by the introduction of subroutine **bfopt**.
4. The  $1s^2 2s 2p^4 \text{ } ^4\text{P}$  electronic state of N at  $88,135 \text{ cm}^{-1}$  is now included with the  $1s^2 2s 2p^2 ({}^3\text{P}) 3s \text{ } ^2\text{P}$  state at  $86,193 \text{ cm}^{-1}$  to form a composite state at  $87,488 \text{ cm}^{-1}$ . This state was not included in the old code because the active electron is characterized by a

different principal quantum number (2 vs. 3), which can affect the bound-free recombination rate coefficient. However, it has a strong transition probability or rate to the ground state and a multiplicity of 12. These factors make a substantial difference in the population of this composite state in low density environments.

5. The escape factors, discussed below and in Appendix E, have been reformulated to gain a better understanding of this important parameter.

The QSS method, as a first principles method, considers the collisional and optical excitation and de-excitation rates into and out of an “appropriate” number of electronic energy levels. A key assumption in the QSS method states that the rate of change of the population of any electronic energy level is slow compared to the excitation and de-excitation rates into and out of that level. That is, it assumes that the rates into and out of every level are very large and nearly equal, and that the population of each energy level is in a nearly (quasi-) steady state or QSS condition. This condition is advanced to a major assumption by setting the rate of change of the population of each electronic energy level, at all points in the flow, to zero. This step converts the problem of solving a set of differential equations into that of solving a much simpler set of linear algebraic equations for the electronic state populations (ref. 26).

Other approximations made in the QSS procedure are that only a limited number of energy levels need to be considered in the calculation and that several electronic energy levels can be lumped together to form composite levels. Table 2 gives the number of electronic energy levels included for most of the species entered in NEQAIR96. For atomic N, O, and C most of the energy levels are composite levels. Only a few of the lowest energy levels, which contain most of the species population, are composed of single electronic states. The populations of higher energy levels, which are not included in the QSS calculation, are found from equilibrium considerations by using the Saha equation (ref. 44), and the number of atomic ions and electrons at the electronic temperature.

The number of electronic energy levels included for diatomic molecules used in the QSS method are also shown in table 2. Clearly, the number of levels used is very limited, although all are composed of a single electronic state. The largest number of molecular levels considered in the **excitation.data** file is only four. Thus, the molecular results are not well established and may be significantly in error for the higher energy levels such as those near the dissociation limit of the ground state.

The upper states of the  $N_2(1+)$  and  $N_2(2+)$  band systems and many of the NO band systems lie near, and some above, the dissociation limit for the ground state. Thus, the populations of their upper states are of uncertain accuracy. On the other hand, the population of the upper state of  $N_2^+(1-)$  is probably given reasonably accurately because it lies well below the dissociation limit. The populations of the higher energy states that are not included in the QSS calculation are found by placing them in equilibrium with the number of dissociated atoms at the electronic temperature.

Table 2. Number of electronic energy states used in the QSS method

	Atom or molecule	Number of single levels	Number of composite levels
1	N	4	18
2	O	7	12
3	C	5	17
4	H	Not included in QSS	
5	He	Not included in QSS	
1	N <sub>2</sub> <sup>+</sup>	4	0
2	N <sub>2</sub>	4	0
3	NO	3	0
4	CO	4	0
5	CN	3	0
6	O <sub>2</sub>	Not included in QSS	
7	C <sub>2</sub>	Not included in QSS	
8	OH	Not included in QSS	
9	H <sub>2</sub>	Not included in QSS	

The effect of the optical excitation and de-excitation rates on the population of an energy level can be very substantial at low densities. This occurs because particle collisional rates are low at low densities and may approach the usually much lower spontaneous optical rates. The spontaneous optical transition rates can then become a major factor in lowering the populations of the upper states. The upper state populations can then be far below those determined by the collisional rates alone, often by orders of magnitude. Such flows are referred to as “collision limited” because the collision rates are too limited to maintain the state populations when optical emissions occur.

The optical emission rate coefficients [ $s^{-1}$ ] (assumed here to be the Einstein transition probabilities,  $A_{UL}$ ; see Appendix E) tend to lower the population of an energy level, and a suitably defined optical absorption rate coefficient [ $s^{-1}$ ] (not actually identified herein) tends to counter this tendency by repopulating the level. Thus, one can define an effective emission rate coefficient by multiplying the actual emission rate coefficient by a suitable factor that accounts for absorptions. This factor is called the “escape factor” and is defined as

$$\text{escf} = (A_{UL} - \text{absorption rate coefficient})/A_{UL} \quad (12)$$

The escape factor can have any value from 0.0 to 1.0. If all of the photons produced by emissions escape (are not absorbed), the escape factor is 1.0 and  $A_{UL}$  is fully effective in lowering the state population; whereas, if all of the photons are absorbed near the point where they are emitted, the

absorption rate coefficient will equal the local emission rate coefficient and the escape factor is 0.0. The effect of  $A_{UL}$ , as a depopulating rate coefficient, is then completely canceled by absorptions.

Unfortunately, a realistic absorption rate coefficient cannot be calculated, even if defined, until the radiation field is known. But the radiation field cannot be calculated until the QSS calculation is completed. The only way to break out of this dilemma is to use empirically derived values for the escape factor found under similar geometrical and gas dynamic conditions, or to model the escape factor concept with an approximation. As empirical values have not been derived for any condition, the use of an approximation is currently the only option available.

The model used to approximate the escape factor is discussed in Appendix E and is used in subroutine **bbescf** to calculate escape factors for atomic transitions. It is based on the reasonable assumption that the only absorptions that can affect the energy level populations in a local region must be those that occur close to where the emissions occur. Stretching this assumption, the escape factor is assumed to be mimicked by the probability that a photon emitted at a point in a radiating flow field will NOT be absorbed after traveling a distance,  $d$  [cm], through a uniform gas with an absorption coefficient,  $\alpha_\lambda$  [ $\text{cm}^{-1}$ ], equal to that at the point of emission.

The distance,  $d$ , in this approximation is not defined other than it should be chosen to give the correct result. Unfortunately, there are no established criteria for selecting  $d$ . It is surely related to the conditions at the emission point and to the geometry of the flow field, such as that for a shock layer or a wake region. It must also account for the fact that the absorptions at a point in the flow are caused by photons that are emitted from all other points in the flow field that can see the absorption point. Clearly,  $d$  can be selected arbitrarily to give any value of the escape factor from 0.0 to 1.0! However, experience has shown that  $d = 1.0$  cm has given useful quantitative results when compared with experimental data (refs. 45 and 46) from shock layer and shock tube environments, which extend over about 10 cm. Thorough calculations of the actual radiative transport phenomena in representative but simplified flow geometries are badly needed to provide results that will establish realistic values for the escape factor or, equivalently, for the distance  $d$ .

One obvious problem with the QSS formalism is that it cannot describe the energy level populations when the populations are changing rapidly. An important region where this condition exists is within and directly behind the bow shock wave that forms ahead of a blunt entry vehicle. Here the atmospheric gases are raised to a high translational energy condition rapidly, and strong collisions begin the relaxation processes of dissociation, excitation, ionization, and new species formation. The excited electronic states for species present near the shock wave are underpopulated but are being populated at high rates by collisions. Further, the depopulation rates are low because the upper state populations are low. Thus, the conditions for a QSS condition are not met.

In spite of this problem, comparison of the radiation results—using the QSS method with atmospheric entry (ref. 47), shock tube (ref. 48), and ballistic range (ref. 48) data—shows that the radiation profile across the shock layer for many important applications are reproduced in a useful manner. This implies that by the time the flow emits a measurable radiative signal the conditions in the shock layer have reached the point where the QSS formalism is a reasonable approximation. This point is often quite close to the shock wave. But at the very low densities that occur early in an entry trajectory it can be quite large and possibly greater than the shock standoff distance itself. The

intensity of the radiation under such conditions is low, and probably does not make a significant contribution to the total heating rate.

Arguments similar to those made here for the electronic QSS process can be applied to the vibrational and rotational populations as well, but that is not done in NEQAIR96. The total emission intensity from a molecular band system is determined principally by the population of the electronic upper state. The distribution of the total band system intensity among the vibrational bands is controlled by the vibrational populations or temperatures, and the general shape of vibrational bands is controlled by rotational level populations or temperatures. Calculating the vibrational and rotational populations by using “appropriate” temperatures should be viewed only as a starting point in nonequilibrium investigations. These populations may need to be changed substantially to agree with experimental data. Such changes provide insights into the shortcomings of the gas dynamic flow codes and of NEQAIR96 in producing realistic results. This is the research process. It will lead to better flow and excitation codes and encourage progress in determining the multitude of rate coefficients needed to understand these complex flow environments. One case where it was necessary to adjust the vibrational and rotational populations to agree with experimental data is described in reference 9.

The expression used to calculate the escape factors for atomic transitions is discussed and developed in Appendix E. But regardless of how the excited states are populated, the radiation is calculated using those populations and the radiation expressions given in the previous subsection.

## C. Options Available When Using NEQAIR96

NEQAIR96 is a flexible code that gives the User the opportunity to select several run-time options that specify how a particular calculation is to be made. The principal options are mentioned here and are covered again in detail in the How to Use NEQAIR96 section of this manual. The User can choose:

1. Not to create a spectrum, to create a new spectrum, to create and scan a new spectrum, or to scan an existing spectrum.

The option NOT to create a spectrum is effective when only the total radiative heating rate,  $[W/cm^2]$  or  $[W/cm^2-sr]$ , is needed and the radiating source is optically thin. Under such conditions, it is not necessary to spread the lines into a spectrum and then undo the process by integrating over wavelength. A simple summing of the integrated emission from all of the lines and continua is adequate. The total radiative heating rate value for optically thin flow will be the same whether summed or integrated spectrally. Excluding the spreading and integration steps enables the code to execute much faster, as the process of spreading the lines is a major time-consuming activity in the code. Obviously, the spectrum and its specific details are not available for analysis.

2. The spectral units for plot files.

The User can select to print a calculated spectrum to the plot files in terms of wavelength in Angstrom or nm, or in terms of wavenumbers in  $\text{cm}^{-1}$ , or it can be plotted more than once using any or all of these units.

3. Formatted or unformatted plot files.

Unformatted plot files can be transferred electronically, and the data plotted, much faster than formatted files, but they are impossible to check visually for content.

4. Whether to print the **los.data** file and/or spectroscopic data in the standard **Output** file, and/or whether to plot an extra spectrum.

The spectrum calculated at the last grid point in the **los.data** file is always written to the plot file. The User can also print an intermediate spectrum by entering the grid point number where the spectrum is desired. This option is not available for the shock tube option.

5. The kind of flow condition for the calculation, or whether to calculate a group of Black Body spectra.

Spectra can be calculated for three flow conditions: nonBoltzmann, Boltzmann, and Equilibrium; and for the emission from a Black Body surface.

- a. nonBoltzmann, Boltzmann, and Equilibrium flow.

The spectra for these options are calculated in the same way; only the upper state populations are determined differently. For nonBoltzmann flow, the populations of the electronic states are found by the QSS method (ref. 26), whereas for Boltzmann and Equilibrium flows the electronic populations are found using the Boltzmann distribution function, evaluated at the electronic temperature specified in the **los.data** file. The vibrational and rotational populations for nonBoltzmann and Boltzmann flows are found using the Boltzmann function evaluated at the vibrational and rotational temperatures. Only one temperature describes equilibrium flow, and it is used to find all populations.

- b. Black Body spectra.

Spectra are calculated using the Planck function at temperatures from 4000 to 32,000 K in 4000 K intervals, over the wavelength range from 0 to 100,000 Angstroms at 10 Angstrom intervals. One temperature can also be specified by the User and, if entered, it replaces the 4000 K temperature in the calculation.

6. Whether to make an equilibrium calculation.

The User has two options, either for a predetermined flow condition or for the condition behind a normal shock wave. In both options, a one-layer **los.data** file is written to tape unit 20.

a. Predetermined condition.

Enter the temperature [K], density [gm/cm<sup>3</sup>], length of the gas layer [cm], and the gas composition at any known condition.

b. Behind normal shock wave.

Enter the temperature [K] and density [gm/cm<sup>3</sup>] ahead of the shock wave, shock wave velocity, length of the shock layer, and gas composition at any known condition.

7. The type of flow geometry.

NEQAIR96 can handle three kinds of flow geometry: line-of-sight, stagnation point, and shock tube.

8. The radiation geometry of the stagnation flow regime.

The User can select from two options for calculating the total radiative heating rate [W/cm<sup>2</sup>] at the stagnation point. These are an infinite slab model or a spherical cap model (see fig. 13 in the How to Use NEQAIR96 section). The code calculates the specific intensity [W/cm<sup>2</sup>-μ-sr] from the direction of the stagnation streamline and the total radiative heating rate [W/cm<sup>2</sup>] at the stagnation point. The **los.data** file must be appropriate for flow along a stagnation streamline for the results to be realistic. This implies that the flow velocity in the flow calculation goes to zero at the stagnation point and that a boundary layer was included.

9. The parameters for a shock tube flow geometry.

10. The atomic and diatomic band systems included in the calculation and run-time options to:

- a. Calculate the atomic escape factors or set them to a fixed value for all atomic transitions.
- b. Skip weak vibration bands.
- c. Choose the spin multiplicity (singlet, doublet, triplet, or quartet) for each diatomic band system.
- d. Save the **EHL** files produced by the rotational matrix solution.
- e. Calculate a single vibrational band.

- f. Calculate rotational lines for the major branches only.
  - g. Skip vibrational bands whose band origins lie beyond the spectral range entered.
  - h. Limit the number of rotational lines in all branches.
11. Up to 10 wavelength regions for a single spectrum. For each region the User must enter:
- a. Wavelength range.
  - b. Number of spectral intervals.
  - c. Number of line widths, from the line centers, that lines are retained in the spectrum.
  - d. Line shape. The options are rectangular and Voigt. The Voigt shape can be calculated by the code, entered by the User, or set to a Gaussian shape whose line width at half height is equal to 10 times the spectral grid spacing.

Also, the User has the option to enter:

- e. An incident spectrum, except for the stagnation point option.
12. Up to 10 timing gates for shock tube flow.
13. The **los.data** file.
14. Slit and instrument functions.

The slit and instrument functions are used to scan calculated spectra. The slit functions can be described either with Voigt shapes or with a number of linear segments. The scanned spectra are written to tape units 31 to 40.

## How to Use NEQAIR96

The first step in using the code is to make a copy of the **template.input** file. This file specifies the format of the primary input file, which is referred to herein as the **Input** file. Rename the file and open it, so that it is displayed on the computer or terminal screen. Notice that the display contains several groups of lines separated by lines of ---'s. Each of these groups is labeled as LineN where N goes from 0 to 14. Within each of these groups of lines are several words or phrases followed by a 0 (zero), and the 0 is located above a lower case "a." These 0's are referred to here as "check locations." Several of the options displayed on the screen are selected by simply entering a character other than 0 (zero) in the check locations. A capital X is used to select options in the sample cases shown in Appendix J.

Numerical values appropriate for the type of calculation selected also need to be entered at designated places on the screen. In addition, separate files can be used to enter the region, los (line-of-sight), and/or scan file data. The tape unit numbers for these files must be entered on the last three lines of the **Input** file, as described below.

The ability to use the code effectively requires that the User be familiar with the files used for the input of data and the output of results. The tape unit numbers used in the code, and the data or results read or written from or to them, are shown in table 3. These tape unit numbers should not be assigned to any other files during the running of the code.

Table 3. Tape unit number assignments

Tape unit number	File name	Read or write
2	<b>spectroscopic.data</b>	Read
3	<b>excitation.data</b>	Read
4	<b>radiation.data</b>	Read
5	Standard input	Read
6	Standard output	Write
7	Temporary	Read and write
20	Equilibrium <b>los.data</b>	Write
21-30	Calculated plot files	Write and read
31-40	Scanned plot files	Write

Entering data can involve from 4 to 7 files and the results can be written on 1 to 21 files, all but one of these being plot files. Three of the input files are data base files: the **spectroscopic.data**, **excitation.data** and **radiation.data** files. The **excitation.data** file contains the data needed for QSS calculations and the **radiation.data** file contains the data needed to calculate the atomic lines and diatomic band systems selected in Line10. The **spectroscopic.data** file is assigned to tape

unit 2 (default file name fort.2 on the CRAY C-90 computer), the **excitation.data** file to tape unit 3 (fort.3), and the **radiation.data** file to tape unit 4 (fort.4). The data on these three files are read for every calculation. The top portions of these data files are illustrated in Appendix I.

The input files containing the specific data required for a calculation include the **Input** file, and possibly **region.data**, **los.data** and **scan.data** files. Template files for these four kinds of files are shown in figures 9–12. The data in all four files can be entered directly in the **Input** file rather than using the **region.data**, **los.data**, and/or **scan.data** files. The option to use additional files prevents the **Input** file from becoming too long and awkward to read. The User chooses which type of data, if any, are entered in separate files. The **Input** file is assigned to standard input tape unit 5 and the User always assigns the tape unit numbers for the **region.data**, **los.data**, and **scan.data** files. If all of the data are inserted in the **Input** file, the three tape unit numbers for the additional files must be set to 5. The principal subject of this section is to describe the data entered in these four files.

The output files include: the printed **Output** file assigned to standard output tape unit 6, a one layer **los.data** file written to tape unit 20 for the equilibrium option, and up to 20 plot files assigned to tape units 21 to 40. In addition, tape unit 7 is used for temporary storage during input, and for reading and writing the **EHL** files produced by the rotational matrix solution. The **Output** file contains descriptive information about the calculation, results that show the progress of the radiation as it moves along the line-of-sight, and the radiative heating rate at the surface. The surface is located at the last grid point in the **los.data** file.

The radiative heating rates for both an absorbing and an optically thin gas are printed in the **Output** file. The plot files contain the specific intensity spectrum [ $\text{W}/\text{cm}^2\text{-}\mu\text{-sr}$ ] in terms of wavelength in Angstrom and/or nm, and/or in terms of wavenumbers [ $\text{cm}^{-1}$ ]. If all three options are selected, the three spectra are all written to the same plot file. The spectra for both an absorbing and an optically thin gas are written to the plot files. The User can easily change the content of the plot files by changing the write statements in subroutine **transport**.

The User can place an unlimited number of comment lines at the top of all files, as illustrated by the **template.input** file shown in figure 9. The comment lines are contained between two rows of **\*\*\***'s. For the **Input** file only, one of these comment lines is a row of 60 **aaa**'s. All of the comment lines after the first row of **\*\*\***'s and above the row of **aaa**'s are printed as a header in the **Output** file. The row of **aaa**'s is a data format line. Additional comment lines after the row of **aaa**'s and before the second row of **\*\*\***'s are read over by the code and are not printed in the **Output** file.

```

*****
aaaaaaaaaaaaaaaaaaaaaaaaaaaaaaaaaaaaaaaaaaaaaaaaaaaaaaa <- 1st format line
123456789 123456789 123456789 123456789 123456789 123456789
template.input

Template of Input file for NEQAIR(96)

An unlimited number of comment lines can go here.

All lines entered AFTER line of ***'s above, and BEFORE the first format
line (line of aaa's above) will be printed as heading lines in the Output
file. Format for the heading lines is a60.

Enter data ABOVE the format lines shown below.

Line0
*****
SPECTRUM      :Dont Create 0;   Create Only 0;   Create and Scan 0;   Scan Only 0
Line1          a               a               a               a
-----
PLOT UNITS    : Angstroms 0;   NanoMeters 0;   Wave Numbers 0;
Line2          a               a               a
-----
PLOT FORMAT   :Plot File(s) are Formatted 0;   Unformatted 0
Line3          a               a
-----
PRINT OUT     : LOS Data 0;     Data 0;     Extra Plot at Grid # jx= 0;
Line4          a               a               iii
-----
KIND OF FLOW  :nonBoltzmann 0; d= 0.0; Boltzmann 0 Equilibrium 0; BlackBody 0
Line5          a rrrrrrr      a               a
-----
EQUILIBRIUM   : Temp= 0.0 K Rho= 0.000e-0 gm/cm3 LOSlength= 0.0 cm
Line6          rrrrrrr      rrrrrrrrrrrrr      rrrrrr
Species Molfrac :For a known condition where Sum Molfrac=1.0
0.0 :end species entry with blank and 0.0
aaaaaaa rrrrrrrrrrrrr :left justify species (enter above this line)
-----
TYPE OF GEOM.:Line-of-Sight 0; Stag Point 0; Shock Tube 0;
Line7          a               a               a
-----
FOR STAG PT. :Infinite Slab 0; Sphere. Cap 0; Rnose= 0.0 cm; Shock Div= 0.0
Line8          a               a rrrrrr      rrrrrr
-----
FOR SHOCK T. :STwidth= 0.0cm; VS= 0.0 km/s; Rho1= 0.000e-0gm/cc; Temp1= 0.0K
Line9          rrrrrr      rrrrrr      rrrrrrrrrrrrr      rrrrrr
-----

```

NOTE: Line10 Atomic and Diatomic Systems are shown in Fig3b.

```

REGION DATA: Lines11-12      regionfile = 0;
If regionfile=5, data follow; else on unit # =regionfile. iii
-----
LINE-of-SIGHT DATA: Line13      losfile = 0;
If losfile =5, data follow; else on unit # =losfile. iii
-----
SCAN SPECTRA DATA: Line14      scanfile = 0;
If scanfile =5, data follow; else on unit # =scanfile. iii
-----

```

Figure 9(a). Template.input file.

```

SYSTEMS      :Spectral Systems in Spectrum
Line10
      :Atomic Systems
      Escape Factors= Calculated X or 0.0
                        a rrrrr
Atom   smf:b-b      smf:b-f      smf:f-f
N       0.0         0.0         0.0
O       0.0         0.0         0.0
C       0.0         0.0         0.0
H       0.0         0.0         0.0
He      0.0         0.0         0.0
aaaaaaa rrrrr      rrrrr      rrrrr :End with blank and 0.0's.

      :Diatomic Electronic Transition Systems
      IPEAK= -9; Keep vib bands; Ivv>Imax*10**IPEAK
      iiii

      Save                      Major
      Rot EHL One Band SpinMult Branches vvExtend Nmax
      smf Files YN (vu,vl) Use Real Only! [Ang's]
-----
1 N2+ 1- 0.0 X 0 ( 0, 0) 1 2 X 0.0 0
2 N2 1+ 0.0 X 0 ( 0, 0) 1 3 X 0.0 0
3 N2 2+ 0.0 X 0 ( 0, 0) 1 3 X 0.0 0
4 N2 BH2 0.0 X 0 ( 0, 0) 1 1 X 0.0 0
5 NO beta 0.0 X 0 ( 0, 0) 1 2 X 0.0 0
6 NO gam 0.0 X 0 ( 0, 0) 1 2 X 0.0 0
7 NO del 0.0 X 0 ( 0, 0) 1 2 X 0.0 0
8 NO eps 0.0 X 0 ( 0, 0) 1 2 X 0.0 0
9 NO bp 0.0 X 0 ( 0, 0) 1 2 X 0.0 0
10 NO gp 0.0 X 0 ( 0, 0) 1 2 X 0.0 0
11 O2 SR 0.0 X 0 ( 0, 0) 1 3 X 0.0 0
12 CN VIO 0.0 X 0 ( 0, 0) 1 2 X 0.0 0
13 CN RED 0.0 X 0 ( 0, 0) 1 2 X 0.0 0
14 CO 4+ 0.0 X 0 ( 0, 0) 1 1 X 0.0 0
15 C2 Swan 0.0 X 0 ( 0, 0) 1 3 X 0.0 0
16 OH A-X 0.0 X 0 ( 0, 0) 1 2 X 0.0 0
17 H2 B-X 0.0 X 0 ( 0, 0) 1 1 X 0.0 0
18 H2 C-X 0.0 X 0 ( 0, 0) 1 1 X 0.0 0
19 H2 B'-X 0.0 X 0 ( 0, 0) 1 1 X 0.0 0
      0.0 0 0 ( 0, 0) 0 0 0 0.0 0:End Line
aaaaaaa rrrrr a a ii ii i i a rrrrrr iii

      :Diatomic Infra-Red Transition Systems

      Save                      Major
      Rot EHL One Band SpinMult Branches
      smf Files YN (vu, vl) Use Real Only!
-----
1 NO 0.0 X 0 ( 0, 0) 1 2 X
2 CN 0.0 X 0 ( 0, 0) 1 2 X
3 CO 0.0 X 0 ( 0, 0) 1 1 X
4 OH 0.0 X 0 ( 0, 0) 1 2 X
5 NH 0.0 X 0 ( 0, 0) 1 3 X
6 CH 0.0 X 0 ( 0, 0) 1 2 X
      0.0 0 0 ( 0, 0) 0 0 0:End Line
aaaaaaa rrrrr a a ii ii i i a

```

Actual spin mult. does not need to be entered, it is informational only.  
Bands with origins from w1-vvExtend to w2+vvExtend of the wavelength range  
w1-w2 are included. Enter vvExtend=0.0 to include all bands.  
Nmax limits the number of rotational lines; enter 0(zero)to keep all rot lines.

Figure 9(b). *Template.input file (concluded).*

Data format lines are used in the input files to illustrate on screen the columns where data are to be entered, and the type of data required. An “a” on a data format line indicates that an alphanumeric character is to be entered, an “i” indicates an integer, and an “r” indicates a real number. The data format lines are read over by the code and are only used to help the User with data entry. The entire group of comment lines at the top of the **Input** file is referred to as Line0. Corresponding to this designation, LineNumber0 is used to designate that portion of subroutine **input** where these lines are read. The **Input** file is divided into 15 such groups of lines and each group is referred to in a similar manner (LineN) in this manual and in the **Input** file, and as LineNumberN in subroutine **input**, where N = 0 to 14. The only exception to this is the combined designation of Lines11–12. The shock tube timing gates entered on Line12 never occur alone, as they are intertwined with the other region data on Line11. This issue is discussed below where the data for each input LineN is described.

Only three lines are used to define the data entered on Lines 1 to 5, 7 to 9 and possibly 11–12, 13, and 14. Each of these groups contains a line of data, a data format line, and a line of ---’s. The last line of every group is always a line of ---’s. These lines are used to separate the data groups and their only purpose is clarity. If the data on Lines 11–12, 13, and 14 are entered in the **Input** file, rather than in separate files, the format for these lines is still defined by the appropriate **template.region**, **template.los**, and **template.scan** files (see figs. 10–12).

The format used for the remaining two groups of data lines, Line6 for equilibrium flow and Line10 for the spectral systems, are longer and contain comment lines in addition to the data, format, and ---’s lines. These comment lines include blank lines that are essential and must not be deleted without making the appropriate changes to subroutine **input**.

Most of the run-time options in the **Input** file are selected by entering a nonzero (anything but “0”) character in the location specified by the format line. Obviously, entering a “0” means the option is not selected. In the three sample cases discussed in Appendix J, a capital X is used to select options. All of the options on lines Line2 for PLOT UNITS and Line4 for PRINT options can be selected. On most other lines, only one of the options is allowed. The code tests for these restrictions, prints an error message in the **Output** file, and terminates the run if an error in the input is found.

Subroutine **input** reads over Lines and parameters that are not needed by the options selected. This flexibility allows the User to leave old data in the **Input** file, such as an incident spectrum or shock tube parameters entered for an earlier run, even though they are not needed in the current run.



```

*****
template.los file

Template of LOS file for NEQAIR96

An unlimited number of comment lines can go here.

Enter Data AFTER the data-format lines!

(1) Enter species in any order; limited to atoms, diatomics, triatomics,
    atomic ions, diatomic ions, and electrons. Left-justify the species
    symbols in the fields. Dimensioned up to 25 species. End entry
    with a blank line.

(2) Properties entered at each grid point along line-of-sight. The
    properties apply to the layer between the grid point and the
    previous grid point. Thus, the properties at the first grid point
    are not used. This grid point only establishes the origin of the
    line-of-sight.

(3) Enter species number densities [cm-3] in the same order that the species
    symbols are entered. End data entry at each grid point with a blank
    line.

(4) End line-of-sight data entry, with a line of 0's as shown.

*****
          aaaaaaaa      aaaaaaaa      aaaaaaaa      aaaaaaaa      (2x,(7x,a8))
                                     :Species symbols.
-----
no.   x,cm  total partcc      t      tr      tv      te (i5,f8.3,
iiii  rrrrrr rrrrrrrrrrrrrr rrrrrrrr rrrrrrrr rrrrrrrr rrrrrrrrrre15.7,4f10.1
      rrrrrrrrrrrrrr rrrrrrrrrrrrrr rrrrrrrrrrrrrr rrrrrrrrrrrrrr (6x,4e15.7)
      Include these 9 lines (from --- to --- lines) for first grid point only!!
      End each grid point entry with a blank line.
      End data file with a line of zero's as shown on the next line.
0      0.0      0.0      0.0      0.0      0.0      0.0
-----

```

*Figure 11. Template.los file.*

```

*****
template.scan file

Template of Scan file for NEQAIR96.

An unlimited number of comment lines can go here.

An unlimited number of slit functions & instrument calibrations
functions can be entered.

Repeat lines below from "SCAN NO." to line of +++'s for each scan.

To end scan entry, enter 8 blank characters in the first 8
locations, after the line of +++'s for the last scan.

Enter Data ABOVE the data format lines!

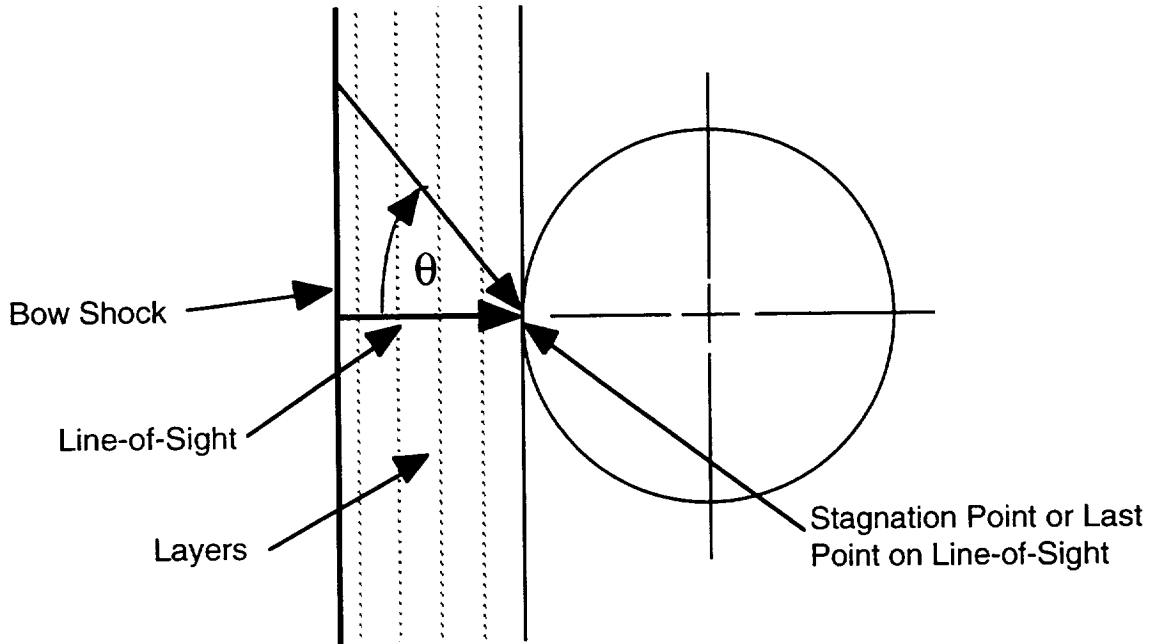
*****
SCAN NO. 1. Enter "SCAN NO." for new scan or 8 blanks to end scans.
aaaaaaaa                                     <- 1st format line.
          :Enter Cap V in first character for Voigt slit function.
          0 :Enter Type Slit Function, and Region or Gate Number.
aaaaaaaaaaaaaaaa iiii (a15,i5)                                     <- 2nd format line.
-----
          Enter Slit Parameters. (Next 2 lines are each the 2nd format line.)
          rrrrrrrrr rrrrrrrrr iiii Voigt Slit : widthg[A], widthl[A], range.
          rrrrrrrrr rrrrrrrrr aaaa Linear slit: lam[A], height, plus "line" at line
          format (5x,2e10.0,a5)                                     center point; " end" at last point.
-----
          Enter Spectral Interval for scan and scan step [A].
          0.0      0.0      0.0
          rrrrrrrrr rrrrrrrrr rrrrrrrrr (3e10.0)                 <- 3rd format line.
-----
          Enter Instrument Function. Wavelength [A] and Instrument Calibration.
          (At least 2 lines must be entered, including the line of 0.0's to end entry.)
          0.0      0.0      : Enter 0.0's to end instrument function.
          rrrrrrrrr rrrrrrrrr (2e10.0)                             <- 4th format line.
          ++++++
          :Enter SCAN NO. for new slit, or 8 spaces to end entry.

```

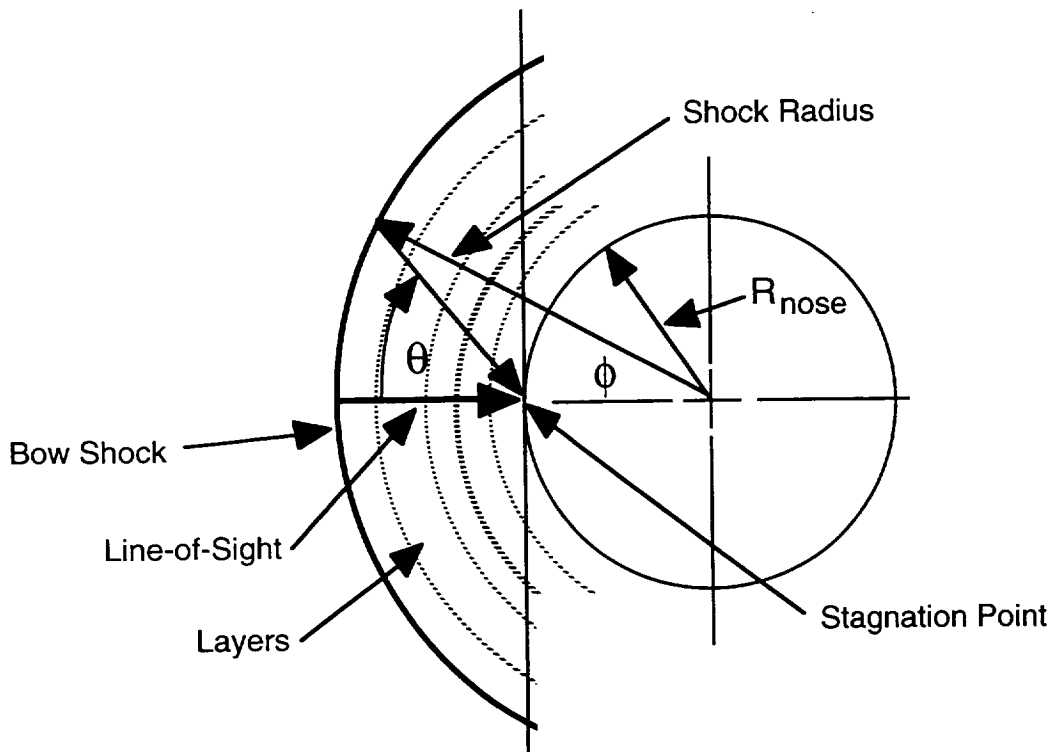
*Figure 12. Template.scan file.*

The geometry of the flow field can have a significant influence on how a calculation is conducted. For example, when calculating the integrated radiative heating rate at a point on a surface it is often necessary to make many line-of-sight calculations to describe the radiant field as a function of solid angle seen by the surface. For the stagnation point option, this process is simplified by using model geometries to perform the integration over solid angle. Two models are included in the code, the infinite slab and spherical cap models shown in figure 13. They are referred to in the following descriptions of the input options.

Subsection A below describes each input Line in detail and discusses the various run-time options. The effect of several of the options is examined in Subsection B.



a. Infinite Slab Approximation



b. Spherical Cap Approximation

*Figure 13. Model flow field geometries used in NEQAIR96.*

## A. Description of the Input File

Line0:

```
*****
aaaaaaaaaaaaaaaaaaaaaaaaaaaaaaaaaaaaaaaaaaaaaaaaaaaaaaa <- 1st format line
1234567879 123456789 123456789 123456789 123456789 123456789
                                template.input

                                Template of Input file for NEQAIR(96)

An unlimited number of comment lines can go here.

All lines entered AFTER line of ***'s above, and BEFORE the first format
line (line of aaa's above) will be printed as heading lines in the Output
file.  Format for the heading lines is a60.

Enter data ABOVE the format lines shown below.

Line0
*****
```

Allows the User to enter an unlimited number of comment lines at the top of the **Input** file and to print as many of these lines as desired as a heading in the **Output** file.

Line1:

SPECTRUM	:Dont Create 0;	Create Only 0;	Create and Scan 0;	Scan Only 0
Line1	a	a	a	a
-----				

Allows the User to select one of four options that specify whether a new spectrum is created and/or whether a spectrum is scanned. For all of these options, except the “scan only” option, the integrated radiative heating for an optically thin gas using the infinite slab model is printed in the **Output** file. This is the only output for the “don’t create” option.

### 1. Don’t create

This option is used to calculate the optically thin radiative heating rate [ $\text{W}/\text{cm}^2$ ] at the last grid point in the **los.data** file without creating a spectrum. A diagram of the infinite slab approximation is shown in figure 13(a).

The optically thin radiative heating rate is calculated by adding the contributions per steradian from all layers along the line-of-sight and multiplying by  $2\pi$ , which is the solid angle “seen” by a flat surface. The layers are the increments between grid points along the line-of-sight, and the contribution from each layer is the total emission [ $\text{W}/\text{cm}^3\text{-sr}$ ] times the layer width [cm]. The total emission is the sum of the emission from all atomic and rotational lines plus the integrated values from the bound-free and free-free continua. This process gives the radiative heating rate at the surface (last grid point on the line-of-sight) produced by an infinite slab of gas that is optically thin and tangent to the surface. The gas properties in each of the layers of the infinite slab are those entered in the **los.data** file.

This option provides the fastest way to run the code. It is a useful option when the gas is nearly optically thin and spectral details are not needed. The integrated line emissions [W/cm<sup>3</sup>-sr] are calculated using equation 1 but are not spread into the spectrum. The spreading process can be a major time-consuming part of a run when large numbers of lines are calculated.

## 2. Create only

This option creates a new spectrum but does not scan the spectrum.

## 3. Create and scan

This option creates and scans a new spectrum.

The scanning process occurs after the spectrum is calculated and requires that the User also enter the slit and instrument functions for the scan(s). An unlimited number of scans can be made on any spectrum. The scan data are entered in the **Input** file or in a separate **scan.data** file. If the tape unit number entered on Line14 below is 5, the entire **scan.data** file, including the comment lines at the start of the file, are entered in the **Input** file on Line14 after the line containing "iii" and before the line of ---'s. (See discussion below for Line14.)

## 4. Scan only

This option scans an existing spectrum.

The plot file containing the spectrum to be scanned must be located on the tape unit whose number is 10 greater than the region or gate number, entered on the first data line in the **scan.data** file. The data format of the file to be scanned must be the same as that used to write the plot files in subroutine **transport**. (See discussion below for Line14.)

The User enters the slit and instrument functions for the scan(s). An unlimited number of scans can be made on any spectrum calculated. These data are entered in the **Input** file or in a separate **scan.data** file. If the tape unit number entered on Line14 below is 5, the entire **scan.data** file, including the comment lines at the start of the file, are entered in the **Input** file on Line14 after the line containing "iii" and before the line of ---'s. (See discussion below for Line14.) The scanning process is discussed in reference 2 and in Appendix H.

The only Lines used in the **Input** file for this option are Lines0, 1, 2, 3, and 14. But uniformity has its value, so a complete **Input** file with all Lines present can be entered. The code reads over all Lines that are not needed.

Line2:

PLOT UNITS	:	Angstroms 0;	NanoMeters 0;	Wave Numbers 0;
Line2		a	a	a
-----				

Allows the User to select from one to three options that specify the units for the wavelength or wavenumber axis in the plot files. The options available are to print the files in terms of wavelength in Angstroms and/or nm, and/or in terms of wavenumbers. The spectra are written to the plot files for each option selected. This choice produces large plot files when large spectral arrays are specified on Line11.

Line3:

PLOT FORMAT	:	Plot File(s) are	Formatted 0;	Unformatted 0
Line3			a	a
-----				

Allows the User to select whether the plot files are formatted or unformatted. This does not affect the results of the calculation, but unformatted files on most computers can be transferred and plotted faster than formatted files. However, they are impossible to check visually for their content.

Line4:

PRINT OUT	:	LOS Data 0;	Spectros Data 0;	Extra Plot at Grid # jx= 0;
Line4		a	a	iii
-----				

Allows the User to select whether the spectroscopic data and/or the line-of-sight data are printed in the **Output** file, and whether an additional spectrum is written to the plot files. The plotting of an additional spectrum is selected by entering the line-of-sight grid point number where the additional spectrum is wanted. The spectrum produced at the last grid point in the line-of-sight data is always printed.

Line5:

KIND OF FLOW	:	nonBoltzmann 0;	d= 0.0;	Boltzmann 0	Equilibrium 0;	BlackBody 0
Line5		a	rrrrrrr	a	a	a
-----						

Allows the User to select one of three kinds of flow conditions for the spectral calculation, or to calculate a group of Black Body spectra.

## 1. nonBoltzmann

This option calculates the populations or number densities [ $\text{cm}^{-3}$ ] of the electronic energy levels using the QSS method. The QSS method can only be applied to those species whose excitation rate coefficients are entered in the **excitation.data** file (fort.3). The species included at the writing of this manual are the atoms C, N, and O and the diatomic molecules  $\text{N}_2^+$ ,  $\text{N}_2$ , NO, CN, and CO.

The populations of the vibrational and rotational levels are determined by using the Boltzmann equation at the vibrational and rotational temperatures entered in the **los.data** file.

An escape distance, d [cm], must also be entered for this option (see Appendix E).

## 2. Boltzmann

This option calculates the populations in the electronic, vibrational, and rotational energy modes using the Boltzmann distribution function at the electronic, vibrational, and rotational temperatures entered with the line-of-sight data.

## 3. Equilibrium

This option is available if either the line-of-sight or shock tube option is selected on Line7. It is not available at this time for the stagnation point option. The thermodynamic conditions for the equilibrium calculation are entered on Line6 for the line-of-sight option and on Lines 6 and 9 for the shock tube option.

**WARNING:** The codes in the subroutines called by subroutine **eqgas** may not converge if the temperature entered for a gas mixture is too low. Values of  $T = 300$  K or greater usually work satisfactorily.

## 4. Black Body

This option allows the User to produce a group of Black Body spectra for a range of temperatures and print them in the **Output** file. These spectra are generated by the Planck function at temperatures from 4000 to 32,000 K in 4000 K intervals, and over the wavelength range from 0 to 100,000 Angstroms in 10 Angstrom increments.

The value of d used in the nonBoltzmann option is not needed when the Black Body option is selected. The User can, therefore, enter a temperature in the input field for "d," which the code then uses to replace the 4000 K calculation with one using the temperature entered. These calculations are made in subroutine **planck**.

Line6:

```
EQUILIBRIUM : Temp= 0.0 K Rho= 0.000e-0 gm/cm3 LOSlength= 0.0 cm
Line6      rrrrrr      rrrrrrrrrrr      rrrrrr
           Species Molfrac :For a known condition where Sum Molfrac=1.0
                        0.0 :end species entry with blank and 0.0
           aaaaaaaa rrrrrrrrrr :left justify species (enter above this line)
-----
```

Allows the User to enter data needed to perform an equilibrium calculation for either the line-of-sight option (selected on Line5 above) or the shock tube option (selected on Line7 below). Both options require that the temperature [K] and density [gm/cm<sup>3</sup>] for the calculation be entered and that the mole fractions at some known condition be entered, so that the atomic fractions can be calculated. For a line-of-sight calculation the length of the gas layer is also needed, and all of the data are entered on Line6. For a shock tube calculation the only data entered on Line6 are the mole fractions of the initial gas composition; the other data are entered on Line9 below.

All species in the **spectroscopic.data** file that are consistent with the atoms contained in the initial gas composition, plus the electron, are included in the equilibrium calculation. Additional species may need to be entered into the **spectroscopic.data** file by the User to produce realistic equilibrium compositions. Additional species may include highly ionized atomic and diatomic species and polyatomic molecules. The only limitations on polyatomic molecules entered in the initial gas composition and the **spectroscopic.data** file are that only neutral polyatomic molecules (no ions) be entered, the chemical symbols used must not contain more than seven characters, and the numbers used must be only single digits. For example, CO<sub>2</sub>, C<sub>2</sub>H<sub>4</sub>, CH<sub>3</sub>O<sub>2</sub>N, and Na<sub>3</sub>AsO<sub>4</sub> are acceptable, but C<sub>16</sub>H<sub>16</sub>O<sub>2</sub> is not, as it contains eight characters and double-digit numbers. These restrictions can be removed by changing the coding in subroutines **eqInput**, **reorder**, and **reorderions**.

The partition functions for polyatomic molecules are calculated in subroutine **eqPf**. However, at the time of publication of this manual, only the expressions for CO<sub>2</sub> have been entered. The appropriate expressions for calculating the partition functions for other polyatomic molecules must be entered by the User.

The data on Line6 are read in subroutine **input**. The thermochemical state of the gas is calculated in subroutines **eqgas**, **eqInput**, **findspecies**, **reorder**, **reorderions**, and **eqTrho**. The equilibrium solution is treated as a single layer **los.data** file and is written on tape unit number 20. Thus, an external **los.data** file is not required, and if one is specified on Line13 below it is not read.

**WARNING:** The codes in the subroutines called by subroutine **eqgas** may not converge if the temperature entered for the gas mixture or free stream is too low. Values of T = 300 K or greater usually work satisfactorily.

Note that the data entered in the **los.data** file for any of the other options, except the Black Body option, can represent equilibrium conditions. The four temperatures entered at each grid point for such a case would then all be equal. The single layer **los.data** file written to tape unit 20 is an example of such a case. This file, once created, can be used as the **los.data** file in any other kind of calculation.

Line7:

TYPE OF GEOM.:Line-of-Sight 0; Stag Point 0; Shock Tube 0;
Line7                                   a                                   a                                   a
-----

Allows the User to select one of three types of geometry for the calculation.

### 1. Line-of-sight

This option calculates the specific intensity [ $\text{W}/\text{cm}^2\text{-}\mu\text{-sr}$ ] along the line-of-sight to the last grid point given in the **los.data** file. The data in the line-of-sight are not calculated by the code, except for the equilibrium option, and must otherwise be provided from an external calculation. The radiative heating rate per steradian [ $\text{W}/\text{cm}^2\text{-sr}$ ] is found from the specific intensity by integrating over wavelength.

### 2. Stagnation point

This option assumes that the data in the **los.data** file corresponds to the properties along a stagnation streamline. A realistic condition for this case is that the data correspond to a flow environment whose velocity is zero at the stagnation point, and that the last grid point specifies the shock standoff distance. Note, however, that the **los.data** file itself does not contain the flow velocity. The radiative heating rate at the stagnation point is calculated by using either an infinite slab or a spherical cap flow model. This choice is made on Line8.

### 3. Shock tube

This option assumes that the data in the **los.data** file correspond to the properties behind a normal shock traveling down a shock tube, and that the optical instrument recording the spectrum is looking normal to the shock tube flow. Therefore, the instrument views only a small slice of the flow field as it passes by the entrance slit of the instrument. The shock tube data are entered on Line9 below.

Line8:

FOR STAG PT. :Infinite Slab 0; Sphere. Cap 0; Rnose= 0.0 cm; Shock Div= 0.0			
Line8	a	a	rrrrrrr rrrrrr
-----			

Allows the User to select whether an infinite slab or a spherical cap model is used to calculate the radiative heating rate at the stagnation point (see fig. 13). The effective nose radius of the vehicle,  $R_{nose}$  [cm], and the shock divergence parameter,  $c1$  [cm/radian], must also be entered if the spherical cap model is selected. These calculations are performed in subroutine **transport**.

#### 1. Infinite slab model

The infinite slab model assumes that an infinite slab of gas is tangent to the stagnation point and normal to the stagnation streamline, as shown in figure 13(a). The gas properties in the slab along any line normal to the slab are assumed to be identical to those along the stagnation streamline given in the **los.data** file.

The radiative heating rate is found by calculating the specific intensity [ $W/cm^2\text{-}\mu\text{-sr}$ ] at the stagnation point along 10 equally spaced rays that cover the solid angle “seen” by the stagnation point. These rays range from the stagnation streamline itself, to a ray that is tangent to the stagnation point. The radiative heating rate [ $W/cm^2$ ] is then found by integrating the specific intensity over wavelength and solid angle.

If the infinite slab is optically thin, the radiative heating rate [ $W/cm^2$ ] is equal to  $2\pi$  steradians times the integral, over wavelength, of the specific intensity at the stagnation point from the direction of the stagnation streamline,  $I_\lambda$  [ $W/cm^2\text{-}\mu\text{-sr}$ ]. This result occurs because the optically thin specific intensity increases with the angle,  $\Phi$ , from the stagnation streamline as  $I_{\lambda_0}/\cos(\Phi)$ , and the surface area,  $A$ , decreases with  $\Phi$ , as  $\cos(\Phi)dA$ .

If the gas adjacent to the stagnation point is optically thick, the radiative heating rate at the stagnation point is equal to  $\pi$  steradians times the integral, over wavelength, of the specific intensity,  $I_{\lambda_0}$ , along any ray to the stagnation point. This result occurs because, if the gas is truly optically thick, the specific intensity along any ray at the stagnation point is equal to the Black Body spectrum at the gas temperature at the stagnation point. Thus, the specific intensity does not change with the angle  $\Phi$ .

If the gas is neither optically thin nor optically thick, the radiative heating at the stagnation point will fall between the above two values.

## 2. Spherical cap model

The spherical cap model assumes that the shock layer is bounded by a spherical vehicle surface and by a bow shock wave that is nearly concentric with the vehicle nose radius, as shown in figure 13(b). The model allows the shock wave to diverge away from the surface as the distance from the axis of symmetry increases.

This option requires that the effective nose radius,  $R_{\text{nose}}$  [cm], of the vehicle and the shock divergence coefficient,  $c1$  [cm/radian], for the shock wave be entered. The location of the bow shock wave, as a function of angle from the direction of the stagnation streamline, is calculated using the linear relationship

$$\text{shock radius} = R_{\text{nose}} + \delta + c1 * \phi \quad (13)$$

where  $\delta$  [cm] is the shock standoff distance at the stagnation point and  $\phi$  [radian] is the angle between the stagnation streamline and a point on the bow shock wave measured from the center of the sphere described by  $R_{\text{nose}}$ .

The radiative heating rate is found using the same steps as those used for the infinite slab model; that is, by calculating the specific intensity [ $\text{W}/\text{cm}^2\text{-}\mu\text{-sr}$ ] at the stagnation point along 10 rays between the stagnation streamline and the tangent to the stagnation point, and then integrating these specific intensities over wavelength and solid angle. The gas properties are assumed to be constant in nearly concentric zones between the surface and the shock wave and specified by the data in the **los.data** file.

The results from the spherical cap model are typically about 80% of the values from the infinite slab model (ref. 5).

Line9:

FOR SHOCK T. :STwidth=	0.0cm;	VS=	0.0 km/s;	Rho1=	0.000e-0gm/cc;	Temp1=	0.0K
Line9	rrrrr	rrrrrr	rrrrrrrrr	rrrrrr			
-----							

Allows the User to enter the shock tube width [cm], the shock velocity [km/s], the free steam density,  $\rho_1$  [gm/cm<sup>3</sup>], and temperature, Temp1 [K], ahead of the shock wave, if the shock tube option is selected on Line7. When the equilibrium option is also selected on Line5, the species mole fractions in the free stream ahead of the shock at some known condition are entered on Line6.

The time that each grid point along the line-of-sight passes the entrance slit of the optical instrument is calculated using the continuity equation,  $\rho_i V_i = \rho_1 V_s$ . The time that each grid point in the **los.data** file passes the entrance slit is given by

$$t_i = t_{i-1} + (x_i - x_{i-1}) / (V_s - V_i) \quad (14)$$

assuming that the time that the shock wave passes the entrance slit is set to 0.0. The densities,  $\rho_i$  [gm/cm<sup>3</sup>], along the line-of-sight are calculated from the line-of-sight data. These calculations are performed in subroutine **acntrol**.

The transport of the radiation across the width of the shock tube, STwidth [cm], is calculated to give the specific intensity as a function of time at each grid point. The specific intensity is then integrated over the time that the timing gate is open and divided by the time the gate is open to give a time average specific intensity spectrum [W/cm<sup>2</sup>-μ-sr]. These calculations are performed in subroutine **transport**.

Line10:

```

SYSTEMS      :Spectral Systems in Spectrum
Line10
      :Atomic Systems
      Escape Factors= Calculated X or 0.0
                        a rrrrr
      Atom    smf:b-b      smf:b-f      smf:f-f
      N        0.0         0.0         0.0
      O        0.0         0.0         0.0
      C        0.0         0.0         0.0
      H        0.0         0.0         0.0
      He       0.0         0.0         0.0
      0.0      0.0         0.0         0.0 :End with blank and 0.0's.
      aaaaaaaa rrrrr      rrrrr      rrrrr

      :Diatomic Electronic Transition Systems
      IPEAK= -9; Keep vib bands; Ivv>Imax*10**IPEAK
      iiii

      Save          Major
      Rot EHL One Band SpinMult Branches vvExtend Nmax
      Diatomic smf Files YN (vu, vl) Use Real Only! [Ang's]
      -----
1  N2+ 1-    0.0  X    0 ( 0, 0)  1  2    X    0.0    0
2  N2 1+    0.0  X    0 ( 0, 0)  1  3    X    0.0    0
3  N2 2+    0.0  X    0 ( 0, 0)  1  3    X    0.0    0
4  N2 BH2   0.0  X    0 ( 0, 0)  1  1    X    0.0    0
5  NO beta  0.0  X    0 ( 0, 0)  1  2    X    0.0    0
6  NO gam   0.0  X    0 ( 0, 0)  1  2    X    0.0    0
7  NO del   0.0  X    0 ( 0, 0)  1  2    X    0.0    0
8  NO eps   0.0  X    0 ( 0, 0)  1  2    X    0.0    0
9  NO bp    0.0  X    0 ( 0, 0)  1  2    X    0.0    0
10 NO gp    0.0  X    0 ( 0, 0)  1  2    X    0.0    0
11 O2 SR    0.0  X    0 ( 0, 0)  1  3    X    0.0    0
12 CN VIO   0.0  X    0 ( 0, 0)  1  2    X    0.0    0
13 CN RED   0.0  X    0 ( 0, 0)  1  2    X    0.0    0
14 CO 4+    0.0  X    0 ( 0, 0)  1  1    X    0.0    0
15 C2 Swan  0.0  X    0 ( 0, 0)  1  3    X    0.0    0
16 OH A-X   0.0  X    0 ( 0, 0)  1  2    X    0.0    0
17 H2 B-X   0.0  X    0 ( 0, 0)  1  1    X    0.0    0
18 H2 C-X   0.0  X    0 ( 0, 0)  1  1    X    0.0    0
19 H2 B'-X  0.0  X    0 ( 0, 0)  1  1    X    0.0    0
      0.0  0    0 ( 0, 0)  0  0    0    0.0    0:End Line
      aaaaaaaa rrrrr      a    a ii ii  i  i    a    rrrrrr    iii

      :Diatomic Infra-Red Transition Systems

      Save          Major
      Rot EHL One Band SpinMult Branches
      Diatomic smf Files YN (vu, vl) Use Real Only!
      -----
1  NO        0.0  X    0 ( 0, 0)  1  2    X
2  CN        0.0  X    0 ( 0, 0)  1  2    X
3  CO        0.0  X    0 ( 0, 0)  1  1    X
4  OH        0.0  X    0 ( 0, 0)  1  2    X
5  NH        0.0  X    0 ( 0, 0)  1  3    X
6  CH        0.0  X    0 ( 0, 0)  1  2    X
      0.0  0    0 ( 0, 0)  0  0    0:End Line
      aaaaaaaa rrrrr      a    a ii ii  i  i    a

```

Actual spin mult. does not need to be entered, it is informational only.  
Bands with origins from w1-vvExtend to w2+vvExtend of the wavelength range  
w1-w2 are included. Enter vvExtend=0.0 to include all bands.  
Nmax limits the number of rotational lines; enter 0(zero)to keep all rot lines.

Allows the User to select the spectral systems to be included in the calculation, and several options and parameters. The format for this Line is illustrated in the **template.input** file shown in figure 9. The format does not allow the entering of species or systems that are not in the **radiation.data** file. When the **radiation.data** file is changed, the **template.input** file needs to be changed also.

The method of selecting the spectral systems is to enter a nonzero strength multiplication factor (smf) for each system. The smf value provides a simple way to alter the integrated intensity of an entire spectral system; that is, all of the lines or continua of an atomic system, or all of the rotational lines of a diatomic band system. The smf's, therefore, allow the User to experiment with the effect of changing the total species concentration for an atomic system, or of changing the product of the transition moment squared and the population of the upper electronic state for diatomic band systems.

The other options and parameters that can be selected are:

1. A "check location" that specifies whether the escape factors for the atomic QSS calculation for nonBoltzmann (nonequilibrium) flow are calculated or set to a single value for all atomic levels. If the check location for the "Escape Factors = Calculated" is set to zero, the escape factors are not calculated by the code, and a fixed value from 0.0 to 1.0 must be entered. This value is then used for all atomic escape factors. Note, the values of the escape factors for all atomic continua and all molecular systems are set to 1.0 in subroutines **qss** and **molext**. These values can be changed by the User as desired.
2. The parameter (ipeak) that eliminates weaker vibrational bands from diatomic electronic band systems. To eliminate the weaker bands, approximations to the strongest line, in each band, in all of the band systems included in the calculation are found. The strongest of these strong lines is identified, and all bands whose strongest line is less than the product of the "strongest line of all" multiplied by  $10^{\text{ipeak}}$ , are not included in the calculation.

The process of eliminating weak vibrational bands speeds the spectral calculations for electronic band systems. The vibrational band data in the **radiation.data** file includes large numbers of bands for most of the band systems. Many of these bands are very weak in many (most?) calculations, yet together they can contain several thousands of rotational lines. These lines do not make a significant contribution to the spectrum, but they require just as much time to calculate and spread into the spectrum as do strong lines.

Entering a value of  $\text{ipeak} = -2$  will include most strong bands. However, it will also leave gaps in the spectrum where the weak bands tend to provide a low level background spectrum. A value of  $-2$  includes only those bands that are more than 1% as strong as the strongest band. It is a good value to use in the early period of an investigation. A value of  $\text{ipeak} = -5$  will select most of the significant radiation and a value of  $-9$  is about as far as one needs to go. However, to ensure that all bands are included, a value of  $\text{ipeak} = -20$  or smaller can be entered. The effect of  $\text{ipeak}$  on a spectrum and on the time required to generate the spectrum are illustrated in the following subsection.

3. A “check location” that selects whether the files containing the rotational energies and Hönl-London factors (**EHL** files) are saved or deleted after the calculation. The time to generate these files and their sizes are shown in table 1. Saving them means they only need to be calculated once. However, a significant amount of memory is required to store them, and at least some effort is required to keep track of them. Perhaps the biggest worry about keeping these files is that they may become outdated and still be used. This situation occurs if the spectroscopic constants in the **spectroscopic.data** file or the vibrational bands in the **radiation.data** file are changed, but the old **EHL** file is not deleted. The code will continue to use the old **EHL** file until it is deleted and then it will generate a new **EHL** file.

The file names for the **EHL** files are formed in subroutines **vuvi** and **irvuvi**. The first two characters in the name are either “EL” for electronic transitions or “IR” for IR transitions. The next one or two characters identify the band system. The characters are assigned based on their order in the **Input** file format for Line10. The last character is the spin multiplicity used for the calculation. Thus, if the NO gamma band system, a doublet transition (band system 6 in Line10), is run as a singlet, its file name is **EL61**, and if run as a doublet its file name is **EL62**. If it is foolishly run as a quartet, its name is **EL64**.

The **EHL** files produced when either or both the **vvExtend** and **Nmax** options are selected are discussed in item 7 below. They are named as outlined above but with a leading character of “X.” Thus, if NO gamma is run as a singlet and with a value of **Nmax** = 10, its **EHL** file is named **XEL61**. The purposes of adding the X character are to mark them for deletion and to preserve the complete **EHL** files already calculated. The “X” files are deleted because their **EHL** files are usually only valid for the particular case run. The User can save these files by changing the delete statements located near the bottom of subroutine **acntrol**.

4. A “check location” and two integer numbers for selecting a single vibrational band in any band system. This is a convenient option that is often used to investigate a spectrum piece by piece.
5. The spin multiplicity used to calculate the band structure. The actual spin multiplicity for each band system is shown in the **template.input** file. Using a lower multiplicity than the actual multiplicity enables the code to run faster. The results may still be realistic unless high resolution is needed or significant absorption occurs in the radiation environment.
6. A “check location” that allows only the “major” branches to be included in the calculation. This option enables the code to run faster, particularly for high spin multiplicities, as many weak lines are eliminated from the calculation. The major branches are those where  $\Delta J = \Delta N$  (see refs. 13 and 14). For doublets this eliminates half of the branches, for triplets two-thirds, and for quartets three-quarters! This is usually a very good approximation and is recommended for most calculations.
7. Two parameters, **vvExtend** and **Nmax**, can increase the speed of calculating diatomic electronic band systems, but their use has some risks:

- a. **vvExtend**. Eliminates vibrational bands whose band origin is **vvExtend** [Angstrom] beyond the bounds of the wavelength region entered on Line 11. Entering a value of 0.0 instructs the code to ignore this option. The default value **vkeep** set in subroutine **epeak** is used. The value of **vkeep** at the publication of this manual is 300 [Angstroms].
- b. **Nmax**. Limits the maximum number of rotational lines in all branches, in all bands, in a band system. Entering a value of 0 (zero) instructs the code to ignore this option and include all rotational lines.

Although these two parameters increase the speed of the calculation, they can reduce the total radiant power emitted by a factor of 2 or more. They are effective options in the early stages of an investigation or for special circumstances such as calculating the low rotational lines as shown in figure 6. These options should be used with caution. Their effects are illustrated in the following subsection.

The spin multiplicity of any diatomic band system is a fixed value, and it may seem odd that it is entered as a parameter that can be selected. The purpose of this option is to allow the User to approximate a band system with a spin multiplicity that is lower than its actual value. The effect of doing this, as noted above, can reduce substantially the computer time required to run a calculation when the spin multiplicity is high. This reduction is due to the large number of branches and rotational lines that occur in vibrational bands with high spin states.

The number of branches, as a function of the spin multiplicity, in each vibrational band for electric dipole allowed transitions (the only transitions currently included in NEQAIR96) is:

Multiplicity	Name	Number of branches	
		$\Sigma^+ - \Sigma^+$ and $\Sigma^- - \Sigma^-$ transitions	All other transitions
1	Singlet	2	3
2	Doublet	6	12
3	Triplet	15	27
4	Quartet	24	48

The occurrence of fewer branches for  $\Sigma - \Sigma$  transitions is due to the quantum mechanical selection rules  $\Delta J = 0$  or  $\pm 1$ ; and positive parity levels can only transition to negative parity levels, or negative to positive (see Appendix G). Also, in  $\Sigma^+$  states all even N levels have positive parity, and all odd N levels have negative parity, where N is the total rotational quantum number without spin. The opposite parities hold for  $\Sigma^-$  states. Thus, transitions between J-levels where  $\Delta N$  is zero or an even value cannot exist because the parity of these levels is the same. This effect is used in subroutine **band** to limit the number of branches and, thus, the number of rotational lines calculated.

Each branch has about the same number of lines, often on the order of 100 to 300. Thus, the amount of computer time required to calculate and spread the rotational lines in the spectrum increases substantially for transitions between higher spin states.



For cases using a single wavelength region and whose incident spectrum is entered on a few lines, the data needed are easily entered directly in the **Input** file. However, when more than one region is specified, or when the incident spectrum for any region is long, placing the region data in a separate **region.data** file keeps the **Input** file shorter and easier to read.

The region data are entered in a separate **region.data** file when the tape unit number entered by the User for "regionfile," on Lines11–12 in the **Input** file, is other than 5, the standard input unit number. If 5 is entered for regionfile, then the region data are entered directly in the **Input** file.

The **region.data** file format is always the same, whether the data are entered in the **Input** file or in a separate **region.data** file. The format for these data is illustrated in the **template.region** file shown in figure 10. If the region data are placed in the **Input** file, the entire **region.data** file is placed after the format line for Lines11–12 (line ending with "iii") and before the line of ---'s.

The format for the **region.data** file allows an unlimited number of comment lines to be entered at the top of the file. These comments are bounded by lines of \*\*\*'s. The first format line in the **region.data** file shows the location of the "check location" for an incident spectrum. Entering any character other than 0 (zero) in this location specifies that an incident spectrum will be entered for this region. The second format line gives the format for the spectral data that define the region, and the third format line gives the format for an incident spectrum. The data are entered directly above the format lines. An incident spectrum is not always entered, but the region file format always allows for one. Thus, if an incident spectrum is NOT wanted, these lines can be removed or they can be left in, as the code will simply read over them.

The format for a region, as shown in figure 10, also contains an embedded group of lines (Line12) for entering the timing gate data needed when the shock tube option is selected on Line7. This subgroup of lines contains a line of ---'s, three comment lines, a line of 0's, and a data format line. Although timing gates are only entered if the shock tube option is selected, the **region.data** file format always allows for them. If timing gates are not needed, these lines are read over. If they are needed, they are entered on the Line12 portion of Lines11–12.

The following spectral data must be entered for each region:

1.  $w_1$

The shortest wavelength [Angstrom] for the region.

2.  $w_2$

The longest wavelength [Angstrom] for the region.

3.  $narray$

The number of spectral points. However, the code assumes that the User enters the number of spectral intervals, because that appears to be the number that is most intuitive. For example, if Users want the spectrum to cover from 2000 to 3000 Angstroms with 1000 equally spaced points, they are probably expecting the spectral intervals to be 1.0 Angstrom. But, if they enter 1000 for  $narray$  they will have only 999 spectral intervals, and each interval is slightly greater than 1.001 Angstroms. As the code must work with the number of grid points along the wavelength axis, the code adds 1 to the number entered and redefines this sum as  $narray$ .

The number of spectral points must provide for at least 5, and preferably 10, spectral intervals per full line width at half height. This ensures that an integration over the line shape returns a value close to the integrated power density that is calculated before the line is spread into the spectrum.

4.  $range$

Range is the distance from the line center that Voigt profile lines are added into the spectrum, specified as an integer number of line widths. The User can elect to include the contribution of lines over the entire wavelength range from  $w_1$  to  $w_2$  by setting  $range$  equal to 0 (zero). A value of 3 is usually adequate for Gaussian profile lines and a minimum value of 5 is suggested for other Voigt profile lines. A larger value of  $range = 20$  has been recommended for the O<sub>2</sub> Schumann-Runge band system by Christophe Laux of Stanford University.

5.  $lwidth$

The parameter that sets the line shape. The following values can be entered:

= 0 The line shape is rectangular and is spread uniformly over 4 spectral intervals or 5 spectral grid points. This shape is not realistic and should only be used for optically thin gases when the spectral resolution is broader than about 5–10 Angstroms. Only the spectrum for the optically thin case is calculated for this option because the absorption results are meaningless. It is a fast option and can be helpful in the early stages of an investigation.

A comparison of the effect of Voigt and rectangular line shapes on the shape of a spectrum and on computer time is shown in the following subsection.

- = 1 The line shape is a Voigt profile and its Gaussian and Lorentzian component line widths, widthg and widthl, are determined by the code (see Appendix D). The line width in NEQAIR96 is always the full line width at half height.
- = 2 The line shape will be a Gaussian profile whose width is  $10 \cdot \text{dellam}$ , where dellam [Angstrom] is the spectral interval (spacing between spectral grid points). The Lorentzian width is set to 0.0 for this option. This is often the option of choice for most calculations where absorption is not important.
- = 3 The line shape is a Voigt profile and the User enters the widths of the Gaussian and Lorentzian components, widthg and widthl [Angstrom].

## 6. An incident spectrum

An incident spectrum is specified by entering the wavelength [Angstrom] and the specific intensity [ $\text{W}/\text{cm}^2\text{-}\mu\text{-sr}$ ] for as many points as required. The wavelength values must start at the shortest wavelength and proceed to the longest wavelength monotonically. The first wavelength must be less than or equal to  $w_1$  for the region, and the last wavelength must be equal to or greater than  $w_2$ . A line of 0.0's is entered to terminate the entry of the incident spectrum. The incident spectrum is read in subroutine **incident**.

Note that an incident spectrum is not allowed if the stagnation point option is selected on Line7. In this case, the integration to find the radiative heating rate at the stagnation point involves integrating the shock layer over  $2\pi$  steradians, whereas the incident spectrum is only entered per steradian along the line-of-sight. Thus, when the stagnation point option is selected, the code reads over the incident spectrum lines, even if data are entered.

Line12:

```
-----
Line12      :Shock tube timing gates, as needed.  10 gates allowed all regions.
              Enter gates for region after next line.  End entry with all 0.0's.
tstart [s] topen [s]  lam1 [A]  lam2 [A]  planckT[K]
          0.0      0.0      0.0      0.0      0.0
          rrrrrrrr rrrrrrrr rrrrrrrr rrrrrrrr rrrrrrrr (5e10.0)          <- 4th.
          +-----+
          :Repeat REGION to +++'s line for new region, or end as noted above.
```

Allows the User to enter the timing gate data when the shock tube option is selected on Line7.

The format for a region (see fig. 10), also contains an embedded group of lines for entering timing gate data that are needed when the shock tube option is selected on Line7. This subgroup of lines contains a line of ---'s, three comment lines, a line of 0.0's, and a data format line. Although timing gates are only entered if the shock tube option is selected, the

**region.data** file format always allows for them. If timing gates are not needed, they can be removed or left in, as the code reads over them.

There is an intertwining of the timing gate data with the other data entered for the regions on Line11. For example, up to 10 timing gates can be entered, and they can be distributed among the 10 possible wavelength regions in any way the User chooses. For example, all of them can be entered in a single region, even though more than one wavelength region is specified. The timing gates are entered after the incident spectrum for each region is entered. A line of 0.0's is entered to terminate the entering of gates in each region.

A timing gate is specified by entering five data values on a single line with a format of (5e10.0). The data entered for each gate are:

1.  $t_{\text{start}}$

The time [s] from the time the shock wave passes the entrance slit of the optical instrument until the gate is initiated.

2.  $t_{\text{open}}$

The time increment [s] that the gate is open, also known as the width of the gate.

3.  $\lambda_1$

The shortest wavelength [Angstrom] for the spectrum recorded while the gate is open.

4.  $\lambda_2$

The longest wavelength [Angstrom] for the spectrum recorded while the gate is open.

5.  $\text{planckT}$

A temperature that, if entered, instructs the code to calculate a Black Body spectrum for this temperature and write it in the plot file along with the calculated spectrum for the gate. This temperature is not used, even if entered, in the equilibrium option. In the equilibrium case, a Black Body spectrum is always calculated at the equilibrium temperature.

The transport of the radiation across the width of the shock tube is calculated to give the specific intensity, as a function of time at each grid point in the **los.data** file. These spectra are then integrated over time and divided by  $t_{\text{open}}$ , the time the gate is open, to give a time average specific intensity spectrum [ $\text{W}/\text{cm}^2\text{-}\mu\text{-sr}$ ]. The width of the shock tube is entered on Line9 above. These calculations are performed in subroutine **transport**.

Line13:

```

LINE-OF-SIGHT DATA: Line13                losfile      = 0;
If losfile  =5, data follow; else on unit # =losfile.    iii
-----
          aaaaaaaa      aaaaaaaa      aaaaaaaa      aaaaaaaa      (2x,(7x,a8))
                                     :Species symbols.
-----
no.  x,cm  total partcc      t      tr      tv      te (i5,f8.3,
iiii rrrrrr rrrrrrrrrrrrrr rrrrrrrr rrrrrrrr rrrrrrrr rrrrrrrre15.7,4f10.1
      rrrrrrrrrrrr rrrrrrrrrrrr rrrrrrrrrrrr rrrrrrrrrrrr      (6x,4e15.7)
      Include these 9 lines (from --- to --- lines) for first grid point only!!
      End each grid point entry with a blank line.
      End data file with a line of zero's as shown on the next line.
0      0.0      0.0      0.0      0.0      0.0      0.0
-----

```

Allows the User to enter the line-of-sight data. These data are entered either in the **Input** file at this point or in a separate **los.data** file. The line-of-sight data are entered in a separate **los.data** file when a tape unit number other than 5 is entered by the User for "losfile" on Line13. If 5 is entered for losfile, then these data are entered directly in the **Input** file.

The **los.data** file format is the same, whether the data are entered in the **Input** file or in a separate **los.data** file. The format for these data is illustrated in the **template.los** file shown in figure 11. If the line-of-sight data are placed in the **Input** file, the entire **los.data** file is placed after the format line for Line13 ending with "iii" and before the line of ---'s.

The format allows for an unlimited number of comment lines to be entered at the top of the file. These comments are contained between two rows of \*\*\*'s. The **los.data** file contains the symbols for the species in the flow field; the line-of-sight grid; the total number density of all species (including those not in the species list); the translational, rotational, vibrational, and electronic temperatures; and the number densities of the species.

The atomic and molecular species symbols are entered immediately after the second row of \*\*\*'s ending the comment lines. The format for these data is (2x,4(7x,a8)), and data entry continues until a blank line is read. The code then determines the number of species. The atomic symbols used to specify the species can contain one or two characters. If two characters are used, the first one must be a capital letter and the second one a lowercase letter. Do NOT leave any blanks in a species name. The last character of a species name must be a blank. Thus, although the format for the name is a8, only seven characters can be used.

The species may be entered in any order, but their number densities must be entered in the same order. The species are reordered after they are entered, and placed in the order of atoms, diatomic molecules, polyatomic molecules, atomic ions, diatomic ions, and electrons. The ions for each atom and each diatomic molecule are grouped together and reordered to be in the order of ionization. These reorder operations are performed in subroutines **reorder** and **reorderions**.

The data for each grid point are read after the species symbols are entered. The grid number; the grid location [cm]; the total number density (including species not in the species list); and the

translational, rotational, vibrational, and electronic temperatures are read from the first line of data for each grid point, using a format of (i5,e8.0,e15.0,4e10.0). The number densities of the species are then read using a format of (6x,4e15.7). After the data for each grid point have been entered, a blank line is read. The reading process is terminated when the first line for a new grid point is a line of 0.0's. The number of grid points is determined by the code.

Line14:

```
SCAN SPECTRA DATA: Line14          scanfile = 0;
If scanfile =5, data follow; else on unit # =scanfile.   iii
-----
```

```
SCAN NO. 1.  Enter "SCAN NO." for new scan or 8 blanks to end scans.
aaaaaaaaa                                     <- 1st format line.
              :Enter Cap V in first character for Voigt slit function.
              0 :Enter Type Slit Function, and Region or Gate Number.
aaaaaaaaaaaaaaa iiiii (a15,i5)               <- 2nd format line.
-----
              Enter Slit Parameters. (Next 2 lines are each the 2nd format line.)
rrrrrrrrrr rrrrrrrrr iiiii Voigt Slit : widthg[A], widthl[A], range.
rrrrrrrrrr rrrrrrrrr aaaa  Linear slit: lam[A], height, plus "line" at line
format(5x,2e10.0,a5)                      center point; " end" at last point.
-----
              Enter Spectral Interval for scan and scan step [A].
0.0      0.0      0.0
rrrrrrrr rrrrrrrrr rrrrrrrrr (3e10.0)      <- 3rd format line.
-----
              Enter Instrument Function. Wavelength [A] and Instrument Calibration.
              (At least 2 lines must be entered, including the line of 0.0's to end entry.)
0.0      0.0      : Enter 0.0's to end instrument function.
rrrrrrrr rrrrrrrrr (2e10.0)                <- 4th format line.
+++++
              :Enter SCAN NO. for new slit, or 8 spaces to end entry.
```

Allows the User to enter an unlimited number of slit and instrument functions for scanning a calculated spectrum (see sample case 1 in Appendix I). The present code only allows the first spectrum at the left side of the plot file to be scanned. However, this can be changed by changing the format statements in subroutines **voigtscan** and/or **linearscan**. The line-of-sight and stagnation point options print two spectra in three columns. The first column is the wavelength, in Angstroms or nm, or the wavenumber. The second column is the specific intensity with absorption, and the third column is the specific intensity for an optically thin gas. For the shock tube option four spectra are printed in five columns. The first column is again the wavelength or wavenumber, and the second column is the time-averaged specific intensity over the slit. The other spectra are described in part 3 of the next subsection.

Each slit and its associated instrument function are used to produce a scan directly after being entered. They are not saved in memory. Thus, an unlimited number of scans can be made on any spectrum. The spectral scanning method used is described in Appendix H and in reference 2.

The User can enter two kinds of slit functions: those modeled by a Voigt profile and those approximated by a group of linear line segments. The kind of slit is read in subroutine **bandpass**, and the specific slit and instrument functions are read in either subroutine **voigtscan** or **linearscan**. The maximum number of line segments allowed for approximating a slit function is presently set

at 1001, but this number can be increased by changing the dimensions of the **Bandlam** and **rBand** arrays in subroutine **linearscan**.

The instrument functions express the sensitivity of spectral instruments, as a function of wavelength, in units such as  $[V/(W/cm^2-\mu\text{-sr})]$  or its inverse. They can be used in two ways:

1. To transform an experimental spectrum, recorded as a function of  $V$  (or other parameter), to specific intensity.
2. To transform a calculated spectrum, as a function of specific intensity, to  $V$  (or other signal parameter).

Here, of course, we are concerned with the second of these ways.

The maximum number of points describing an instrument function is presently set at 5001, but this number can be increased by changing the dimensions of the **caliblam** and **rcalib** arrays in subroutines **voigtscan** and **linearscan**.

The length of the scanning data can become quite long for slit functions composed of linear segments and for large instrument function arrays. Thus, it is often desirable to remove the scanning data from the **Input** file and enter it in a separate **scan.data** file. The scanning data are entered in a separate **scan.data** file when the tape unit number entered by the User for "scanfile" on Line14 is other than 5, the standard input unit number. If 5 is entered for scanfile the scan data are entered directly in the **Input** file.

The **scan.data** file format is the same whether the data are entered in the **Input** file or in a separate **scan.data** file. The format for these data is illustrated in the **template.scan** file shown in figure 12. If the scanning data are placed in the **Input** file, the entire **scan.data** file is placed after the format line for Line14 ending with "iii" and before the line of ---'s.

The format for the **scan.data** file allows an unlimited number of comment lines to be entered at the top of the file. These comments are bounded by lines of \*\*\*'s.

Four kinds of scanning data are entered for each slit function using the format statements shown in the **template.scan** file. The specific data needed for each kind of data are:

1. First data line: Type of slit function and the location of the plot file to be scanned, using a format of (15a,i5).
  - a. The User enters the type of slit function in the first field on this line. The format allows 15 characters to define the type of slit function for printing in the **Output** file, but only the first character is examined by the code. The first character **MUST** be a lower case "v" to select a Voigt slit function. If the first character is not a "v" the code assumes that a linear slit function is specified.

- b. The User also enters the number, N, that specifies where the spectrum to be scanned is located. The spectrum must be loaded on tape unit 20+N and have a format compatible with that used to write the plot files in subroutine **transport**. The scanned spectrum is written to the plot file located on tape unit 30+N.
  2. Second data line or lines: The specification of the slit function, format (2x,2e10.0,a5).
    - a. Voigt slit function, one line:
      - 1) Width of Gaussian component,  $w_g$  [Angstrom].
      - 2) Width of Lorentzian component,  $w_l$  [Angstrom].
      - 3) Distance slit function extends from the slit center, specified as an integer number of slit widths.
    - b. Linear segment slit function, many lines:
      - 1) Wavelength of slit coordinate [Angstrom].
      - 2) Height of slit coordinate [Arbitrary]. Enter up to 1000 slit coordinates. Enter the word "end" (right justified) in the third field to terminate the entry of the slit function.
      - 3) Wavelength coordinate of slit "center." The slit center is specified by placing the word "line" in the data line whose wavelength coordinate identifies the slit center. The slit center can be difficult to define in a mathematically satisfying manner if the slit is not roughly symmetrical. But it must be assigned in all cases to provide the location on the slit that is used to align the slit with the spectrum for each calculation.
3. Third data line: The scanning range and step size.
  - a. The starting wavelength [Angstrom] for a scan; shortest wavelength.
  - b. The ending wavelength [Angstrom] for a scan; longest wavelength.
  - c. The wavelength interval [Angstrom] for stepping the scan. Entering a value of 0.0 instructs the code to set the interval as follows:
    - 1) Voigt slit, slit width divided by 10.
    - 2) Linear segment slit, effective slit width divided by 10. The effective slit width is found by calculating the area under the slit function and dividing by the peak height of the slit.

#### 4. Instrument Function.

- a. Wavelength [Angstrom] of instrument function.
- b. Value of instrument function. Enter up to 5000 instrument function values and then a line of 0.0's to terminate the entry of the instrument function. These values must be entered monotonically from the shortest to the longest wavelengths.

The scanning process can also simulate a fixed slit such as a radiometer. In this case the starting and ending wavelengths for the scan are identical. Note that an instrument function defined at single point is then possible.

### B. Effect of Options and the Output File

The purpose of this subsection is to illustrate the effects of the run-time options on results and briefly discuss the **Output** file. This subsection is structured in three parts:

- Part 1. Options for atomic systems.
- Part 2. Options for diatomic systems.
- Part 3. Brief statement about the **Output** file and plot files.

The **los.data** file used for these calculations is identical to the last layer of the 38 layer **los.data** file used for sample cases 1–2 shown in figure J2 in Appendix J. This shortened one layer **los.data** file is shown in figure 14. Note, the data at the first grid point is not used, as the gas properties for the first layer are given at the second grid point. The first grid point only establishes the starting location (x value) of the data, here set equal to 0.0. The other data shown for the first grid point are simply a repeat of the data at grid point 2, although these data fields could have been filled with zeros. The width of the layer is 1.0 cm, as shown by the x value or location of the second grid point.

The spectral range for all of the calculations made for this subsection is from 2000 to 10,000 Angstroms. The number of spectral intervals is 8000 and the line shapes are Gaussian line profiles with a line width at half height of 10.0 Angstroms. The one exception to this is a calculation for a rectangular line, and all rectangular lines are spread over 4 spectral intervals, or 4 Angstroms in this case.



## Part 1. Effect of Options for Atomic Systems

The effect of options for atomic systems is shown in table 4 by the tabulation of two input parameters and three output results for four calculations. The calculations included all atomic N, O, and C lines within the spectral range 2000 to 10,000 Angstroms. The two input options tabulated are:

1. The type of flow. The options used are either Boltzmann, B, or nonBoltzmann, nonB. nonBoltzmann means that the QSS code in subroutine **qss** is used to calculate the electronic state populations.
2. Whether the escape factors, **escf**, for nonBoltzmann flow are calculated. If not calculated, the value assigned to the escape factors is shown.

The three output results tabulated are:

1. The total time in seconds needed to complete the run,  $t_{\text{tot}}$ .
2. The number of atomic lines calculated and spread into the spectrum,  $N_{\text{lines}}$ .
3. A radiative heating rate at the end of the line-of-sight [ $\text{W}/\text{cm}^2$ ], **RadH**, calculated by multiplying the specific intensity [ $\text{W}/\text{cm}^2\text{-}\mu\text{-sr}$ ] by  $2\pi$  steradians and integrating over wavelength. These heating rates are intended only to provide values for comparison purposes and are not considered to be a correct integration over solid angle and wavelength.

Table 4. Summary of four calculations for atomic systems to illustrate NEQAIR96 options

	Flow	escf	$t_{\text{tot}}$ [s]	$N_{\text{lines}}$	RadH [ $\text{W}/\text{cm}^2$ ]
1	B	Calculated	1.68	207	4.275
2	nonB	Calculated	1.88	207	3.318
3	nonB	0.0	1.80	207	4.241
4	nonB	1.0	1.80	207	3.318

Conclusions from an examination of table 4 are:

1. The atomic line systems contain only 207 lines in the wavelength range from 2000 to 10,000 Angstroms, and they are calculated very quickly.
2. The nonBoltzmann flow calculations run slower than the Boltzmann calculation. This is true even when the escape factors for each electronic state are set to a specific value rather than calculated in subroutine **bbescf**.

3. The radiative heating rate for nonBoltzmann flow, with  $\text{escf} = 0.0$ , is nearly equal to the rate for Boltzmann flow. This implies that the populations of the excited electronic levels would be very close to the Boltzmann populations if radiative depopulation did not occur.
4. The radiative heating rates for nonBoltzmann flow using calculated escape factors and escape factors set to 1.0 are equal. This means that the calculated escape factors are very close to 1.0, and emission lowers the populations of the excited electronic states.
5. The radiative heating rates for nonBoltzmann flow using escape factors set equal to 0.0 and 1.0 are not equal. Thus, the flow is at least somewhat collision limited, and the emission rate is lowering the populations of the excited electronic states.

## Part 2. Effect of Options for Electronic Diatomic Systems

The effect of options for electronic diatomic systems is shown in table 5 by the tabulation of 6 input parameters and 5 output results for 13 calculations. The last run made (number 13) is for a rectangular line profile. The calculations included 15 of the 19 electronic band systems for diatomic molecules shown in the **template.input** file in figure 9(b). The OH band system is not included because it is not included in the **los.data** file used.

The six input options tabulated are:

1. The type of flow. The options used are either Boltzmann, B, or nonBoltzmann, nonB. nonBoltzmann means the QSS code in subroutine **qssm** is used to calculate the electronic state populations.
2. The value entered for **ipeak**.
3. The spin multiplicity. All band systems are treated as singlets, Singlet, or all treated correctly, Correct.
4. The branches spread into spectrum. All branches, All, or just the major branches, Major. The major branches are those where  $\Delta J = \Delta N$  (refs. 13 and 14).
5. The **vvExtend** value. Either 0.0 or 50.0 Angstroms.
6. The **Nmax** value. Either 0 or 50.

Descriptions of these parameters are given under Line10 in the previous subsection. The effects for input options 1, 3, and 4 also apply to IR diatomic systems.

The five output results tabulated are:

1. The total time in seconds needed to complete the run,  $t_{\text{tot}}$ .
2. The time in seconds needed to calculate and spread the rotational lines,  $t_{\text{lines}}$ .
3. The number of rotational lines calculated,  $N_{\text{calc}}$ , in thousands of lines.
4. The number of rotational lines spread into the spectrum,  $N_{\text{spread}}$ , in thousands of lines.
5. A radiative heating rate at the end of the line-of-sight [ $\text{W}/\text{cm}^2$ ],  $\text{RadH}$ , calculated by multiplying the specific intensity by  $2\pi$  steradians and integrating over wavelength. These heating rates, as noted above, are intended only to provide values for comparison purposes and are not considered to be a correct integration over solid angle and wavelength.

More lines are calculated than spread because the test for keeping the rotational lines within the spectral range occurs after the integrated line emissions are calculated. This may seem inefficient, but placing this test within the loop over rotational lines destroys the ability of the CRAY computer to vectorize the code. Without vectorization the computer time required increases substantially. For all of the cases shown in table 5, the radiative heating rate values for both the optically thin and absorption cases were equal. Thus, only one heating rate value is shown for each calculation.

Table 5. Effect of options for electronic diatomic systems

	Flow	IPEAK	Spin	Brn	vvExt [Ang]	Nmax	$t_{\text{tot}}$ [s]	$t_{\text{lines}}$ [s]	$N_{\text{Calc}}$ [ $\times 10^{-3}$ ]	$N_{\text{spread}}$ [ $\times 10^{-3}$ ]	RadH [ $\text{W}/\text{cm}^2$ ]
1	B	-9	Singlet	Major	0.0	0	4.62	2.34	515	445	0.1244
2	nonB	-9	Singlet	Major	0.0	0	4.52	2.34	515	445	0.1505
3	B	-9	Correct	Major	0.0	0	7.20	4.92	1120	991	0.1235
4	B	-9	Correct	All	0.0	0	14.00	11.72	2742	2473	0.1244
5	B	-20	Correct	Major	0.0	0	7.44	5.36	1457	1018	0.1236
6	B	-5	Correct	Major	0.0	0	6.73	4.45	998	891	0.1235
7	B	-3	Correct	Major	0.0	0	5.28	3.00	661	581	0.1233
8	B	-2	Correct	Major	0.0	0	3.40	1.11	229	181	0.1198
9	B	-1	Correct	Major	0.0	0	2.61	0.32	24	17	0.0947
10	B	0	Correct	Major	0.0	0	2.53	0.23	0	0	0.0
11	B	-9	Correct	Major	50.0	0	6.95	4.67	1021	975	0.1232
12	B	-9	Correct	Major	0.0	50	4.50	2.23	459	398	0.0588
13	B	-9	Correct	Major	0.0	0	3.52	1.24	1120	991	0.1235

Conclusions from an examination of table 5 are:

The first four rows compare the effects of Boltzmann flow, nonBoltzmann flow, spin multiplicity, and number of branches.

1. The calculation for nonBoltzmann flow, shown in row 2, runs slightly faster than the identical Boltzmann flow calculation, shown in row 1. The QSS method usually requires more, not less, time to calculate. The opposite effect may occur here because the Boltzmann calculation calls the partition function routine (function `qevr`) more frequently than does the QSS method. Also, the nonBoltzmann heating rate value in row 2 is almost 20% greater than the Boltzmann result in row 1. This means that some excited electronic states have higher populations under the QSS method than under the Boltzmann method.
2. The effect of using the singlet spin multiplicity for all band systems, rather than the correct spin multiplicity, is shown by comparing the results in rows 1 and 3. The calculated radiative heating rates in column 12 are nearly identical, but the number of lines calculated and spread into the spectrum (columns 10 and 11) for the correct multiplicities is more than twice that for the singlet approximation. The greater number of lines accounts for the increase in time required to calculate and spread the lines from 2.35 to 4.92 seconds (column 9) and for the 50% increase in the run time,  $t_{\text{tot}}$ , from 4.62 to 7.20 seconds shown in column 8.
3. The effect of including all of the branches in the calculation, compared to including only the major branches, is found by comparing the results in row 4 and row 3. The radiative heating rates are nearly identical in this case, but the number of lines calculated and spread for all branches, is about 2.5 times that for major branches only (columns 10 and 11). The run time, for all branches is also nearly double that for the major branches (column 8). Thus, nearly 60% of the rotational lines are very weak and need not be included in a calculation unless fine spectral detail is required.

Rows 5 to 10 in the table, plus row 3, show the effect of `ipeak` on the run time and the radiative heating rate.

4. The effect of changing `ipeak` (see Line10 in previous subsection for discussion of `ipeak`) is shown by examining rows 3 and 5–10. A better illustration of the effect on run time is shown in figure 15. In this figure the run time minus a “base” time is plotted against `ipeak`. The code does not run with `ipeak` = 0, as all bands would be skipped in the calculation. However, an equivalent time for a case with `ipeak` = 0 was found by running with `ipeak` = -9 and inserting an if-statement in the code to skip over all bands in subroutine `vuvl`. Figure 15 shows that the time to calculate the rotational lines and spread them in the spectrum is reduced by about 75% when `ipeak` is changed from -9 to -2.

The effect of using low absolute values of `ipeak` on the run time is substantial when large numbers of lines are calculated, i.e., cases with many band systems and many layers in the `los.data` file.

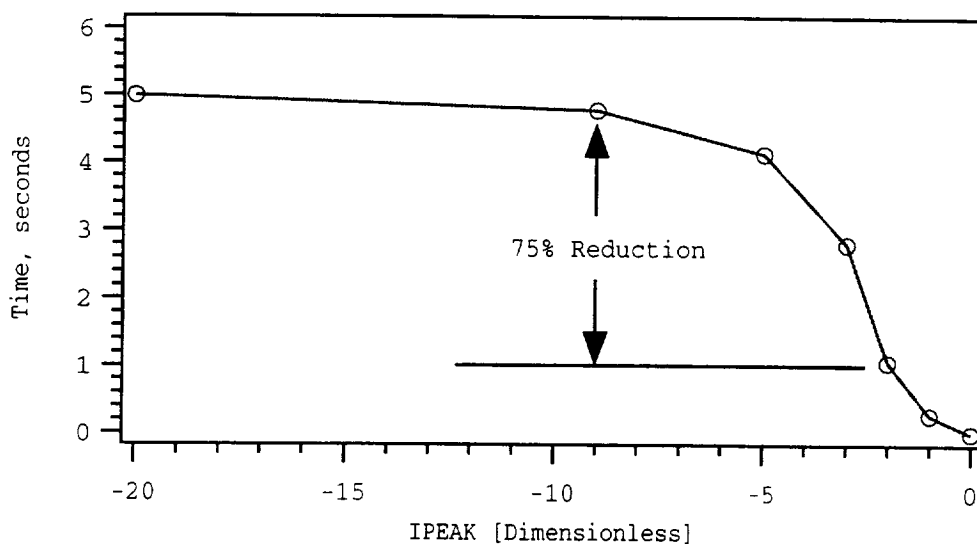


Figure 15. Effect of the IPEAK option on the time to calculate and spread the rotational lines.

The effect on the spectrum of setting  $\text{ipeak} = -2$  is shown in figure 16. The upper spectrum plotted with a solid line is considered to be the “correct” spectrum. It is for the case shown in row 4 in table 5, which includes the correct spin multiplicities and all branches. The spectrum plotted with a dotted line is the spectrum for  $\text{ipeak} = -2$ . The spectrum plotted with a dashed line is for the Nmax option, which is discussed below.

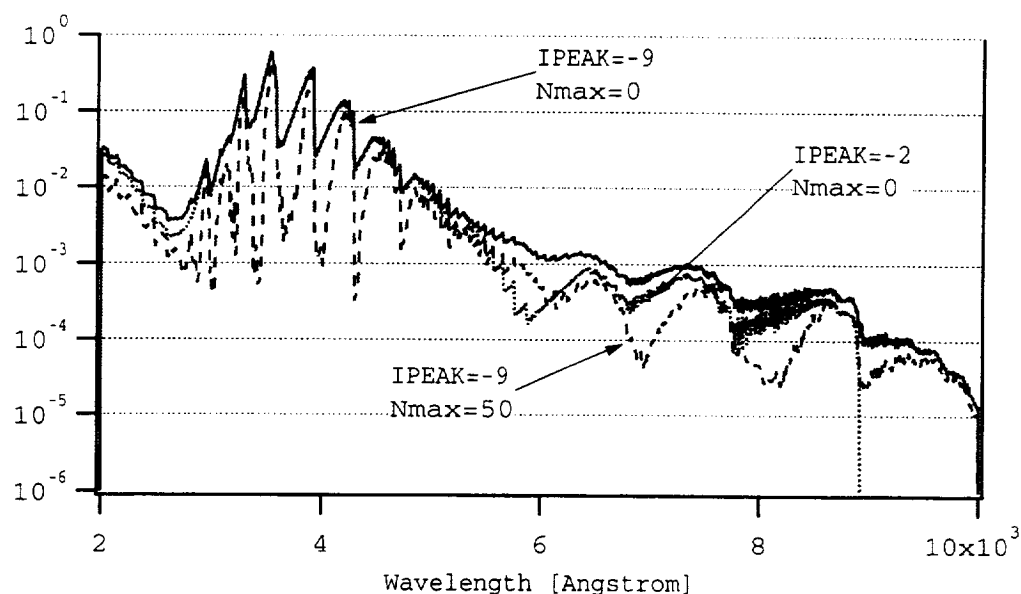


Figure 16. Electronic diatomic spectra for testing effect of IPEAK and Nmax options.

Although the radiative heating for the  $i_{\text{peak}} = -2$  case is only about 2% less than that for  $i_{\text{peak}} = -9$  (compare column 12 for rows 4 and 8), the spectrum loses its correct shape in the valleys between the bands when the intensity is low. Notice that the group of bands on the right side of the figure have dropped out of the calculation altogether. The strong bands are present, however, and the spectrum is valuable for preliminary analysis and requires less computer time to run.

The last three rows in table 5 show the effects of using the `vvExtend`, `Nmax`, and rectangular line shape options.

5. The effect of reducing the number of vibrational bands in the calculation by using `vvExtend` [Angstrom] is shown in the table by comparing row 11 with row 3. This option eliminated all bands whose band origins [Angstrom] are more than 50.0 Angstroms beyond the wavelength range of the calculation, i.e., less than 1950 Angstroms or greater than 10,050 Angstroms.

The time to calculate the lines with `vvExtend` = 50 is only about 5% less than that for row 3, and the radiative heating rate is reduced even less. However, this option preferentially reduces the intensity of the spectrum near the ends of the spectral range. The reduction in this case is only about 8% at 2000.0 Angstroms. The reduction of the computer run time and the radiative heating can be significant when the spectral range is small, and strong vibrational bands are eliminated because their band origins lie just outside of the range. The calculated spectrum for this option is not plotted in figure 16 because of the small change from the `vvExtend` = 0 case shown by the solid line.

6. The effect of changing the value of `Nmax`, the maximum number of rotational lines allowed in each branch, is shown by comparing row 12 with row 3 in table 5. A value of `Nmax` = 0 includes all of the rotational lines in each vibrational band until rotational dissociation occurs. Clearly, using a low value of `Nmax`, but one that is greater than 0, speeds the calculation. However, the calculated radiative heating rate also drops by over 50%, so one needs to use this option with caution.

The effect that a low value of `Nmax` has on the spectrum is shown in figure 16. The upper spectrum in this figure, as noted above, is considered to be very close to the correct spectrum. The dashed spectrum is for `Nmax` = 50, which means that only the lowest 50 rotational lines are included in the calculation. The general shape of the spectrum shows that bands are truncated fairly close to the band heads. This effect makes the spectrum appear to have a large variation in intensity, although the peak heights of the stronger bands are in good agreement with those for the correct spectrum. Thus, one can use a low absolute value of `Nmax` to get a good, preliminary look at the strongest radiating systems while using less computer time. Another example of using the `Nmax` option is shown in figure 6, where only the first few rotational lines in the  $\text{C}_2$  Swan (0,0) band were calculated.

7. The effect of using a rectangular line profile spread uniformly over 4 spectral intervals, or 5 grid points, is seen by comparing row 13 with row 3 in table 5. The comparison can only be made with optically thin spectra because the absorption case is not calculated for rectangular lines. The rectangular shape is not realistic and calculated absorption values would be meaningless. Fortunately, for the calculations in table 5 the flow is nearly optically thin, as noted in the paragraph just prior to table 5. Thus, all radiative heating rate results with absorption, given in the table, are equal to the optically thin results, and a comparison is possible.

The time to calculate the lines and spread them into the spectrum is significantly less for the rectangular line shape, with a saving of 3.68 seconds or 75% (comparing column 8 and column 9 between rows 3 and 13). The quality of the spectrum produced by the rectangular line profile in this case is illustrated in figure 17. Comparing this spectrum with the upper spectrum in figure 16 shows that they are very similar at the fairly low spectral resolution for these cases, and that mean values along the spectrum are nearly identical. The rectangular line spectrum appears to have higher resolution than the Gaussian line spectrum, but resolution is difficult to define for rectangular lines. The differences in the spectra will be quite pronounced at high resolution, of course.

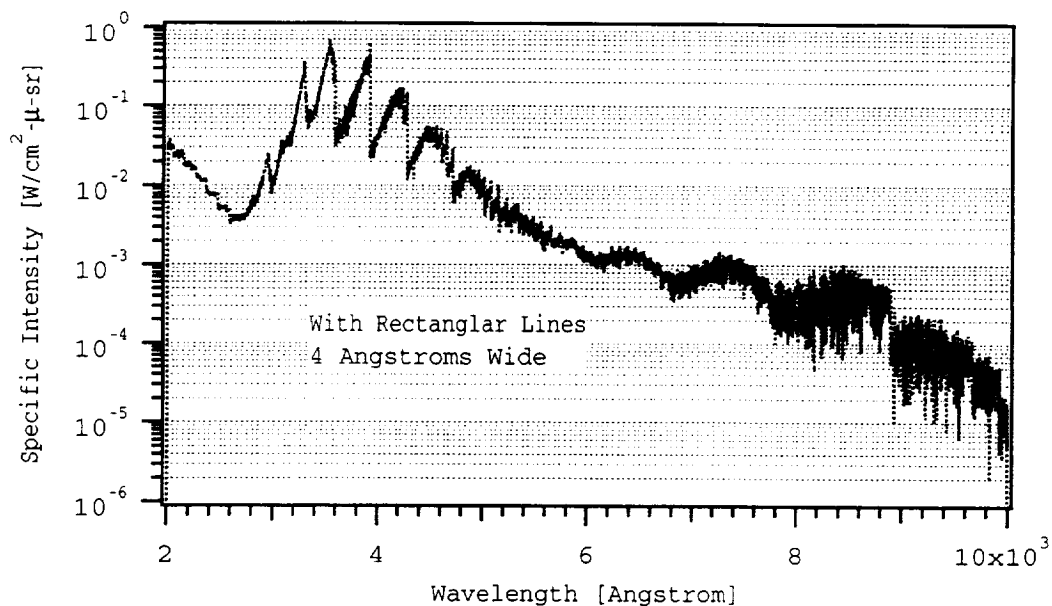


Figure 17. Electronic diatomic spectra for testing effect of rectangular line shape option.

### Part 3. Brief Statement About the Output File and Plot Files

The information contained in the **Output** file identifies the type of run made and presents results related to the radiative heating rate. The three sample cases discussed in Appendix J show in detail the various kinds of information contained in the **Output** file. The sample cases are:

- Sample case 1. Uses the line-of-sight option and includes two scans over a calculated spectrum.
- Sample case 2. Uses the stagnation point and the spherical cap model options to calculate the radiative heating rate at the stagnation point.
- Sample case 3. Uses the shock tube and equilibrium options. It includes two regions, with an incident spectrum in region 2, and uses calculated Voigt line profiles for the line shapes.

The radiative heating rates per steradian [ $\text{W}/\text{cm}^2\text{-sr}$ ] for both an absorbing and an optically thin gas along the line-of-sight are printed at the grid points for both the stagnation point and line-of-sight options. Also, for the stagnation point option only, the total radiative heating rate at the stagnation point and the distribution of the total radiative heating rate, as a function of angle from the stagnation streamline, are printed.

The optically thin heating rates [ $\text{W}/\text{cm}^2$ ] at the grid points in the **los.data** file are calculated for all cases, except the "scan only" option. These approximate heating rates are found by using the infinite slab approximation and summing the integrated power density of all lines and continua in each layer along the line-of-sight. These values are tabulated near the end of the **Output** file. This is the only heating rate calculation made if the "don't create" a spectrum option is selected. A good check on whether a spectral calculation is consistent with the approximate heating rate value [ $\text{W}/\text{cm}^2$ ] is to multiply the optically thin heating rate value [ $\text{W}/\text{cm}^2\text{-sr}$ ] (mentioned in the prior paragraph) printed for the last grid point of the line-of-sight by  $2\pi$  and compare this value to the approximate value printed in the last line of the **Output** file, in the rightmost column.

For the shock tube option, the spectral regions, timing gates for each region, and average heating rates [ $\text{W}/\text{cm}^2\text{-sr}$ ] for each gate are printed. The calculation of these values is performed in subroutine **transport**. An effective emission value [ $\text{W}/\text{cm}^3\text{-sr}$ ] for each gate is also found by dividing the average heating rate for the gate by the shock tube width. This calculation is performed in subroutine **acontrol**.

When the equilibrium option is selected, the equilibrium gas properties and species number densities are printed in the **Output** file. If the shock tube option is also selected, the equilibrium gas properties in the free stream and behind the shock wave are both printed.

The plot files are the principal output from the code. They are generated for all options, except the "don't create" a spectrum option. Specific intensity spectra [ $\text{W}/\text{cm}^2\text{-}\mu\text{-sr}$ ] for an absorbing and an optically thin gas are written to the plot files for the line-of-sight and stagnation point options. However, if the rectangular line shape option is selected, only the optically thin results are printed.

The line-of-sight and stagnation point options print the two spectra in three columns. The first column is the wavelength in Angstroms or nm, or the wavenumber in  $\text{cm}^{-1}$ ; the second column is the specific intensity with absorption; and the third column is the specific intensity for an optically thin gas.

The shock tube option prints 4 time averaged specific intensity spectra in 5 columns for each timing gate:

Column 1. The wavelength or wavenumber of the spectral points.

Column 2. The spectrum with absorption.

Column 3. A Planck function if a temperature is entered or the equilibrium option is selected.

Column 4. The spectrum with absorption, but without the incident spectrum included.

Column 5. The optically thin spectrum without the incident spectrum included.

The calculated spectra for up to 10 regions or timing gates are written to tape units 21 to 30. The scanned spectra, if calculated, are written to tape units 31 to 40. The tape unit number for a scanned spectrum is 10 greater than the tape unit number of the original spectrum. Also, the **scan.data** files are printed in the **Output** file, when the scan option is selected.

The code is presently formatted to scan only the first spectrum at the left side of the plot file. For the shock tube option, this is the time averaged specific intensity over the timing gate. The spectrum that is scanned can be changed by changing the appropriate write format statements in subroutine **transport** and read format statements in subroutine **bandpass**.

## Appendix A

### Radiation

This appendix is organized in four parts:

- Part 1. Bound-bound radiation.
- Part 2. Bound-free radiation.
- Part 3. Free-free radiation.
- Part 4. Brief comments about the use and validity of a nonequilibrium absorption coefficient.

#### Part 1. Bound-Bound Radiation

There are three radiative mechanisms operating at all times in a radiating medium: spontaneous emission, stimulated emission, and absorption. Scattering also occurs, but it is not included in NEQAIR96 and is not discussed. Spontaneous emission, as its name implies, is based on an “uncaused” process, defined as the probability per particle per second,  $A_{UL}$  [ $s^{-1}$ ], that a transition will occur from an upper energy level,  $E_U$  [ $cm^{-1}$ ], to a lower energy level,  $E_L$  [ $cm^{-1}$ ], and a photon will be emitted. The expression for the radiant power density emitted by spontaneous emission from a unit volume of gas, under isotropic and unpolarized conditions, in the direction of a line-of-sight is

$$E = g_U N_U A_{UL} hc \bar{\nu}_{UL} / 4\pi \quad [W/cm^3-sr] \quad (A1)$$

where  $N_U$  [ $cm^{-3}$ ] is the population (number density) of a nondegenerate upper level;  $h$  [J-s] is Planck's constant;  $c$  [cm/s] is the speed of light; and  $\bar{\nu}_{UL} = (E_U - E_L)$  [ $cm^{-1}$ ] is the energy, or wavenumber, of the transition and of the emitted photon. The group of factors “ $hc \bar{\nu}_{UL}$ ” [J] also gives the energy of the photon. The wavelength,  $\lambda$  [Angstrom], of the emitted photon is given by  $\lambda = 10^8 / \bar{\nu}_{UL}$ .

The spectral spontaneous emission in a specified direction is found by multiplying the emitted power density by a line shape function,  $\phi_\lambda$  [ $\mu^{-1}$ ], that is,

$$E_\lambda = g_U N_U A_{UL} hc \bar{\nu}_{UL} \phi_\lambda / 4\pi \quad [W/cm^3-\mu-sr] \quad (A2)$$

where  $\phi_\lambda$  is normalized so that its integral over all wavelengths is 1.0.

As soon as a photon is emitted it begins to move away from the emission point at the speed of light. The emitted photons encounter other atoms and molecules as they move, and some of the photons are absorbed. Others stimulate the emission of additional photons that are emitted with the

same energy and direction as the stimulating photons. All photons moving away from a point, within a small cone, that cross a plane surface produce a spectrum of the radiant energy flux  $[(J/cm^2-\mu-sr)/s]$  or  $[W/cm^2-\mu-sr]$  hitting the plane from the direction of the point. This is the quantity that NEQAIR96 is designed to calculate. It is referred to herein as the “specific intensity,”  $I_\lambda$ , but is also referred to in the literature as the spectral radiance. The specific intensity is found by integrating the radiative transport equation along the path the photons travel, as described later in this appendix.

Stimulated emissions and absorptions, unlike spontaneous emissions, are “caused” by the presence of photons in the neighborhood of the emitting or absorbing species. The greater the density of the photons with the correct wavelength (spectral radiant energy density  $[J/cm^3-\mu]$ ) the faster the rate of stimulated transitions. The Einstein coefficients for stimulated emission and absorption,  $B_{UL}$  and  $B_{LU}$ , reflect this dependence and are expressed in units of  $[1/(J/cm^3-\mu)-s]$ .

The spectral radiant energy density of the photons can be written as

$$\rho_\lambda = \int_0^{4\pi} I_\lambda / c \, d\Omega \quad [J/cm^3-\mu] \quad (A3)$$

where  $I_\lambda$  is the local specific intensity  $[W/cm^2-\mu-sr]$  in a direction and  $c$  is the speed of light  $[cm/s]$ .

The expressions for the spectral power densities emitted and absorbed by stimulated transitions in a specified direction in terms of  $B_{UL}$  and  $B_{LU}$  are

$$\begin{aligned} E_\lambda(\text{emitted}) &= g_U N_U B_{UL} (I_\lambda / c) hc \bar{\nu}_{UL} \phi_\lambda \\ &= C_\lambda(\text{emitted}) I_\lambda \quad [W/cm^3-\mu-sr] \quad (A4) \end{aligned}$$

$$\begin{aligned} E_\lambda(\text{absorbed}) &= g_L N_L B_{LU} (I_\lambda / c) hc \bar{\nu}_{UL} \phi_\lambda \\ &= C_\lambda(\text{absorbed}) I_\lambda \quad [W/cm^3-\mu-sr] \quad (A5) \end{aligned}$$

where the line shape functions,  $\phi_\lambda$ , for stimulated emission and absorption are assumed to be identical to that for spontaneous emission. The  $C_\lambda$  factors in these equations contain all factors except  $I_\lambda$ , and are defined as appropriate volumetric stimulated emission and absorption coefficients  $[cm^{-1}]$ .

The Einstein A and B coefficients (ref. 43) are related to each other and are fundamental properties for each transition. The relationships between them can be found under equilibrium conditions and then applied universally. Under equilibrium the specific intensity is given by the Planck (Black Body) function:

$$B_\lambda = c_1 / (\pi 10^4 \lambda^5 (e^{c_2 \bar{\nu}/T} - 1)) \quad [W/cm^2-\mu-sr] \quad (A6)$$

where

$$c_1 = 2\pi hc^2 = 3.7405 \cdot 10^{-12} \quad [\text{W cm}^2] \quad (\text{A7})$$

is the first radiation constant and

$$c_2 = hc/k = 1.43879 \quad [\text{cm K}] \quad (\text{A8})$$

is the second radiation constant. The wavelength,  $\lambda$  in equation A6, is in units of [cm], and the  $10^4$  factor converts one of the cm's to  $\mu$ 's to provide the spectral interval for the specific intensity per micron [ $\mu^{-1}$ ]. The principle of detailed balance in equilibrium states that the rates of exchange of any process between two energy levels must be equal. For the optical processes described here, the sum of the spontaneous and stimulated emission rates from the upper to the lower level in a given direction must be equal to the absorption rate from the lower to the upper level in the same direction. Thus,

$$g_U N_U A_{UL}/4\pi + g_U N_U B_{UL}(B_\lambda/c) = g_L N_L B_{LU}(B_\lambda/c) \quad [1/\text{cm}^3\text{-s-sr}] \quad (\text{A9})$$

At equilibrium the Boltzmann expression gives the ratio of the populations of two nondegenerate levels as

$$N_U/N_L = e^{-c_2 \bar{\nu}_{UL}/T} \quad (\text{A10})$$

Also, the Planck function does not change appreciably over the width of a line, so that the exponential factor in equation A6 can be written as  $N_L/N_U$ , and the Planck function is expressed as

$$B_\lambda = 2hc^2/(10^4 \lambda^5 (N_L/N_U - 1)) \quad [\text{W/cm}^2\text{-}\mu\text{-sr}] \quad (\text{A11})$$

which enables the relationships between the Einstein A and B coefficients to be expressed as (ref. 13)

$$A_{UL} = 8\pi hc/(10^4 \lambda^5) B_{UL} \quad [1/\text{s}] \quad (\text{A12})$$

$$g_U B_{UL} = g_L B_{LU} \quad [1/(\text{J/cm}^3\text{-}\mu\text{-s})] \quad (\text{A13})$$

As noted above,  $\lambda$  in equations A11 and A12 is expressed in cm, and the factor of  $10^4$  converts one of the cm's to  $\mu$ 's. These expressions relate fundamental atomic properties that hold for any thermodynamic condition.

The local, or point, radiation properties discussed above are critical factors in the analysis of the radiation field, and of radiative transport as the photons move away from the local emission point. Perhaps the most familiar equation of radiative transport is Lambert's law, which is usually referred to as Bouguer's law (ref. 49) or Beer's law (ref. 50). (See ref. 51.) This law describes the decrease in the specific intensity of a beam passing through a nonemitting layer of gas with constant properties, i.e.,

$$I_{\lambda}(x) = I_{\lambda}(0)e^{-\alpha_{\lambda}x} \quad (\text{A14})$$

where  $I_{\lambda}(x)$  is the specific intensity at location  $x$  [cm] and  $\alpha_{\lambda}$  [ $\text{cm}^{-1}$ ] is the volumetric absorption coefficient. This equation is a solution of the differential equation of radiative transport without emission along the light path. The situation in NEQAIR96 is slightly more complicated, as the gas also emits radiation along the path through a series of layers, each with constant properties. The one-dimensional form of the differential radiative transport equation for this case is written as (ref. 44)

$$dI_{\lambda}/dx = -\alpha_{\lambda}(I_{\lambda} - B_{\lambda}) \quad (\text{A15})$$

where  $\alpha_{\lambda}$  is the effective volumetric absorption coefficient that includes stimulated emission and absorption.

The integration of this equation across a layer of gas with constant properties gives

$$I_{\lambda}(x) = I_{\lambda}(0)e^{-\alpha_{\lambda}x} + B_{\lambda}(1 - e^{-\alpha_{\lambda}x}) \quad (\text{A16})$$

The effective volumetric absorption coefficient in this equation can be written in terms of the stimulated emission and absorption coefficients given in equations A4 and A5 as

$$\alpha_{\lambda} = \{C_{\lambda}(\text{absorbed}) - C_{\lambda}(\text{emitted})\} \quad (\text{A17})$$

which can be manipulated to give

$$\alpha_{\lambda} = (g_L N_L B_{LU} - g_U N_U B_{UL}) h \bar{\nu}_{UL} \phi(\lambda) \quad (\text{from eqs. A4 and A5})$$

$$= (N_L/N_U - 1) g_U N_U B_{UL} h \bar{\nu}_{UL} \phi(\lambda) \quad (\text{from eq. A13})$$

$$= (N_L/N_U - 1) g_U N_U A_{UL} 10^4 \lambda^5 / (8\pi hc) h \bar{\nu}_{UL} \phi(\lambda) \quad (\text{from eq. A12})$$

$$= (N_L/N_U - 1) E_{\lambda} / (B_{\lambda}(e^{c^2 \bar{\nu}/T} - 1)) \quad (\text{from eqs. A2 and A6})$$

and finally, using equation A10, the expression for the effective volumetric absorption coefficient, which includes the effects of stimulated emission and absorption, is written as

$$\alpha_{\lambda} = E_{\lambda}/B_{\lambda} \quad (\text{A18})$$

This equation expresses Kirchhoff's law (ref. 52) that the ratio of emission to absorption at any surface under equilibrium conditions is the Planck function. Its applicability for nonequilibrium conditions is discussed later in this appendix.

The principal equations used in NEQAIR96 to calculate atomic and rotational line spectra are

1. Equation A2      For spontaneous emission.
2. Equation A16      For the one-dimensional equation of radiative transport.
3. Equation A18      For the effective volumetric absorption coefficient. Equation A18 is also used to calculate the bound-free and free-free continuum emission spectrum,  $E_\lambda$ , from tabulated absorption coefficients.

## Part 2. Bound-Free Radiation

Bound-free continuum radiation is calculated from absorption cross sections per particle for the photo ionization of neutral atoms. This calculation is done in subroutine **bfcont**. It is assumed that the translational energy mode of the free electrons is described by the electronic temperature entered in the **los.data** file. The absorption cross sections,  $\sigma_\lambda$  [ $\text{cm}^2$ ], are defined for the process of ejecting an electron by the absorption of a photon, in terms of the energy (or wavelength) of the absorbed photon. These data are given in reference 45 and are approximated in NEQAIR96 by the product of the cross section for the hydrogen atom multiplied by a correction factor called the gaunt factor. The hydrogenic cross sections are given by Kramers' formula (see page 265 in ref. 53) as

$$\sigma_{\lambda H} = 7.9 \cdot 10^{-18} n (\lambda/\lambda_n)^3 \quad [\text{cm}^2] \quad (\text{A19})$$

where  $n$  is the principal quantum number of the atomic energy level, and  $\lambda_n$  is the maximum wavelength [Angstrom] (minimum energy) of a photon capable of removing an electron from the  $n^{\text{th}}$  energy level. The value of  $\lambda_n$  can be expressed as  $n^2 10^8 / I_H$ , where  $I_H$  is the ionization potential of atomic hydrogen, that is,  $109,679 \text{ cm}^{-1}$ .

The gaunt factors (ref. 1) are determined by comparing the cross sections in reference 45 to those for the hydrogen atom for each energy level in terms of the photon energy from 0.0 to 0.45 Rydberg in steps of 0.05 Rydberg (note,  $1.0 \text{ Rydberg} = 109737.31 \text{ cm}^{-1}$ ). The gaunt factor data for the bound-free process are entered in the **radiation.data** file. The bound-free volumetric absorption coefficient for each energy level is then found by multiplying the cross section by the population of the energy level, i.e.,

$$\alpha_{\lambda_i}^{\text{b-f}} = \text{gaunt } \sigma_{\lambda H} N_i \quad [\text{cm}^{-1}] \quad (\text{A20})$$

The bound-free emission is calculated from  $\alpha_{\lambda}^{\text{b-f}}$  using equation A18 and the Planck function as shown in equation A11. In this case  $N_U$  is taken as the population of an imaginary level, located at the ionization potential. This population is found from the Saha equation (ref. 46) as

$$N_U = 2.07 \cdot 10^{-16} N_{\text{ion}} N_e / (Q_{\text{ion}} T_e^{1.5}) e^{-c2(E_{\text{ion}})/T_e} \quad (\text{A21})$$

where  $N_{\text{ion}}$  is the total number density of the first positive atomic ion,  $N_e$  is the electron number density,  $Q_{\text{ion}}$  is the electronic partition function of the ion,  $E_{\text{ion}}$  is the ionization potential [ $\text{cm}^{-1}$ ], and  $T_e$  [K] is the electronic temperature entered with the line-of-sight data. The lower state population,  $N_L$  is the population of the energy level,  $E_i$  associated with  $\alpha_\lambda$ . However, the population of the lower level must be greater than the population of the fictitious level located at the ionization threshold. This in effect restricts the effective temperature between these two levels to be finite. The bound-free spectral emission is then found from equation A18

$$E_\lambda^{b-f} = \alpha_\lambda^{b-f} B_\lambda \quad (\text{A22})$$

which is added into the emission array.

The above procedure is also used in the process of calculating the optical bound-free rate coefficients used in the atomic QSS calculation. In that process, the emission intensity for transitions to each bound state is divided by the photon energy to get the rate that photons are emitted, as a function of wavelength. The rate at which photons are emitted is, of course, equal to the rate at which electrons enter the bound state. These rates are then integrated over wavelength and divided by the electron and atomic ion number densities, to get the effective optical recombination rate coefficients. This process gives results that are in good agreement with the rate coefficients given in reference 47, which were used in the earlier versions of NEQAIR.

### Part 3. Free-Free Radiation

The free-free radiation for neutral, singly ionized, and doubly ionized atoms is also calculated from tabulated absorption cross section from reference 45 in terms of the energy of the photons,  $e_p$  [Rydberg]. These calculations are done in subroutine **ff.cont**. The process is similar to that for bound-free radiation, except that the radiation is caused only by the electrons, and the electrons are assumed to be in thermal equilibrium with the electron temperature entered with the line-of-sight data. Further, hydrogenic-like free-free cross sections are used as a basis for all of the cross sections. and then corrections are applied to these hydrogenic data to get the cross sections for other atoms and their ions.

The hydrogenic-like cross sections,  $\sigma_{\lambda H}$ , for neutral, singly ionized, and doubly ionized species are tabulated in reference 45. These cross sections were found to be reproduced within about 2% with the following expression:

$$\sigma_{\lambda H} = (a_1/e_p + a_2)10^{-40}/e_p^3 \quad [\text{cm}^5] \quad (\text{A23})$$

where  $a_1$  and  $a_2$  are functions of temperature and degree of ionization only. For the neutral atom

$$a_1 = 0.006805 - 0.00934 e^{-1.16 \cdot 10^{-4} T_e} \quad (\text{A24})$$

$$a_2 = 0.508 + 1.046 e^{-5.77 \cdot 10^{-4} T_e} + 1.85 e^{-3.43 \cdot 10^{-4} T_e} \quad (\text{A25})$$

The corrections to the hydrogenic-like cross sections are in terms of the photon energy and the electronic temperature. The correction data are entered in block data **ffdata** for the seven energy values of 0.025, 0.050, 0.10, 0.15, 0.20, 0.25, and 0.30 Rydberg and for several electronic temperatures at each of these energy values. The temperatures range from a value of  $T_{\text{low}}$  to a value of  $T_{\text{high}}$  in 1000 K intervals. As examples, the values of  $T_{\text{low}}$  and  $T_{\text{high}}$  for the neutral C atom are 4000 to 36,000 K, and for neutral N and O are 10,000 to 48,000 K. The data are entered in block data **ffdata** rather than in subroutine **ffcont** to keep this subroutine easier to read.

The tabulated correction values are interpolated and extrapolated where necessary on temperature and photon energy to arrive at the correction factor, **dd**, that is applied to the hydrogenic cross sections.

The free-free cross sections of any atom and ionization are then given by (ref. 45)

$$\sigma_{\lambda}^{\text{f-f}} = (N_{\text{ion}} N_{\text{e}} / N_{\text{a}}) \sigma_{\lambda\text{H}} (1 + \mathbf{dd}) \quad [\text{cm}^2] \quad (\text{A26})$$

where here  $N_{\text{ion}}$  is the number density of the first ion above the ionization of  $N_{\text{a}}$ .  $N_{\text{a}}$  is the number density of the neutral atom, singly ionized atom, or doubly ionized atom as appropriate. The correction factor, **dd**, is defined in the prior paragraph.

The absorption coefficient for free-free radiation, as for the bound-free radiation, is found by multiplying  $\sigma_{\lambda}^{\text{f-f}}$  by the appropriate species concentration of the deflecting atom. For free-free radiation the appropriate concentration is the species concentration,  $N_{\text{a}}$ , which cancels the same factor in equation A26. The neutral free-free absorption coefficient is then given by

$$\alpha_{\lambda}^{\text{f-f}} = N_{\text{ion}} N_{\text{e}} \sigma_{\lambda\text{H}} (1 + \mathbf{dd}) \quad [\text{cm}^{-1}] \quad (\text{A27})$$

The free-free emission is calculated from  $\alpha_{\lambda}^{\text{f-f}}$  using equation A18 and the Planck function as shown in equation A6, at the electronic temperature entered with the line-of-sight data, i.e.,

$$E_{\lambda}^{\text{f-f}} = \alpha_{\lambda}^{\text{f-f}} B_{\lambda} \quad (\text{A28})$$

which is added into the emission array.

## Part 4. Nonequilibrium Absorption Coefficient

The use of a volumetric “nonequilibrium” absorption coefficient is believed to be valid for many cases encountered in atmospheric entry, ballistic ranges, shock tubes, and arc jet facilities. Clearly, when the state of a gas is not in thermal equilibrium, it cannot be described by a single temperature. However, for any particular atomic or rotational line equation A11 shows that the population ratio,  $N_{\text{L}}/N_{\text{U}}$ , can replace the exponential term in the Planck function.

In this form, the Planck function expresses the equilibrium radiation field at  $\lambda$ , only if all transitions producing photons with a wavelength of  $\lambda$  have the same temperature or population ratio,

$N_L/N_U$ , and if the state populations are at least quasi steady. The populations must be nearly steady to give the radiation field at  $\lambda$  the opportunity to become equilibrated with the transitions occurring at  $\lambda$ . For equilibrium, these criteria are true for all wavelengths. But for thermal nonequilibrium the case is not so simple. Thus, one cannot simply form the total emission spectrum over a wavelength range and divide it by a single Planck function. In the code, the spectral absorption coefficient is calculated separately for each line and it is then added into the spectrum of the total absorption coefficient. But this process is not valid if the rate at which the state populations are changing is faster than the optical transition rates.

The following four statements are given to support the contention that the effective volumetric absorption coefficient, developed in the line-by-line manner mentioned above, seems plausible for many applications where the flow is not in equilibrium.

1. Most atomic and rotational lines are very narrow when looked at in high resolution. That is, most of them do not overlap with other lines. Thus, if the radiation field near a particular wavelength is affected primarily by emission and absorption processes of a single line, then the Planck function in a narrow wavelength interval that contains most of the line is defined by  $N_L/N_U$  for the two energy levels involved. This procedure would not be valid if the photons that are absorbed at the line wavelength are spread to remote wavelengths during a re-emission process. A strong spreading process quickly broadens the lines into continuum bands. As this effect is not observed in the applications mentioned above, the use of a single Planck function for isolated lines seems a good approximation.
2. Atomic and rotational lines do overlap significantly in some cases. Examples of overlapping lines are: groups of hyperfine lines produced by nuclear spin, atomic multiplets, spin multiplets involving two  $\Sigma$  states, lambda doublets involving two non $\Sigma$  states, and the bunching together of rotational lines near the turning point at band heads. However, in all of these cases, the  $N_L/N_U$  ratios are the same for the overlapping lines, as they have nearly the same wavelength and all have the same upper and lower electronic states.

Only one vibrational and one rotational temperature are entered for each layer in the **los.data** file, and these temperatures are used in the Planck distribution function to give the vibrational and rotational state populations for all diatomic species. This limitation implies that in NEQAIR96 the relative vibrational and rotational state populations in all electronic states are the same. Further, the same arguments hold for other groups of rotational lines in the same band system. Thus, the equilibrium radiation field for each of these groups of lines is assumed to be approximated by the Planck function in terms of  $N_L/N_U$ . These approximations are not valid for many nonequilibrium conditions, but at the present time, they at least provide a starting point from which more realistic population distribution functions can be devised to match experimental results.

3. Unrelated lines that overlap, or that overlap with one or more continua at the same wavelength, are potential problems. The  $N_L/N_U$  ratios for the lines and the electronic temperatures for the continua can be quite different. In the actual flow field the population ratios tend to adjust toward an equilibrium condition. However, in the code this is not possible because the radiation calculation is made after the excitation calculations are completed. The importance

of this effect is not known. However, often the spontaneous emission of one of the radiation sources is much stronger than the others, and the Planck function for the stronger source should be a good approximation to the equilibrium radiation field at the wavelength for that transition. The contributions of weaker lines with a different Planck function will not be handled correctly, but their effect on the total specific intensity should not be large.

4. When the radiation field is nearly optically thin, the spontaneous emission is weak relative to the Planck function, and the absorption coefficient is very small. The radiative transport is given to good accuracy by

$$I_{\lambda} = I_{\lambda}(0) + E_{\lambda}x \quad (\text{A29})$$

which does not contain the Planck function.



## Appendix B

### Einstein A Coefficients for Diatomic Rotational Lines

The large number of rotational lines in a diatomic band system makes the task of entering an Einstein A coefficient for each line in the radiation data base a tedious one at best. Rather, the transition probabilities are calculated as needed from a limited number of parameters. The allowed rotational transitions in NEQAIR96 are based on the electric dipole moment. The expression for  $A_{UL}$  under this condition is (ref. 10)

$$A_{UL} = (64\pi^4 \bar{\nu}_{UL}^3 / 3h) e a_0^2 R_e^2 q_{v_U v_L} S_{J_U J_L} / (2J_U + 1) \quad (B1)$$

where

$R_e$  [statcoul-cm] is the electronic transition moment for a vibrational band ( $v_U, v_L$ ) within a band system. It is normalized by  $e a_0 = 2.5416 \cdot 10^{-18}$  statcoul-cm, where  $e = 4.8030 \cdot 10^{-10}$  statcoul is the electron charge and  $a_0 = 5.29167 \cdot 10^{-9}$  cm is the Bohr radius.

$q_{v_U v_L}$  [dimensionless] is the Franck-Condon factor, also known as the “vibrational overlap integral squared” for transitions between the vibrational levels  $v_U$  and  $v_L$ .

$S_{J_U J_L}$  [dimensionless] is the Hönl-London factor, also known as the “rotational line intensity factor,” for transitions between the rotational levels  $J_U$  and  $J_L$ .

A more accurate value of  $A_{UL}$  is calculated by including the variation of the transition moment with internuclear distance in the integration over the vibrational wave functions, i.e.,

$$A_{UL} = (64\pi^4 \bar{\nu}_{UL}^3 / 3h) e a_0^2 |\langle v_U | R_e | v_L \rangle|^2 S_{J_U J_L} / (2J_U + 1) \quad (B2)$$

The band data needed to calculate  $A_{UL}$ , either  $R_e$  and  $q_{v_U v_L}$  or  $|\langle v_U | R_e | v_L \rangle|$ , are entered in the **radiation.data** file for each vibrational band. When the  $|\langle v_U | R_e | v_L \rangle|$  integral is used, it is entered in the field for  $R_e$  and the  $q_{v_U v_L}$  value is set to 1.0. The other data needed for each line in a band are the band origin, rotational energies and Hönl-London factors. The rotational energies and Hönl-London factors are calculated from the solution of the rotational matrices in subroutines **honl**, **solve**, and **diag**. The band origins are calculated from electronic and vibrational energy expressions (see Appendices C and F) or are entered in the **radiation.data** file.



## Appendix C

### Wavelengths for Diatomic Rotational Lines

The large number of rotational lines in a diatomic band system makes entering the wavelength for each line in the radiation data base a tedious task. Instead, they are calculated as needed from a limited number of parameters.

The wavelengths [Angstrom] of rotational lines are calculated from the energy values [ $\text{cm}^{-1}$ ] of the upper and lower levels, i.e.,

$$\lambda = 10^8 / \bar{\nu}_{UL} = 10^8 / (E_U - E_L) \quad [\text{Angstrom}] \quad (\text{C1})$$

The energy levels are determined from electronic, vibrational, and rotational contributions. The electronic and vibrational contributions for the upper and lower states are combined to give the band origin [ $\text{cm}^{-1}$ ]. The band origins are either calculated or entered in the **radiation.data** file. Entering the band origins is the more accurate method, as the calculated vibrational levels beyond the validity of the spectroscopic constants can result in significant errors.

The rotational energy contributions are calculated using the matrix method, except for four states of  $\text{H}_2$  where rotational and vibrational energy levels are entered in block data **enH2**. The matrix method formalism used is discussed in reference 18, which uses the Hund's case A matrix elements, from pages 54 and 55 of reference 13, in the basis matrix. The lambda doubling terms, however, are not included. Together the electronic, vibrational, and rotational contributions give the energy value as

$$E = T_e + G_v + F_J \quad [\text{cm}^{-1}] \quad (\text{C2})$$

where

$T_e$  is the electronic energy at the minimum of the potential energy curve for each electronic state. Zero energy is defined at the minimum of the ground state potential well.

$G_v$  is the vibrational energy measured from  $T_e$ .

$F_J$  is the rotational energy measured from  $G(v)$ .

and

$$\begin{aligned} G_v = & \omega_e(v + 1/2) - \omega_e x_e(v + 1/2)^2 + \omega_e y_e(v + 1/2)^3 + \omega_e z_e(v + 1/2)^4 \\ & + \omega_e a_e(v + 1/2)^5 + \omega_e b_e(v + 1/2)^6 + \omega_e c_e(v + 1/2)^7 \end{aligned} \quad (\text{C3})$$

Again, except for four states of  $H_2$ , where the energy values are entered directly in block data **enH2** (see Appendix F).

Expressions for  $F_J$  are not given here as numerical values are obtained from the solution of the rotational Hamiltonian matrix. Expressions for  $F_J$  for various spin multiplicities are given in reference 13. The numerical values are calculated in subroutines **honl**, **solve**, and **band** and involve the spin orbit interaction parameter,  $A$ , the rotational constant,  $B_v$ , and the centrifugal distortion constant,  $D_v$ , for the upper and lower vibrational levels. The matrix solution for doublet states also includes the spin-rotation interaction constant,  $\gamma$ , and triplet and quartet states include  $\gamma$  and the spin-spin interaction constant,  $\sigma$ . These rotational levels and the Hönl-London factors between levels are stored in the **EHL** files, discussed in the Introduction and the How to Use NEQAIR96 sections of this manual.

All spectroscopic constants are in units of wavenumber [ $\text{cm}^{-1}$ ], and are entered from the **spectroscopic.data** file on tape unit 2 (the default file name for the CRAY computer is fort.2). The high vibrational and rotational levels beyond the validity of the Dunham expansions are approximated to give "reasonable" values (see Appendix F). The best spectroscopic constants to use are those determined by matrix fitting schemes that include many bands and band systems simultaneously, such as the one discussed in reference 23. However, most of the constants available (ref. 15) in the literature are effective values determined from single bands or branches. The accuracy of the wavelengths calculated from the rotational energy levels is compromised if the spectroscopic constants are not appropriate for the matrix method.

## Appendix D

### Atomic and Rotational Line Shapes

The shapes of the atomic and rotational lines are described by either a Voigt or a rectangular profile. The Voigt profile provides a reasonably realistic approximation to the actual line shape in many cases. The rectangular line shape is NOT realistic, but can be used to increase the speed of computation when appropriate.

The line width [Angstrom] for the Voigt profile is defined as the full width of the line at its half-peak intensity value. The width is, of course, an important descriptor of the line. It is also used to specify how far from the line center a line is retained in the spectrum before its contribution is considered unimportant. That is, "range" is an integer number of line widths over which the line is retained.

The shape of a Voigt profile is calculated from the widths of its Gaussian,  $w_g$ , and Lorentzian,  $w_l$ , components. The approximation used for this calculation is taken from reference 54 and gives the profile as a function of the Voigt width,  $w_v$  [Angstrom], and the ratio of  $w_l/w_v$  as

$$\begin{aligned} \phi_\lambda = 10^4 & [(1 - w_l/w_v)e^{-2.772(\Delta\lambda/w_v)^2} + (w_l/w_v)/\{1 + 4 * (\Delta\lambda/w_v)^2\} \\ & + 0.016(w_l/w_v)(1 - w_l/w_v)(e^{-0.4(\Delta\lambda/w_v)^{2.25}} \\ & - 10/\{10 + (\Delta\lambda/w_v)^{2.25}\})]/[w_v\{1.065 + 0.447(w_l/w_v) + 0.058(w_l/w_v)^2\}] \quad [\mu^{-1}] \end{aligned} \quad (D1)$$

where  $\Delta\lambda$  is the distance from the line center [Angstrom] and is always positive. All of the factors in this equation are dimensionless except for the factor  $w_v$  [Angstrom] in the denominator. The  $10^4$  factor [Angstrom/ $\mu$ ] in the numerator converts the wavelength unit from Angstrom<sup>-1</sup> to  $\mu^{-1}$ .

The expression that gives  $w_v$  in terms of  $w_l$  and  $w_g$  is taken from reference 55, that is,

$$w_v = [1 - 0.18121 * (1 - sd^2) - (0.023665 e^{0.6sd} + 0.00418 e^{-1.9sd}) * \sin(\pi sd)](w_l + w_g) \quad (D2)$$

where

$$sd = (w_l - w_g)/(w_l + w_g)$$

Each line is usually spread over a range of 3 or more line widths in both direction from the line center. This results in each line contributing to about 60 or more spectral grid points. The integer value of range, in line widths, is entered by the User for each calculation. A reasonably accurate description of a line requires about 10 grid points per line width, and using less than 5 can produce meaningless results for the integrated radiant power and for the line shape. The code tests for this condition and, if the number of grid points per line width is less than 5, prints an error message and terminates the run.

The code can calculate the line widths for the Gaussian and Lorentzian components of a Voigt profile. The Gaussian component considers the broadening effects of random thermal motion (Doppler broadening), and the Lorentzian component considers natural broadening, Stark broadening (due to collisions with electrons), resonance broadening (due to collisions with identical species), and collisional broadening (due to collisions with other species, an approximation to van der Waals broadening). The equations used to calculate these effects are discussed in reference 26, although in NEQAIR96 the natural broadening of atomic lines is calculated in subroutine **naturalwidth**, rather than using the fixed classical value of  $1.18 \times 10^{-4}$  Angstroms given in reference 26.

The wings of a line extend far from the line center and although they become very weak they are extremely important when strong self-absorption occurs. In such cases, the range over which the line is retained in the spectrum might be a thousand or more (refs. 35 and 36) line widths. The code will include all lines over the entire wavelength range if a value of 0 (zero) is entered for range.

The rectangular line shape, when specified, is arbitrarily spread uniformly over 5 spectral grid points or 4 spectral intervals. It is not, of course, a physically realistic line shape, but its use reduces the computer time needed to calculate a spectrum. Only the optically thin emission and radiative transport are calculated for this option. The results are quite good for a nearly optically thin gas and when the resolution is about 5–10 Angstroms or greater. It is useful in providing a quick look at spectra in the early stages of a project. A comparison of spectra calculated using a Voigt profile and a rectangular line shape is shown in table 5 and figures 16 and 17 in Subsection B of the How to Use NEQAIR96 section.

The use of a realistic line shape is particularly important when significant self-absorption occurs. The absorption coefficient is given by the spectral emission profile of the line, divided by the Planck function for the appropriate temperature or population ratio. The absorption coefficient is maximum near the line center where the spectral emission is the greatest. Further, the emission intensity and the absorption coefficient at a line center are increased by squeezing the total integrated emission into a narrower line shape. Thus, the correct, or at least a reasonably realistic, line shape must be used to calculate realistic spectra and radiative transport when absorption is important.

Often, however, using realistic line shapes and widths are unnecessary and will waste resources. If absorption is not important, using a realistic line shape may produce a resolution much greater than necessary and cause the spectrum to appear as a very large collection of individual lines. Such a picket fence pattern of lines makes it difficult to see and identify even familiar band shapes. The spectral range covered might also be limited to a fairly small value, perhaps no more than 10 Angstroms, to keep the number of grid points within the dimensions of the spectral arrays. Further, these results might be of less value than a spectrum calculated using a Gaussian line width equal to the resolution desired in the spectrum or present in the data. Such a spectrum gives the widest spectral coverage, produces recognizable band shapes, and increases the speed of the calculation.

A useful indicator for estimating whether absorption is important is simply the wavelength. Often the dividing line between an optically thin spectral region and one where absorption effects are important occurs at about 2000 Angstroms. Above this wavelength, flow fields are often nearly optically thin, and below this wavelength one usually needs to consider absorption. For example, in

room air O<sub>2</sub> absorbs almost all radiation below 2000 Angstroms, which is why this region is referred to as the vacuum ultraviolet.

Strong absorption below 2000 Angstroms occurs because:

1. Transition probabilities tend to be stronger for higher energy transitions, other factors being equal.
2. The Planck function decreases rapidly toward shorter wavelengths and occurs in the denominator of the expression for the absorption coefficient (see eq. A18).

Both of these effects tend to make absorption an important consideration below 2000 Angstroms. Clearly though, each situation must be investigated on its own merits.



## Appendix E

### The Escape Factor

The purpose of the escape factor is to account for the lowering of the excited state populations in low density flows in QSS nonequilibrium calculations. It does this by adjusting the optical emission rate coefficients in the calculation of the state populations. Like all radiative transport phenomena, the escape factor depends on both spontaneous and stimulated optical transitions.

The escape factors for atomic bound-bound transitions are calculated in subroutine **bbescf** and are discussed in this appendix. The escape factors for atomic bound-free transitions, **escfbf**, and diatomic transitions, **escf**, are not calculated, but are set arbitrarily to 1.0 in data statements in subroutines **qss** and **molext**. These may need to be changed in some calculations. A test of the importance of the escape factors can be made by running the code with them set to 1.0 and then set to 0.0. If a significant change occurs in the spectrum or the radiative heating rate values, the issue needs to be addressed.

Exact radiative transport calculations are complicated because all field points are coupled by the photons that are emitted and absorbed. The photon density, or radiant energy density (see eq. A3), needed at each point in the field is produced by photons that are emitted from all other points that are NOT absorbed before they reach the point in question. Thus, the radiation emitted and absorbed at every point in the flow field is coupled to the radiation emitted and absorbed at every other point. The solution of this highly coupled optical problem is difficult to obtain even in highly simplified flow geometries and is impractical to consider in a code such as NEQAIR96.

The approach used in NEQAIR96 is to bypass the actual complex physical situation with a conceptually simple point of view, called the escape factor. The escape factors for atomic transitions are then calculated by using a simplified model for approximating their values.

The escape factor is defined as the probability that a photon emitted at a point in the flow will NOT be matched by the absorption of an identical photon near the same point. Emitted photons that are NOT matched by absorptions will appear to have escaped from the region of emission and will contribute to the optical depopulation of the excited state. Contrarily, any emitted photons that are matched by the absorption of identical photons will tend to repopulate the upper state. If all of the photons emitted from a small region escape from the region the escape factor is 1.0, and if all of the emitted photons are matched by absorptions the escape factor is 0.0. The result of all such emissions and absorptions can be expressed conceptually as

$$A_{UL}(\text{effective}) = (A_{UL} - \text{Absorption rate coef.}) = \text{escf } A_{UL} \quad (\text{E1})$$

where

$A_{UL}(\text{effective})$  is the effective optical depopulating rate coefficient of an upper state due to optical transitions to a specific lower energy state.

$A_{UL}$  is the Einstein rate coefficient for spontaneous emission.

Absorption rate coef. is the result of all stimulated emissions and absorptions between the same upper and lower states, in the region of the emission point, caused by the unknown photon density in that region.

$\text{escf}$  [dimensionless] is defined as the escape factor.

The escape factor, as stated above, accounts for the tendency of optical transition rates to lower the population of excited states in low density flows. This kind of flow is often present under non-equilibrium conditions and is usually referred to as “collision limited” flow. The populating and depopulating rates due to electrons and heavy particles depend on the collision rates of the particles, which are related to the product of the number densities for the species involved. The collision rates, therefore, change quadratically with the density. In high density flows, the collision rates greatly exceed the optical rates and the state populations stay close to the Boltzmann values, regardless of the value of the escape factor. In low density flows, however, the collision rates are low and can become on the order of the optical rates or even lower. Then, the optical rates have an important effect on state populations, as electrons are drained to lower energy states by the emission of photons.

Having a useful conceptual picture of the escape process is helpful, but by itself it does not provide any computational advantage. One still needs to perform a complete solution of the optical transport problem to find the escape factors to use. One basis for an approximation is to recognize that the local volumetric absorption coefficient strongly influences the amount of absorptions that take place in a small local region and, hence, the value of the escape factor in that region. A descriptive definition of the model used in NEQAIR96 to evaluate the escape factors is stated as:

**The escape factor is the probability that a photon emitted at a point in a radiating flow field will NOT be absorbed after traveling a distance,  $d$  [cm], through a uniform gas with an effective volumetric absorption coefficient equal to that at the point of emission.**

The distance,  $d$ , in this approximation is not defined other than it should be chosen to give the correct result and, unfortunately, there are no established criteria for selecting its value. It is surely related to the conditions at the emission point and to the geometry of the flow field, such as a shock layer or a wake region. But presently the only way for the escape factor to account for absorptions caused by photons from other points in the flow field is through an appropriate value of  $d$ . Clearly,  $d$  can be selected, arbitrarily, to give any value of the escape factor from 0.0 to 1.0! Our limited experience (refs. 48 and 56–58) indicates that a value of  $d = 1.0$  cm gives reasonable results for the specific intensity spectrum when comparing with experimental spectra from shock layers and shock tubes. Whether this provides useful guidance or is simply fortuitous is unknown at this time.

Several thorough calculations of the actual radiative transport phenomena in representative, but simplified, flow geometries are needed to provide more realistic guidance in the selection of escape factors. Such results would enable realistic values of  $d$ , or the escape factor itself, to be established empirically. Not having such results available, the escape factor is calculated with an expression derived from the definition given above.

The effective volumetric absorption coefficient,  $\alpha_\lambda$  (see the unnumbered equation following eq. A17), is given by

$$\alpha_\lambda = (g_L N_L B_{LU} - g_U N_U B_{UL}) h \bar{\nu}_{UL} \phi_\lambda \quad [\text{cm}^{-1}] \quad (\text{E2})$$

The first term in this expression, except for the line shape factor,  $\phi_\lambda$ , is the volumetric absorption coefficient, and the second term is the volumetric stimulated emission coefficient. Combining these terms in the same expression means that  $\alpha_\lambda$  includes the effects of both absorptions and stimulated emission.

The line shape function is normalized so that its integral over all wavelengths is 1.0, and gives the probability of a photon being emitted or absorbed between  $\lambda$  and  $(\lambda + \delta\lambda)$  [ $\mu$ ] as  $\phi_\lambda * \delta\lambda$ . The line shapes for emission and absorption are assumed to be identical.

The Einstein A and B coefficients are related by (see eqs. A12 and A13)

$$A_{UL} = 8\pi hc/(10^4 \lambda^5) B_{UL} \quad [1/\text{s}] \quad (\text{E3})$$

$$g_L B_{LU} = g_U B_{UL} \quad [1/(\text{J}/\text{cm}^3\text{-}\mu)\text{-s}] \quad (\text{E4})$$

where  $\lambda$  is in cm and the  $10^4$  factor in equation E3 converts one of the cm's to  $\mu$ 's. Using these expressions, equation E2 can be written as

$$\alpha_\lambda = 10^4 (N_L/N_U - 1) N_U g_U A_{UL} \bar{\nu}_{UL} \lambda^5/(8\pi c) \phi_\lambda \quad (\text{E5})$$

The volumetric absorption coefficient can also be written in a simple form as  $E_\lambda/B_\lambda$  (see eq. A18), but that form cannot be used here because the upper state population,  $N_U$ , is not known before the calculation is made. Neither, of course, is the lower state population, but an initial lower state population is estimated by using a Boltzmann distribution.

Normally, the only levels that are populated adequately to enable significant absorption to occur are the lowest two or three electronic energy states. The populations of these levels are usually well approximated using the Boltzmann equation at the electronic temperature found during the calculation of the flow field. This electronic temperature is entered in the **los.data** file.

The value of  $N_L/N_U$  in equation E5 is usually a very large number with a value of at least a few hundred and possibly several thousand. Thus, this equation is further approximated by setting  $N_L/N_U - 1 = N_L/N_U$ . This step allows an approximate volumetric absorption coefficient to be expressed as

$$\alpha_{\lambda} = 10^4 N_L g_U A_{UL} \bar{v}_{UL} \lambda^5 / (8\pi c) \phi_{\lambda} \quad (E6)$$

which does not contain the upper state population.

The major premise of the escape factor model, as noted above, is that the escape factor is the fraction of the local spontaneous emission remaining (NOT absorbed) after traveling a limited distance,  $d$ . The radiation remaining is found using Lambert's law (usually referred to as Beer's law (ref. 57)) using the approximate volumetric absorption coefficient given by equation E6 acting over a distance,  $d$ , that is,

$$\text{escf} = \frac{\int_0^{\infty} E_{\lambda} e^{-\alpha_{\lambda} d} d\lambda}{\int_0^{\infty} E_{\lambda} d\lambda} = \frac{\int_0^{\infty} \phi_{\lambda} e^{-\tau_{\lambda}} d\lambda}{\int_0^{\infty} \phi_{\lambda} d\lambda} = \int_0^{\infty} \phi_{\lambda} e^{-\tau_{\lambda}} d\lambda \quad (E7)$$

as  $E_{\lambda} = E \phi_{\lambda}$  and  $\int_0^{\infty} \phi_{\lambda} d\lambda = 1.0$

where escf is the escape factor and  $E$  is the total spontaneous emission in the line  $[\text{W}/\text{cm}^3\text{-}\mu]$  given in equation A1. Notice that the total line emission cancels from this equation. Thus, under the assumption made above ( $N_L/N_U \gg 1.0$ ), not only is  $\alpha_{\lambda}$  not a function of the upper state population but neither is the escape factor. This allows  $N_U$  to be set to zero for the calculation of the escape factor!

The expression for the escape factor can be further simplified by making the reasonable assumption that the line width is narrow compared to the line wavelength. This limits the range of the integration in equation E7 to a narrow region around the line center. This is a good approximation for nearly all atomic lines, and under this condition  $\bar{v}_{UL}$  and  $\lambda$  can be replaced with their values at the line center. The approximate volumetric absorption coefficient can then be written as

$$\alpha_{\lambda} = \alpha_t \phi_{\lambda} \quad [\text{cm}^{-1}] \quad (E8)$$

where  $\alpha_t$  is the total (integrated) value of  $\alpha_{\lambda}$  over the line shape, i.e.,

$$\alpha_t = 10^4 N_L g_U A_{UL} \bar{v}_{CL} \lambda_{CL}^5 / (8\pi c) \quad [\mu/\text{cm}] \quad (E9)$$

The optical depth,  $\tau_{\lambda} = \alpha_{\lambda} d$ , can then be written as

$$\tau_{\lambda} = \alpha_t d \phi_{\lambda} \quad [\text{dimensionless}] \quad (E10)$$

and the optical depth in terms of the optical depth at the line center,  $\tau_0$ , as

$$\tau_{\lambda} = \tau_0 \phi_{\lambda} / \phi_{\lambda_{CL}} \quad [\text{dimensionless}] \quad (E11)$$

where  $\phi_\lambda/\phi_{\lambda_{CL}}$  defines a line shape function normalized to 1.0 at the line center. Then from equations E10 and E11

$$\tau_0 = \alpha_t d \phi_{\lambda_{CL}} \quad [\text{dimensionless}] \quad (\text{E12})$$

The escape factor can then be expressed as

$$\text{escf} = \int_{\lambda_1}^{\lambda_2} \phi_\lambda e^{-(\alpha_t d \phi_\lambda)} d\lambda \quad (\text{E13})$$

Values of the escape factor, calculated using equation E13 and an escape distance of  $d = 1.0$  cm, are plotted against  $\tau_0$  in figure E1. The value of  $\tau_0$  is calculated using equation E12, where the value of  $\phi_{\lambda_{CL}}$  is established by the line shape function in subroutine **lineshape**. Curves for the escape factor are shown for four Voigt profiles: a pure Gaussian ( $w_l = 0.0$ ), a pure Lorentzian ( $w_g = 0.0$ ), and  $w_l/w_g$  values equal to 0.3 and 1.0. A curve for  $w_l/w_g = 5.0$  was not included because it lies nearly on top of the pure Lorentzian curve. Clearly, the escape factor increases as one moves from the Gaussian to the Lorentzian line shape. This effect is consistent with the increased height of the line wing intensity as the Lorentzian component increases. Thus, there is more emission from the wings, and it is the weak radiation in the line wings that is more likely to escape from the flow field.

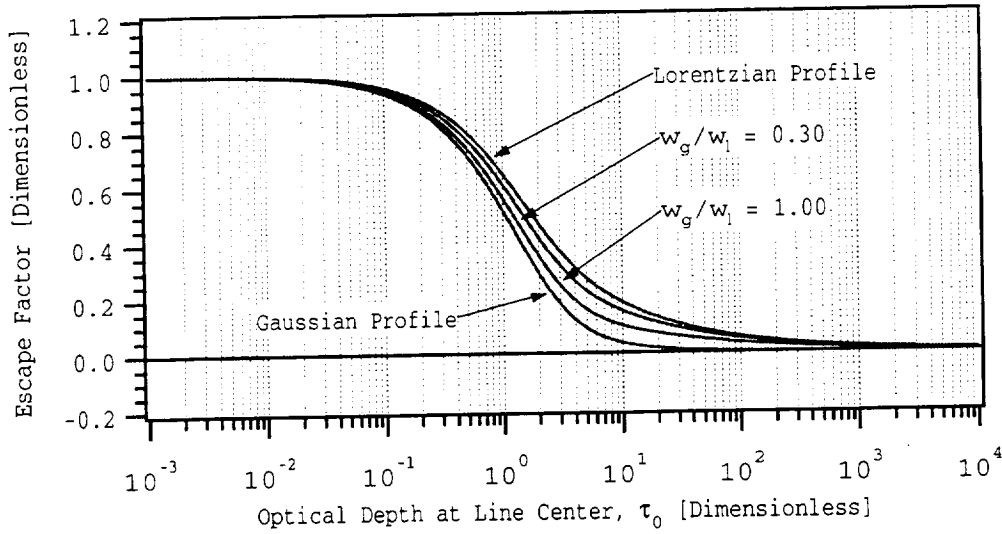


Figure E1. Effect of line shape on the escape factor.

Note that the value of  $\tau_0$  is proportional to both  $\phi_{\lambda_{CL}}$  and  $d$  (see eq. E12). Thus, a change in  $\tau_0$  by changing  $d$  moves one along the same  $w_l/w_g$  curve to a new value of  $\tau_0$ . The change in the escape factor by changing  $d$  is substantial, if the escape factor is in the mid range of values between 0.0 and 1.0. A change in  $\tau_0$  caused by a change in  $\phi_{\lambda_{CL}}$ , which is equivalent to changing the line width, is not clear from an examination of the above equations. Calculations show that a shift in  $\tau_0$  while keeping  $w_l/w_g$  fixed also moves one along the same  $w_l/w_g$  curve. Thus, a shift in  $\tau_0$  caused by a change in the line width is exactly compensated for by a corresponding shift in  $d$ .

The escape factor curves shown in figure E1 were checked using NEQAIR96 to calculate the absorption in atomic lines. Using the code in this way is identical to using the leftmost expression in equation E7. The calculations were made for the atomic nitrogen line at 149.262 nm, a Gaussian line shape with a width of 0.06 Angstrom, and an upper state population of  $10^{-10}$  [cm<sup>-3</sup>]; the transport was made over a distance of 1.0 cm. The upper state population could not be set to 0.0 because the code calculates the absorption coefficient from the spontaneous emission. The unrealistic low value of  $10^{-10}$  for  $N_U$  approximates a value of 0.0 and allows the code to work. The lower state population was varied as a convenient method of changing the values of  $\alpha_\lambda$  and  $\tau_0$ . Increasing the lower state population, while keeping the upper state population fixed, decreases the electronic temperature, which narrows the line width and increases the values of  $\alpha_\lambda$  and  $\tau_0$ . The results from these calculations are in exact agreement with the results shown in figure E1.

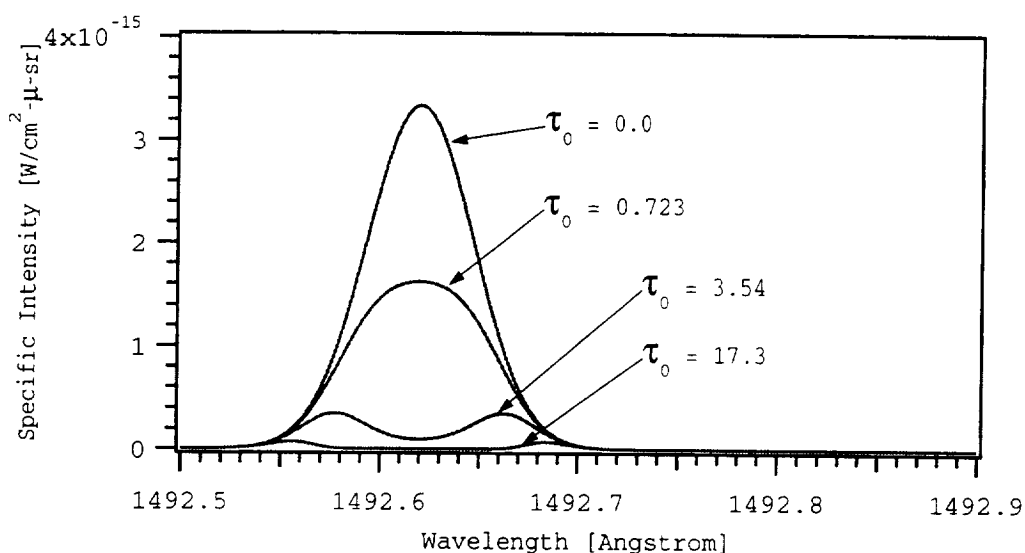


Figure E2. Effect of optical density at the line center,  $\tau_0$  on the absorption in Gaussian profile lines with  $d = 1.0$  cm.

The results from four of these runs are shown in figure E2. The value of the escape factor is equal to the area under a curve for  $\tau_0$  divided by the area under the curve for  $\tau_0 = 0.0$  (see eq. E7). The optical densities at the line center for these calculations are shown on the figure. At very low optical density, no significant absorption occurs and the escape factor is nearly 1.0. The absorption becomes pronounced at large optical densities, particularly near the line center. At high optical densities, the center of the line is almost totally absorbed, and the only photons that can escape are in the far wings of the line. The escape factor in this case is close to zero.

The escape factors for all of the atomic lines contained in the **excitation.data** file were calculated at the conditions noted above. This included many lines whose lower states were neither the ground state nor one of the two low-lying pseudo ground states. The populations of the three lowest states were estimated with reasonable confidence using the Boltzmann distribution function, but the higher states were a potential problem. However, an initial estimate of the populations of the higher states was made using the Boltzmann function.

The intention in these calculations was to find approximate escape factors using the Boltzmann populations, and then find more realistic populations using these escape factors and the QSS code in subroutine **qss**. An iteration scheme was set up and investigated to determine whether it would converge to reasonable state populations. Surprisingly, the iteration converged in a single iteration!—and yet, in several cases, the upper state population changed markedly, some by orders of magnitude. The escape factors and state populations changed insignificantly after the first iteration.

This finding shows that escape factors can be calculated for all transitions. However, all of the escape factors calculated for transitions whose lower state was not a ground or pseudo ground state were close to 1.0, and the value of calculating them is probably not worth the computer time required. Thus, to speed the calculation, the escape factors for atomic states are calculated only for transitions whose lower state is one of the three lowest electronic states. All other escape factors are set equal to 1.0. The line of code that controls which escape factors are calculated is located in subroutine **bbescf**, and is set by the integer constant “LSlimit” in that subroutine.

Interestingly, the process of calculating the escape factors for high energy states is not very sensitive to the initial estimate of the state populations, even when the initial estimate is wrong by a few orders of magnitude. This occurs because the state populations of excited states are quite low, even as given by the Boltzmann equation, and results in escape factors near 1.0. The use of these values in the QSS method will tend to lower the original estimate of the state population because the photons are escaping from the region of emission. The new, lower populations will result in still higher escape factors, but the escape factors are already nearly 1.0 and cannot change appreciably on a second iteration. The emission and collisional rates from higher levels to the level in question can alter this effect and increase the state population. But the state population will still be a small value, and the escape factor will probably decrease very little.

The escape factors used in earlier versions of the code were not calculated using the integration shown in equation E7 or E13. Instead, other approximations were used. The approximations assumed that the line shapes were pure Gaussian and evaluated the escape factors using one of two expressions: an expansion or a closed form equation based on the value of  $\tau_0$ . When the value of  $\tau_0$  was less than 4.0, the following expansion, approximation 1, was used:

$$\text{escf} = 1.0 - \sum_{n=1}^{15} \frac{(-1)^n \tau_0^n}{n! (n+1)^{1/2}} \quad (\text{E14})$$

The inclusion of 15 terms in this expansion is clearly adequate when  $\tau_0$  is less than 4.0, as can be checked with a few calculations. When the value of  $\tau_0$  was greater than or equal to 4.0, the following equation, approximation 2, taken from page 24 of reference 59 was used:

$$\text{escf} = \frac{1.0}{\tau_0 (\pi \log_{10}(\tau_0))^{1/2}} \quad (\text{E15})$$

This equation approximates the integration over a line from the wavelengths where  $\tau = 1.0$  toward the line wings. The curves given by equations E14 and E15 are plotted in figure E3. The combination of these two expressions is seen to be an excellent approximation to the complete curve for the Gaussian line shapes shown in figure E1.

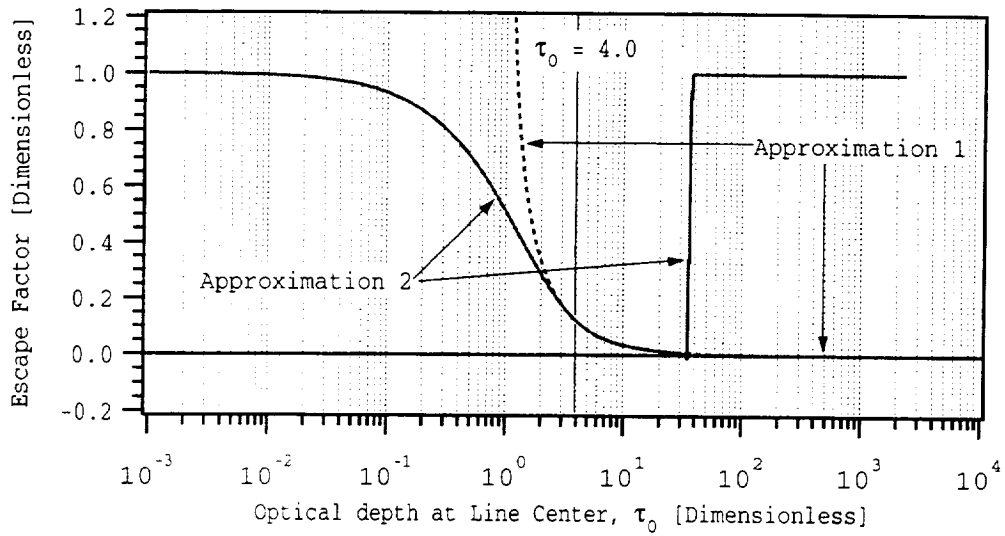


*Figure E3. Effect of approximate Gaussian profiles on escape factor.*

## Appendix F

### Diatomic Internal Partition Function

The internal partition function of a species is the sum of the number densities in all of its nondegenerate energy levels,  $N_i$ , normalized to one particle in a nondegenerate sublevel of the lowest energy state,  $N_1$ . The partition function is thus given by

$$Q = \sum N_i/N_1 \quad (F1)$$

Under equilibrium conditions at a temperature  $T$  [K] the partition function is calculated from the Boltzmann distribution function and is given by

$$Q = \sum g_i e^{-c_2 E_i/T} \quad (F2)$$

where  $g_i$  is the degeneracy of an energy level,  $E_i$  [cm<sup>-1</sup>] is the energy of energy level  $i$ , and  $c_2 = hc/k = 1.43879$  [cm K] is the second radiation constant. Under nonequilibrium conditions the Boltzmann distribution function does not accurately reproduce the population distribution. In this case, the internal partition function can only be expressed in terms of the population ratios as given in equation F1.

The only true degeneracy in the absence of strong magnetic or electric fields is the rotational degeneracy  $(2J + 1)$ , where  $J$  is the quantum number for the total angular momentum. However, as a practical manner, the degeneracy is usually defined to include all energy substates that are reasonably close to the same energy value and that can be easily identified.

Thus, in most calculations the number of substates included in  $g_i$  is equal to the product of the electronic spin multiplicity,  $(2S + 1)$ , lambda doubling multiplicity,  $(2 - \delta_{\Lambda,0})$ , and  $(2k + 1)$ , where  $S$  is the resultant electronic spin quantum number,  $\Lambda$  is the quantum number for the component of the electron orbital angular momentum along the internuclear axis, and  $k$  is the rotational quantum number without spin. See reference 14 for discussion and explanation of the symbols used in these expressions.

The standard symbol for the rotational quantum number without spin is “N,” but  $k$  is used in this manual to be consistent with the NEQAIR96 code. The symbol  $k$  is used in the code because the symbols “N” and “n” are used frequently as do-loop indices or limits, and for other integer variables.

The nuclear spin multiplicity,  $g_{\text{nuc}}$ , is normally not included in the degeneracy because its effect usually cancels or can be handled with simple approximations when the partition function is applied. However, this is not always true and in NEQAIR96 the nuclear spin multiplicity is included in the degeneracy. The total degeneracy is then expressed as

$$g_i = g_{\text{nuc}}(2S + 1)(2 - \delta_{\Lambda,0})(2k + 1) \quad (F3)$$

The values for, and use of,  $g_{\text{nuc}}$  are discussed in Appendix G.

One of the important uses of the internal partition function is to find the population of an energy state,  $N_i$ , from the total number density for a species,  $N_t$ , that is,

$$N_i = (N_t/Q) g_i e^{-c_2 E_i/T} \quad (\text{F4})$$

The energies of the energy levels,  $E_i$ , in the case of diatomic molecules is usually written as a sum of the electronic, vibrational, and rotational components of the total energy. Further, if a temperature for each energy mode is specified, the first step toward calculating a nonequilibrium internal partition function is made by writing equation F2 as

$$Q = \sum g_i e^{-c_2(E_e/T_e + G_v/T_v + F_k/T_k)} \quad (\text{F5})$$

Under equilibrium conditions all of the temperatures are equal, of course.

The magnitude of the internal partition function,  $Q$ , at  $T = 0.0$  K is equal to  $g_1$ , as only the ground state is occupied. At high temperatures  $Q$  approaches  $\sum g_i$ , as all nondegenerate states are equally populated as  $T$  approaches infinity. At other temperatures its value depends on the number of energy levels and their energy values. At high temperatures the number of levels is often more important than the actual energy values. This effect occurs because the exponential factors,  $e^{-c_2 E_i/T}$ , approach 1.0 as  $T$  increases. Furthermore, most diatomic molecules have several excited electronic states (about 20 for  $\text{N}_2$ ) located, energywise, near the dissociation limit of the ground state. The number of energy levels in these states strongly influences the value of the partition function at temperatures above about 5000 K. However, errors in the energy values, by perhaps  $100 \text{ cm}^{-1}$  or more, do not change the partition function appreciably.

The remainder of this appendix comments on two particular issues involved in the calculation and application of the partition function. These are:

1. Energy levels and vibrational-rotational dissociation.
2. Partial partition functions for single electronic states.

The nuclear spin multiplicity, as noted above, is included, but is not discussed in detail in this appendix. Heteronuclear diatomic molecules have a single nuclear spin multiplicity, which provides a constant multiplying factor in all terms of the internal partition function. This constant factor cancels when the internal partition function is applied to the number density for an energy level, and for other thermodynamic properties such as the internal energy and specific heat. Homonuclear molecules have two nuclear spin multiplicities that alternate from rotational level to rotational level. An average of these two multiplicities can be used in many calculations, in the same manner as the single value is used for heteronuclear molecules.

Unfortunately, using the average value of the two spin multiplicities for homonuclear molecules removes the special effect of alternating line intensities in the spectra emitted by them. The alternation can then only be included by an empirical approximation. The approach in NEQAIR96 is to

include the correct nuclear spin multiplicities in the internal partition function and calculate correct line intensities even when line alternation occurs. A more complete discussion of nuclear spin multiplicities is presented in Appendix G.

## Part 1. Energy Levels and Vibrational-Rotational Dissociation

The number of electronic-vibration-rotation energy levels in diatomic molecules, as well as the energies of these levels, obviously effects the value of the partition function. The number of levels included in the summations depends on the degeneracies, as noted above, and on limitations imposed by dissociation. Dissociation can be caused by pure vibration, pure rotation, or a combination of both energy modes.

The procedure used in NEQAIR96 for finding the vibration-rotation dissociation limits begins by applying the rotational energy to the nonrotating potential curve of the molecule, and then finding the number of vibrational levels that can exist in the potential well of the rotating potential, if a well exists. The rotating potential is, of course, distorted from the nonrotating potential by the introduction of the centrifugal force of rotation. With adequate rotation, molecules will dissociate without considering the vibrational energy.

The expression for the rotating potential can be expressed as (see ref. 14):

$$U(k,R) = E_0(R) + h k(k+1) 10^7 / (8\pi^2 c \mu R^2) \quad (F6)$$

where  $E_0(R)$  [ $\text{cm}^{-1}$ ] is the nonrotating potential curve,  $h$  [J s] is Planck's constant,  $k$  is the quantum number for rotational angular momentum without spin,  $c$  [cm/s] is the speed of light,  $\mu$  [gm] is the reduced mass of the molecule, and  $R$  [cm] is the internuclear separation. The factor of  $10^7$  is included so that Planck's constant can be expressed in [J s] rather than [erg s].

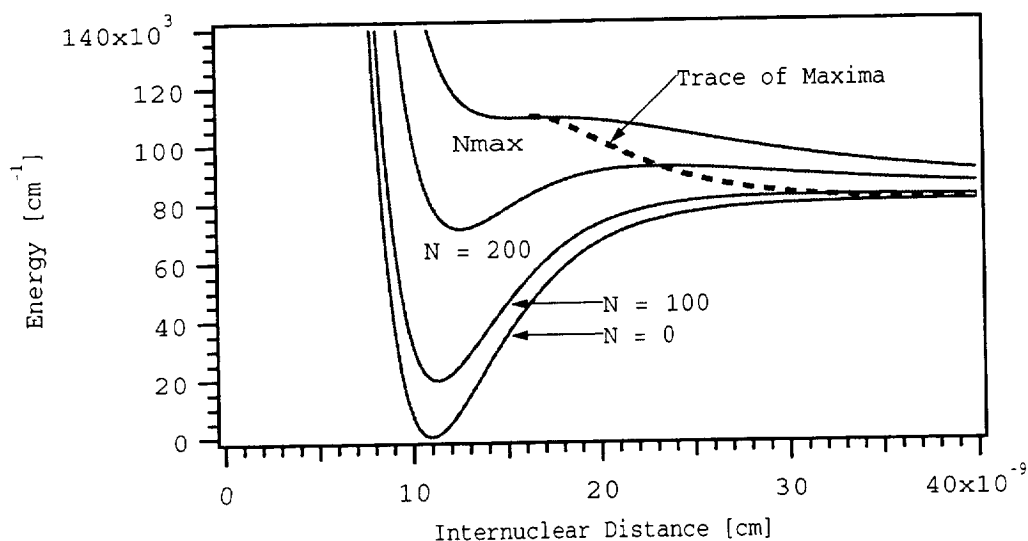


Figure F1. Potential curves of  $N_2$  ground state.

The effect of rotation on a potential function is shown in figure F1. The lower curve in this figure is the ground state of the N<sub>2</sub> molecule, approximated by a Morse potential (ref. 60). The upper curve shows the limiting potential curve for the maximum rotational condition ( $k = k_{\max}$ ). The maximum rotational condition no longer creates a potential well, but only an inflection point in the curve. Thus, there are no bound energy levels at or beyond  $k_{\max}$ . Any further increase in the rotational energy will cause the molecule to dissociate due to rotation only. The two intermediate curves are for rotational quantum numbers of  $k = 100$  and  $200$ , and each of these curves shows the presence of a rotational hump, or local maximum, at larger  $R$  values.

The effect of rotation on the nonrotating potential function increases the energy at all internuclear distances, as shown by the last term in equation F6. However, for given rotational angular momentum or, equivalently, for a given value of  $k$ , the energy increase is larger for small  $R$  values and becomes less as  $R$  increases. Thus, the effect of rotation causes the minimum energy at the bottom of the potential well to increase faster than the energy at the peak of the rotational hump. Thus, at  $k_{\max}$  the potential minimum and the rotational hump coincide, and only an inflection point remains, as mentioned above.

The dashed curve in figure F1 defines the locations of the rotational humps,  $U(k, R_{\text{hump}})$ , for all rotating potential wells, as a function of internuclear distance, where  $R_{\text{hump}}$  is the value of  $R$  at the peak height of the hump.

The picture presented by equation F6 and the two previous paragraphs shows that the rotational energy is a function of  $R$ , as is the electronic binding energy itself. This makes it impossible to separate fully the electronic, vibrational, and rotational energy modes. However, the simple models, which approximate separate energy modes, have been exceptionally successful in producing useful results. This model has been described many times. Perhaps the most used description is that of Dunham (ref. 16) and the expansion he developed.

A simplified view of the Dunham model is that the electronic energy (including his  $Y_{00}$  term) and vibrational energies for any electronic state are defined by the appropriate nonrotating potential function. The rotational energies are then defined to give the correct value for the total energies of the electronic-vibrational-rotational levels. Here we mention only two of the most important effects of rotation: its effect on raising the energy at the minimum of the potential well and its effect on flattening the potential well.

The effect of rotation on the energy at the minimum of the potential well implies that the principal portion of the rotational energy is usually given as the energy difference between the minima of the rotating and nonrotating potential curves. That is,

$$E'_{\text{rot}}(k) = U(k, R_{\min}) - U(0, R_e) \quad (\text{F7})$$

where  $R_{\min}$  is the  $R$  value at the potential minimum, and  $R_e = R_{\min}$  for  $k = 0$ . If the  $R$  value at the minimum did not change with  $k$ , then the value of  $E'_{\text{rot}}$ , as given in equation F7, would equal the last term in equation F6, which contains the factor  $k(k + 1)$ . But the  $R$  value at the potential minimum increases with  $k$ , and the actual value of  $E_{\text{rot}}$  is somewhat less than this value.

The second effect of rotation mentioned above is to flatten the potential curve. This effect causes the vibrational energy levels to lie a bit lower in the potential well, which causes the vibrational energies to decrease. But to keep the spectroscopic model intact, we want to maintain the energies of the vibrational energy levels as they are found for  $k = 0$ . Thus, the rotational energy is defined as  $E'_{\text{rot}}(k)$  minus the decrease in the vibrational energy due to rotation. If  $\Delta E(v,k)$  is defined as the effect on the rotational energy, due to a change in the  $R$  value at the potential minimum and to the decrease in vibrational energy with rotation, we can write

$$E_{\text{rot}}(v,k) = [U(k,R_{\text{min}}) - U(0,R_e)] - \Delta E(v,k) \quad (\text{F8})$$

This expression is similar to the two term rotational Dunham expansion expressed by

$$E_{\text{rot}}(v,k) = B_v k(k+1) - D_v [k(k+1)]^2 \quad (\text{F9})$$

Equation F8 is, in principle, more accurate than equation F9. However, to gain this accuracy the potential function would need to be known precisely, so that accurate values of  $\Delta E(v,k)$  could be determined. Generally, the spectroscopic constants used in equation F9 are known accurately from experimental data, at least for the lower vibrational and rotational levels, making it the better choice when accurate energy levels are needed. However, one needs to be careful in using equation F9 because it can produce large errors when it is used beyond the range of validity of the spectroscopic constants. A similar warning applies to the use of the vibrational Dunham expansion, even for  $k = 0$ .

Regardless of how the energy levels are determined, it is clear that the molecule will dissociate whenever the sum of the vibrational and rotational energies exceeds the local maximum in the potential well. In NEQAIR96 all electronic spin and lambda substates are assumed to dissociate simultaneously. Some dissociation can occur by quantum mechanical tunneling through the potential barrier before the maximum point is reached, but that effect is not considered in NEQAIR96.

The procedure used in NEQAIR96 to find the vibrational and rotational energy levels that are consistent with equation F6 is to use:

1. The code developed by Liu (refs. 61 and 62) to find the energies at the rotational hump formed by the rotating potential curves, as illustrated by the dashed curve in figure F1. These energy values define the total vibrational-rotational dissociation energies for all possible values of  $k$ , from 0 to  $k_{\text{max}}$ . In the Liu code, the nonrotating potential functions are approximated by either Lippincott (ref. 63) or Hulburt and Hirschfelder (ref. 64) potentials.
2. The vibrational Dunham expansion to calculate the the nonrotating vibrational energy levels,  $E_0(v)$ , up to a cut-off vibrational level,  $v_{\text{DunMax}}$ . The value of  $v_{\text{DunMax}}$  is discussed in Subsection A below. The vibrational spectroscopic constants ( $w_e$ ,  $w_e x_e$ , etc.) needed for these calculations are entered in the **spectroscopic.data** file.
3. The rotational Dunham expansion to calculate the rotational energy levels for each vibrational level,  $E_{\text{rot}}(v,k)$ , up to a cut-off rotational level,  $k_{\text{DunMax}}$ . The value of  $k_{\text{DunMax}}$  is discussed in Subsection B below. The rotational constants,  $B_v$  and  $D_v$ , needed for these

calculations are found from the rotational constants,  $B_e$ ,  $\alpha_e$ ,  $D_e$ , and  $\beta_e$ , entered in the **spectroscopic.data** file.

4. Approximate methods to extend the vibrational and rotational levels beyond the cut-off limits. The approximate methods used are discussed in Subsections A and B below.

The Liu code (ref. 61), as mentioned above in step 1, uses either Lippincott or Hulburt and Hirschfelder potentials to approximate the nonrotating potential functions. A possible problem can occur when using the Hulburt and Hirschfelder potential. This potential is capable of placing a potential hump in the curve, which extends above the dissociation limit even for a nonrotating potential. Such humps do occur in some electronic states. However, in NEQAIR96 these humps are removed by increasing the dissociation energy entered in the **spectroscopic.data** file by the height of the hump. This allows all potential curves to be handled in the same way when calculating the number of vibrational and rotation levels that occur before dissociation occurs.

The use of the steps outlined above results in reasonably accurate energy values for the vibrational and rotational energy levels for all molecular band systems included in the code to date, except  $H_2$ . Even for  $H_2$ , the procedure provides energies that are adequate for the calculation of useful partition functions. However, the  $H_2$  energy values determined in this way are not adequate for realistic spectra.

Thus, a complete departure from the above procedure is taken for the X, B, C, and B' electronic states of  $H_2$ . The energies of the vibrational and rotational levels for these four states are not calculated, but are instead entered directly into the code, in block data **enH2**. This allows accurate spectra to be calculated for the B-X, C-X, and B'-X band systems, as well as providing energy values for the calculation of the partition function. Another 19 electronic states of  $H_2$  are handled as described above for other molecules. More details about the  $H_2$  energy levels entered directly into the code are discussed in Subsection C below.

For most molecules other than  $H_2$ , the Dunham expansions provide good approximations to the known energy levels that have been used to determine the spectroscopic constants. However, the appropriate spectroscopic constants have not been determined for most high vibrational and rotational levels. Thus, significant errors can occur when using the Dunham polynomial expansions to extrapolate beyond the ranges where the spectroscopic constants were determined. This is particularly a problem when calculating the wavelengths of rotational lines.

Even though the spectra produced by transitions from most high vibrational and rotational levels are not well established and contribute mainly to the background radiation, it is important that the calculated spectra produced by NEQAIR96 be somewhat realistic. For example, the vibrational energies should increase with increasing vibrational quantum number, and the rotational energies should increase with increasing rotational quantum number. Using the Dunham expansions beyond their range of validity can sometimes result in unrealistic energies that decrease with increasing quantum numbers.

The best way to limit the vibrational Dunham expansion is to enter into the **spectroscopic.data** file the maximum vibrational quantum number for which the spectroscopic constants were determined. This is done by entering a value for the variable “vlimit,” for each electronic state. Unfortunately, these limits are seldom published. Thus, usually approximations must be relied on to limit the range of validity of the Dunham expansions. The limits used in NEQAIR96 to terminate the use of the Dunham expansions, and the approximations used to calculate reasonable energy levels beyond the Dunham limit, are discussed in the following subsections.

## A. Vibrational Cut-Off Limits and Extension Approximations

Two arbitrary, but we believe reasonable, cut-off limits are used in NEQAIR96 to limit the use of the vibrational Dunham expansions. The User can change these limits by making the appropriate changes in subroutine **energys**. In NEQAIR96 the Dunham expansions are terminated when either:

1. The vibrational energy exceeds 50% of the dissociation energy for the electronic state, or
2. The vibrational quantum number,  $v$ , exceeds 50% of the  $v$  value at the peak of the Dunham vibrational energy curve.

The peak of the vibrational Dunham energy curve occurs when the slope of the  $G_v$  curve is 0.0. Using the two term Dunham expansion

$$G_v = w_e (v+1/2) - w_e x_e (v + 1/2)^2 \quad (\text{F10})$$

and the value of  $v$  at the maximum energy point is

$$v = w_e / (2 * w_e x_e) - 1/2 \quad (\text{F11})$$

Thus, the second criterion is met when  $v$  exceeds 50% of this value or, approximately, when

$$v = v_{\text{DunMax}} = w_e / (4 * w_e x_e) \quad (\text{F12})$$

Limiting the Dunham expansion to  $v \leq v_{\text{DunMax}}$  increases the likelihood that the energies calculated are reasonably close to their correct values. However, the task is not yet complete. A significant number of energy levels may exist between the cut-off limit and the dissociation limit. The energy values of these remaining vibrational states are approximated by repetitively adding an energy increment to the previous energy value, until the dissociation limit is reached. The first energy increment is found from the energy difference between the last two levels calculated with the Dunham expansion.

$$\Delta E = E_0(v_{\text{DunMax}}) - E_0(v_{\text{DunMax}} - 1) \quad (\text{F13})$$

Also, generally, the vibrational energy spacing decreases slightly from level to level as the dissociation limit is approached. This decrease in the energy increment is approximated by the second derivative of equation F8. That is,

$$\Delta(\Delta E) = -2 * w_e x_e \quad (F14)$$

However, if  $\Delta E$  is less than  $\Delta(\Delta E)$ , then  $\Delta E$  is set to  $\Delta(\Delta E)/2$ ; that is,  $\Delta E = -w_e x_e$ . From this point on,  $\Delta E$  is held constant at this value until the dissociation energy is exceeded. This method ensures that all vibrational energies calculated do in fact increase with increasing  $v$ .

## B. Rotational Cut-Off Limits and Extension Approximations

Two arbitrary cut-off limits are used in NEQAIR96 to limit the use of the rotational Dunham expansion. The User can change the limits by making the appropriate changes in subroutine **energys**. The rotational Dunham expansions are terminated when either:

1. The rotational quantum number without spin,  $k$ , exceeds 75% of the  $k$  value at the peak of the Dunham rotational energy curve, or
2. For the  $H_2$  energy levels not entered directly into the code, the rotational quantum number without spin,  $k$ , exceeds 20% of  $k_{\max}$ .

The first criterion involves the two term Dunham expansion for rotational energies, which is

$$F_k = B_v k(k + 1) - D_v [k(k + 1)]^2 \quad (F15)$$

The maximum occurs when the slope of the  $F_k$  curve is 0.0. That is, when

$$k = -1/2 + \sqrt{1/4 + B_v/(2 * D_v)} \quad (F15)$$

Thus, the first criterion occurs when  $k$  is given, approximately, by

$$k = k_{\text{DunMax}} = 3/4 \sqrt{B_v/(2 * D_v)} \quad (F17)$$

The second criterion is only used for  $H_2$ , and only then for the  $H_2$  electronic states whose vibrational and rotational energies are not entered directly in the code. Special treatment of  $H_2$  is necessary because the spectroscopic constants for the rotational Dunham expansion are valid for very few rotational levels. The cut-off limit in this case is set arbitrarily to 20% of the  $k_{\max}$  value found in subroutine **enbarier** (ref. 61). This criterion is not well established, and may actually be too high. It is expressed as

$$k = k_{o5} = k_{\max}/5 + 1 \quad (F18)$$

Again, as for the vibrational levels, many rotational levels may exist above  $k = k_{\text{DunMax}}$ . However, the method of approximating the energies of these additional levels is very different from the method used for the vibrational levels. The method used for calculating additional rotational levels uses modified  $B_v$  and  $D_v$  values that: (1) Reproduce the last energy value calculated by the Dunham expansion,  $E_1$ ; and (2) would produce a rotational energy value,  $E_2$ , at the highest rotational energy value  $k_{\max}$ . The value of  $E_2$  is set equal to the difference between the highest energy value possible,  $U(k_{\max}, R_{\text{hump}})$ , and the energy for the vibrational level without rotation involved,  $E_0(v)$ . That is, by letting

$$E_2 = U(k_{\max}, R_{\text{hump}}) - E_0(v) \quad (\text{see eq. F6 and fig. F1}) \quad (\text{F19})$$

then with

$$k_1 = \text{minimum of } k_{o5} \text{ or } k_{\text{DunMax}}$$

$$k_2 = k_{\max}$$

$$E_1 = E_{\text{rot}}(v, k_1)$$

$$B_v \text{Mod} = (E_1 * x_1^2 - E_2 * x_2^2) / (x_1 - x_2) \quad (\text{F20})$$

$$D_v \text{Mod} = B_v \text{Mod} * x_1 - E_1 * x_1^2 \quad (\text{F21})$$

where  $x_1 = 1/[k_1(k_1 + 1)]$  and  $x_2 = 1/[k_2(k_2 + 1)]$ . The rotational energies from  $k = k_1$  to the vibrational-rotational dissociation limit,  $U(k, R)$ , are then given by

$$E_{\text{rot}}(v, k) = B_v \text{Mod} * k(k + 1) - D_v \text{Mod} * [k(k + 1)]^2 \quad (\text{F22})$$

Using  $U(k_{\max}, R_{\text{hump}})$  in equation F19 is correct only for  $v = 0$ ; however, it will be reasonably accurate for several lower vibrational levels. Errors at higher rotational levels will occur, but the rotational energies for the higher vibrational levels are usually poorly known, so that the need for a better approximation is not clearly evident. The use of  $U(k_{\max}, R_{\text{hump}})$  for high vibrational levels seems reasonable because dissociation occurs at low  $k$  values. Even with its weaknesses, this method ensures that the rotational energies increase with increasing  $k$ . However, as noted above, the User can change this criterion by making the appropriate changes in subroutine **energys**.

### C. Energy Levels for the X, B, C, and B' Electronic States for H<sub>2</sub>

The energy values for the vibrational and rotational levels of the X, B, C, and B' states of H<sub>2</sub> are directly entered in the code in block data **enH2**. To be consistent with the spectroscopic model discussed above, the total energy is separated into electronic, vibrational, and rotational energy modes. The electronic energies,  $T_e$ , as for all electronic states of all molecules, are entered in the **spectroscopic.data** file. The vibration and rotation modes are separated as follows: (1) The vibrational energy without rotation for each  $v$  level,  $E_0(v)$ , is set equal to the experimental or theoretical vibrational-rotational energy for  $k = 0$ ; and (2) The rotational energies  $E_{\text{rot}}(v, k)$  are set equal to the difference between the vibration-rotation energy for  $v$  and  $k$ , and the vibrational energy  $E_0(v)$ .

Experimental vibrational and rotational energy values determined from spectroscopic data are used where available. These experimental data are augmented with theoretical energy levels to complete the list of all energy levels that are believed to exist in the four states identified above. The experimental data for the X, B, and C states are taken from Dabrowski (ref. 65) and the data for the B' state are taken from Dieke (ref. 66).

The theoretical results were calculated using a computer code furnished to the authors by David Schwenke (ref. 67). This code calculates the vibration-rotation energy levels from numerical potential energy curves. The potential energy curves used were those calculated by Wolniewicz

(ref. 68) and Wolniewicz and Dressler (ref. 69). These curves include the adiabatic (same state) corrections, but not the nonadiabatic (other state) corrections.

Nonadiabatic corrections for these states have been calculated (refs. 70 and 71), but are limited either to the vibrational levels only (ref. 70) or to a few of the lowest rotational levels of the ground state (ref. 71), where experimental data are available. Thus, the theoretical nonadiabatic corrections were not included in the calculation of the vibrational-rotational energies. However, the theoretical energy values were adjusted to equal the experimental value, at the highest experimental  $k$  level available for each vibrational level. These shifts act like nonadiabatic corrections, at least as a function of  $v$ .

## Part 2. Partition Functions for Single Electronic States

The partition function is calculated for single electronic states of diatomic molecules as part of the calculation to determine the populations of upper electronic states, when the Boltzmann distribution function is used rather than the QSS method. These conditions can be equilibrium or nonequilibrium if separate temperatures are specified for each energy mode; that is, equation F5 is used. This expression is written as

$$Q = \sum g_e e^{-c_2(E_e/T_e)} \sum g_{vk} e^{-c_2(G_v/T_v + F_k/T_k)} \quad (F23)$$

to show that a vibration-rotation summation is identified with, and can be extracted from, each electronic state. This summation has the form of a vibration-rotation partition function,  $Q_{vk}$ , which is expressed as

$$Q_{vk} = \sum g_{vk} e^{-c_2(G_v/T_v + F_k/T_k)} \quad (F24)$$

$Q_{vk}$  can then be combined with the degeneracy of the electronic state to form a temperature dependent, effective electronic degeneracy for the electronic state. The total partition function is then expressed in a form similar to equation F2, that is,

$$Q = \sum g_{\text{eff}}(T_v, T_k) e^{-c_2 E_e/T_e} \quad (F25)$$

This expression shows clearly that the population of an electronic state CANNOT be calculated simply by using the Boltzmann function with the electronic degeneracy, electronic energy, and electronic temperature, as is often done. This effect is particularly important because the  $Q_{vk}$  values and populations for excited states, with about the same energy, can be very different.

The zero energy reference for the calculation of  $Q_{vk}$  is the electronic energy at the minimum of the electronic potential well; otherwise, the total energy would not be  $T_e + G_v + F_k$ . As  $G_v$  is measured from  $T_e$ , the electronic energy in function **qevr** is set to 0.0 when calculating  $Q_{vk}$ . For the calculation of the full partition function, the zero energy reference is the  $v = 0, k = 0$  level of the ground state.

## Appendix G

### Nuclear Spin Multiplicities and Alternation of Line Intensities for Homonuclear Molecules

The rotational lines of homonuclear diatomic molecules alternate in intensity from line to line (ref. 14). The alternation is caused by the existence of two nuclear spin multiplicities that result in different upper state populations for alternate rotational levels. The method used to calculate this effect in earlier versions of NEQAIR was empirical and not always correct. This problem is corrected in the current version of the code by including nuclear spin multiplicities in the degeneracy of the rotational levels. The discussion below applies to all electronic states, but computationally it is applied fully only for  $\Sigma$  states. This simplification does not affect the final results, and the steps taken to adjust for it are discussed near the end of this appendix.

Normally, the nuclear spin multiplicities are not included in the calculation of partition functions and the populations of energy levels. Heteronuclear diatomic molecules have a single nuclear spin multiplicity, and it provides a constant multiplying factor in all terms of the internal partition function. This constant factor cancels when the internal partition function is applied to find the number density for energy states and other thermodynamic properties, such as the internal energy and the specific heat. Although homonuclear diatomic molecules have two nuclear spin multiplicities, their average is often used in the same manner as the single heteronuclear value in the calculation of most thermodynamic properties. The average value is usually, and accurately, determined by calculating the nuclear spin multiplicity as for a heteronuclear diatomic molecule, and then dividing by 2.

Unfortunately, using the average value for the nuclear spin multiplicity of homonuclear molecules removes the phenomenon that produces alternating line intensities. The alternation of the rotational lines can be restored by including an empirical scheme in the code but, as noted above, such schemes are not always correct. The approach in NEQAIR96 is to include the correct nuclear spin multiplicities from the start and avoid empirical solutions.

The rules for applying correct nuclear spin multiplicities for homonuclear diatomic molecules are given in reference 14 and can be stated in terms of the nuclear spin,  $I$ , of either atom as follows:

1. The nuclear spin multiplicity is  $(2I + 1)(I + 1)$  for “symmetric” rotational levels and  $(2I + 1)I$  for “antisymmetric” rotational levels when  $I$  has an integer value. The spin multiplicities are reversed when  $I$  has a half-integral value.
2. The symmetric rotational levels are those with positive parity in even (gerade) electronic states, and with negative parity in odd (ungerade) electronic states. The positive and negative parities of antisymmetric rotational levels are the reverse of these.
3. The even and odd values of the rotational quantum numbers without spin are associated with the positive and negative parity values as follows:

N values	Positive parity	Negative parity
$N = 0, 2, 4, \dots$	$\Sigma^+, \Pi^+, \Delta^+, \text{etc.}$	$\Sigma^-, \Pi^-, \Delta^-, \text{etc.}$
$N = 1, 3, 5, \dots$	$\Sigma^-, \Pi^-, \Delta^-, \text{etc.}$	$\Sigma^+, \Pi^+, \Delta^+, \text{etc.}$

The first rule implies a firm tenet of quantum mechanics: all rotational levels are separated into two groups, one called symmetric and the other antisymmetric. This rule also states that for homonuclear diatomic molecules the separation into symmetry groups can be done strictly on the basis of whether the nuclear spin is integral or half-integral. The assignments are shown in table G1.

Table G1. Nuclear spin multiplicity

Level symmetry	Multiplicity	nucmult index
Symmetric	$(2I + 1)(I + M)$	1
Antisymmetric	$(2I + 1)(I + 1 - M)$	2

where  $M = 1$  for integral  $I$   
 $M = 0$  for half-integral  $I$

The column labeled “nucmult index” indicates that the nuclear spin multiplicity values are stored in an array called nucmult(is,index) where “is” identifies the diatomic species, and index can take values of 1, 2, or 3. The index value of 3 is used to store the nuclear spin multiplicity of heteronuclear molecules and the average nuclear spin multiplicity value of non $\Sigma$  states of homonuclear molecules, as will be mentioned below. The process of finding the spin multiplicities and assigning the index values occurs in the subroutine **specdata**.

The second and third rules given above lead to the following results:

1.  $\Sigma$  states
  - a. Rotational levels with even rotational quantum numbers without spin,  $N$ , are either all symmetric or all antisymmetric.
  - b. The even rotational levels (even  $N$ ) are symmetric for  $\Sigma_g^+$  and  $\Sigma_u^-$  states, and are assigned an index value of 1. The odd rotational levels are assigned an index value of 2.
  - c. The even rotational levels are antisymmetric for  $\Sigma_g^-$  and  $\Sigma_u^+$  states, and are assigned an index value of 2. The odd rotational levels are assigned an index of 1.
  - d. The odd rotational levels have the opposite symmetry to those for the even rotational levels.

## 2. non $\Sigma$ states

- a. Every rotational level has two lambda substates, one with positive parity and one with negative parity. Also, one lambda substate is symmetric and the other is antisymmetric.
- b. The assignment of nuclear spin multiplicities is the same as that for  $\Sigma$  states except that both multiplicities occur for each N value, one in each substate. The multiplicities alternate between the higher and the lower of the two lambda substates, as the value of N changes by  $\pm 1$  for each  $\Omega$  substate and as  $\Omega$  changes by  $\pm 1$  for each value of N.
- c. The order of the nuclear spin multiplicities in the two lambda substates is the same for all levels with the same value of J, but again they all switch when J changes by  $\pm 1$ .

The average of the nuclear spin multiplicities for the two lambda substates is (from table G1)

$$g_{\text{nuc}}(\text{ave}) = ((2I + 1)(I + M) + (2I + 1)(I + 1 - M))/2 \quad (\text{G1})$$

$$= (2I + 1)(2I + 1)/2 \quad (\text{G2})$$

If  $I_1$  and  $I_2$  are substituted in equation G2 for the two values of I, one sees that the average value of the nuclear multiplicity of a homonuclear diatomic molecule is exactly half of the value calculated as if it were a heteronuclear molecule, i.e.  $(2I_1 + 1)(2I_2 + 1)$ .

The value of index and the nuclear spin multiplicity for the even rotational levels (even N) of  $\Sigma$  states is established in subroutine **specdata** at the time the symbols for the electronic states are read from the **spectroscopic.data** file. The nuclear spin multiplicity of heteronuclear states and the average value of the nuclear spin multiplicity for homonuclear non $\Sigma$  states are also established at this time, which are given an index value of 3. These values are used in the calculation of the internal partition function in function **qevr** and in the calculation of the populations of the upper energy levels in subroutine **band**. In both cases, if the first rotational quantum number, N, in the upper state is an odd value, the starting index value is switched from 1 to 2 or from 2 to 1. This is done in subroutine **band** as the proper multiplicity must be used to get the correct population of the upper level and, thus, the correct line intensity. In the function **qevr** the starting rotational quantum number is always set to an even number. The loss of the contribution from a low rotational energy level to the internal partition function is too small to make any difference in its final value.

An index value of 1 or 2 must be changed from 1 to 2 or 2 to 1 with every value of N or J. This change is made by resetting the index equal to

$$\text{index} = 3 - \text{index} - (\text{index} - 1)(\text{index} - 2)(3/2) \quad (\text{G3})$$

after each rotational level in the calculation of the partition function and after each rotational line in the calculation of line intensities. This expression does not change an index value of 3.

Sample spectra shown in figures G1 and G2 illustrate the line alternation effect for homonuclear diatomic molecules. The spectrum shown in figure G1 is for a portion of the (0,0) band of  $N_2^+(1-)$  [ $B^2\Sigma_u^+ - X^2\Sigma_g^+$ ] and that in figure G2 for a portion of the (0,0) band of  $O_2$  (Schumann-Runge) [ $B^3\Sigma_u^- - X^3\Sigma_g^-$ ]. These spectra were calculated using the singlet approximation, 2000 spectral intervals, Gaussian line shape with a width of 0.1 Angstrom, and the one-layer **los.data** file shown in figure 14.

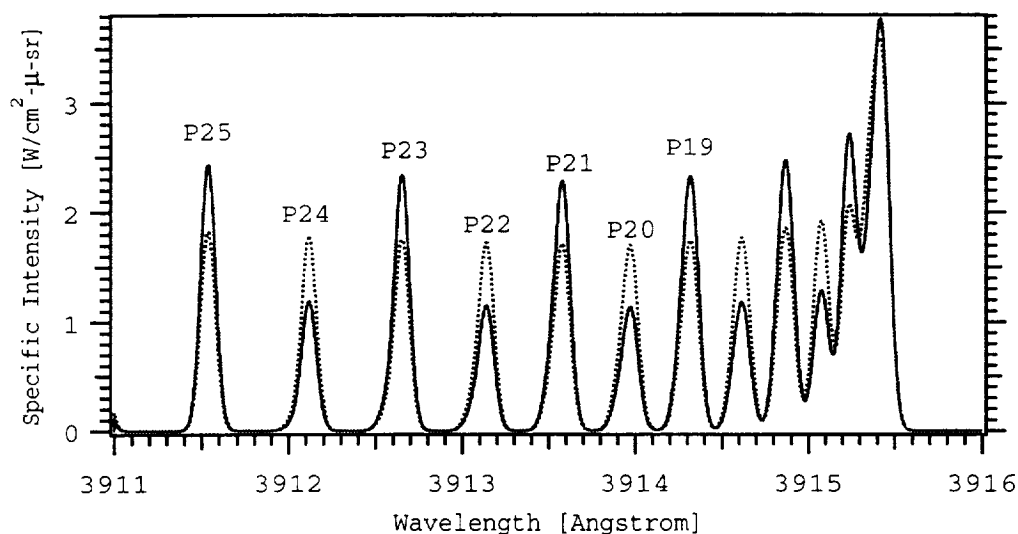


Figure G1. Spectrum of  $N_2^+(1-)$  (0,0) band showing line alternation. Dotted curve is without alternation.

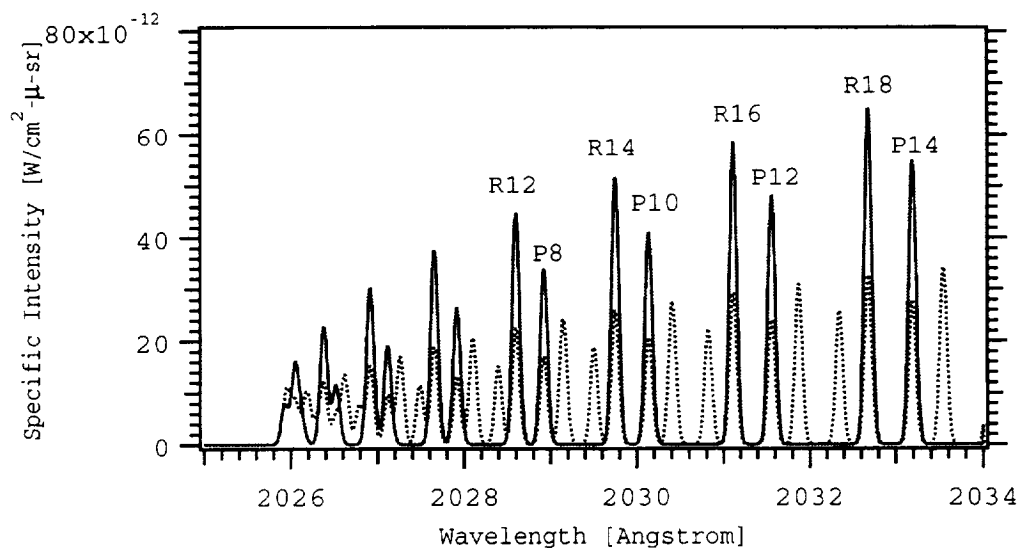


Figure G2. Spectrum of  $O_2$  SR (0,0) band showing line alternation. Dotted curve is without line alternation.

The dotted spectrum in each figure shows how the spectrum would appear if the average value of the nuclear spin multiplicities was used. The nuclear spin of atomic N is 1.0, which makes the line intensities of  $N_2^+$  alternate by a factor of 2 (see table G1). In this case the stronger lines occur for odd values of  $N_U$  because the upper electronic state is  $^2\Sigma_u^+$ . The nuclear spin of atomic O is 0.0 and the upper state of  $O_2$  (Schumann-Runge) is  $^3\Sigma_u^-$ . The rules discussed above show that odd values of  $N_U$  have a nuclear spin multiplicity of 0.0; that is, they do not exist. Thus, the only lines that appear in the spectrum are those for even  $N_U$  values.

The code, as noted in the first paragraph of this appendix, only handles the details of the homonuclear spin statistics when the upper electronic state is a  $\Sigma$  state. All other states are lambda doubled with two very close lambda substates for each rotational energy level. One of these substates is symmetric and the other is antisymmetric. Also, as noted in the Introduction, the code does not include effects of lambda doubling. Instead the code forms a composite upper state by adding the populations of both lambda substates together. This is done by including the lambda multiplicity ( $2 - \delta_{\Lambda,0}$ ), which has a value of 2 for non $\Sigma$  states, as a part of the electronic multiplicity in the internal partition function (see Appendix F).

The procedure described does not affect  $\Sigma$  to  $\Sigma$  transitions because lambda doubling does not occur, and the lambda multiplicity is equal to 1. It also works for non $\Sigma$  to non $\Sigma$  transitions because two very close lambda rotational lines are emitted for each rotational transition. These lines appear in most spectra as a single overlapped line because they are so close together. The emission intensity of this single composite line is equal to the sum of that for the two individual lines. Therefore, approximating them as a single line with twice the intensity is often acceptable. The non $\Sigma$  to non $\Sigma$  transitions of homonuclear and heteronuclear molecules are handled in the same way except for one difference. The nuclear spin multiplicity for the combined upper levels of homonuclear molecules must be the average of the spin multiplicities for the two levels. This average value can be found by forming the nuclear spin multiplicity as if the molecule is a heteronuclear molecule and then dividing this value by 2.0, as shown in equation G2.

The procedure discussed in the previous paragraph is not correct for either homonuclear or heteronuclear  $\Pi$  to  $\Sigma$  transitions, even though the  $\Pi$  state is lambda doubled with one substate having positive parity and the other negative. The explanation of this effect lies in quantum mechanical selection rules. A strong selection rule for dipole allowed transitions, which are the only transitions presently considered in NEQAIR96, only permits transitions from positive levels to negative levels and vice versa. Further, the rotational energy levels in  $\Sigma$  states are not doubled, and each rotational level is either positive or negative. Thus, a transition can occur from only one of the two lambda substates in the  $\Pi$  state to a given rotational level in the  $\Sigma$  state. A detailed look at the effect of these rules on  $\Pi$  to  $\Sigma$  transitions, shows that the transitions from the two lambda substates in the  $\Pi$  state do not form closely spaced lambda doublets but instead form widely separated lines in different branches.

Thus, the populations of the two substates in the  $\Pi$  state must not be added together for  $\Pi$  to  $\Sigma$  transitions, as if they were forming a single line. That is, the lambda multiplicity of 2, which is included in the electronic degeneracy (see Appendix H), must be removed. This is done in subroutine **band** by dividing the electronic degeneracy by 2. Further, the correct nuclear spin multiplicity for each lambda substate of the  $\Pi$  state must be used for homonuclear diatomic molecules.

But, as noted above, the correct nuclear spin multiplicities are only determined for  $\Sigma$  states. The spin multiplicities for the  $\Pi$  substates are found from those for the  $\Sigma$  state by using the selection rule mentioned above, plus those for  $\Delta J = 0, \pm 1$  and the special rule for homonuclear molecules that transitions can only occur from symmetric levels to symmetric levels and antisymmetric to antisymmetric levels. The adjustments mentioned here for  $\Pi$  to  $\Sigma$  transitions are performed in subroutine **band**.

The dipole-allowed selection rule, for both heteronuclear and homonuclear diatomic molecules, permits transitions only from positive rotational levels to negative levels and negative to positive levels. This rule prevents many of the branches in  $\Sigma$  to  $\Sigma$  transitions from occurring (see discussion of Line10 in the How to Use NEQAIR96 section). That is, branches only occur when  $\Delta N = 1, 3, 5$ , etc., in addition to the usual rules for dipole transition that  $\Delta J = 0, \pm 1$ . This effect is used in subroutine **band** to reduce the number of branches, and thus the number of rotational lines calculated, for  $\Sigma$  to  $\Sigma$  transitions.

The combining of the two closely spaced lambda rotational lines into a single line for non $\Sigma$  to non $\Sigma$  transitions can produce errors in the specific intensity if significant absorption occurs. If the lines are not actually overlapped, but are simply close together, then combining them into a single line increases the peak intensity beyond that of the individual lines. The amount of absorption calculated will be too large when absorption is important. The correct absorption is calculated in this case by doubling the line width before adding the two lines together, as the peak intensity of the line would then be preserved. However, if the lines are even partially overlapped, doubling the line width results in calculating too little absorption.

One approach to this problem is to run the code as it is programmed, which adds the two lines together and places the emission under a single line profile. Then run it again after doubling the line width. This approach will determine the two extremes in the specific intensity spectrum and enable an assessment to be made about its importance. If important, it may be necessary to determine the actual lambda doubling as a function of rotational quantum number, and devise a new scheme for calculating the lines separately, with very accurate wavelengths.

## Appendix H

### Scanning a Spectrum

A spectrum calculated for one condition may need to be scanned by a slit and instrument function to satisfy a different constraint or condition. For example, a case may have been run at high spectral resolution to calculate realistic absorption effects, but then needs to be scanned to calculate the output signal that an optical instrument would produce if it observed the calculated spectrum at lower resolution. This task is accomplished by moving (scanning) a slit function across the spectrum and multiplying by the instrument function. The instrument function is often referred to as the instrument sensitivity,  $C_\lambda$ , with units such as  $[V/(W/cm^2-\mu\text{-sr})]$ .

Scanning refers to the process of:

1. Placing a slit function on the calculated spectrum by aligning its “center” with a selected wavelength.
2. Integrating the product of the slit function,  $S_\lambda$ , the spectrum,  $I_\lambda$ , and the instrument calibration or sensitivity,  $C_\lambda$ , over the slit function.
3. Dividing by the integral over the slit function itself.
4. Repetitively moving the slit function to another wavelength and performing the integration again.

The expression for this process is simplified if the slit function is first normalized such that the integral over its shape is 1.0. The instrument response or signal,  $R_\lambda$ , is then

$$R_\lambda = \int_{\text{(slit function)}} S_\lambda I_\lambda C_\lambda d\lambda \quad (\text{H1})$$

Normally, the instrument function varies slowly over the width of the slit function and  $C_\lambda$  can be removed from the integral, giving

$$R_\lambda = C_{\lambda_C} \int_{\text{(slit function)}} S_\lambda I_\lambda d\lambda \quad (\text{H2})$$

where  $C_{\lambda_C}$  is the instrument function at the wavelength where the “center” of the slit function is located.

Two kinds of slit functions are used in NEQAIR96: a Voigt profile or a general profile made up of a number of linear segments. A Voigt slit is specified by entering the slit widths of its Gaussian and Lorentzian components. Again, the width of the slit is its full width at half height. The spectral

range over which the Voigt function is used must also be entered. The range is expressed in terms of the number of Voigt slit widths measured from the slit center. The “center” of a Voigt slit function is selected quite naturally at the center line of the slit, as it is symmetrical about this maximum point. Subroutine **lineshape** calculates the Voigt profile and normalizes the integral of the slit function to 1.0.

A linear segment slit is specified by entering the wavelengths and slit heights of the slit profile. The wavelength points that describe a linear segment slit begin at the shortest wavelength and increase monotonically to the longest wavelength. The integral of the slit over wavelength does not need to be normalized and the slit height values can be entered in any convenient unit. The code integrates over the slit to find the normalizing value and divides equation H2 by this integral. The center of a linear segment slit is not always easy to define. Thus, the User must specify the point on the slit to use as the slit center. This value must be one of the wavelength values entered to describe the slit function.

The remaining items that must be entered are the instrument calibration function, specified by entering pairs of wavelength and sensitivity values, and the wavelength coverage for the scan and the stepping interval for calculating output values. The starting wavelength for the scan must be the shortest wavelength, and the ending wavelength the longest. A stepping interval of 0.0 is entered as a signal for the code to set its value equal to the slit width divided by 10. The equivalent slit width for a linear segment slit is the area under the slit divided by the value of the slit height at its maximum.

The output signal for a fixed bandpass instrument, such as a radiometer, is calculated whenever the starting and ending wavelengths for the scan are equal.

The User may enter an unlimited number of slit and instrument functions for any spectrum calculated. The location of the spectrum to be scanned is specified by a number from 1 to 10 for the wavelength region or timing gate where the spectrum was written or is placed if not generated during the run. The location is identified on the first data line of the slit function (see the description of Line14 in the How to Use NEQAIR96 section). Location 1 corresponds to tape unit 21 and location 10 to tape unit 30.

The plot files, including the scanned files, are the principal output from the code. They are generated for all options, except the “don’t create” option. Specific intensity spectra [ $\text{W}/\text{cm}^2\text{-}\mu\text{-sr}$ ] for both absorption and an optically thin gas are written to the plot files for the line-of-sight and stagnation point options. For the rectangular line option, only the optically thin results are printed. The format for the line-of-sight and stagnation point options prints the two spectra in three columns. The first column is the wavelength in Angstroms or nm, or the wavenumber in  $\text{cm}^{-1}$ . The second column is the specific intensity with absorption, and the third column is the specific intensity for an optically thin gas. The User can, of course, easily change the print format statements in subroutine **transport**.

The format for the shock tube option prints four time-averaged specific intensity spectra in five columns for each timing gate:

- Column 1. The wavelength or wavenumber of the spectral points.
- Column 2. The spectrum with absorption.
- Column 3. A Planck function if a temperature is entered or the equilibrium option is selected.
- Column 4. The spectrum without the incident spectrum included.
- Column 5. The optically thin spectrum without the incident spectrum.

The **scan.data** files are printed in the **Output** file when the scan option is selected. The spectra to be scanned must be on tape units 21 to 30 and the scanned spectra are written to tape units 31 to 40. The tape unit number for a scanned spectrum is 10 greater than that for the tape unit number of the original spectrum.

The present code only scans the first spectrum at the left side of the plot file. For the shock tube option this is the time-averaged specific intensity over the timing gate. The spectral results included in the plot files can be changed by changing the write format statements in subroutine **transport**, and the spectrum to be scanned can be changed by changing the read format statement in subroutine **bandpass**.



## Appendix I

### The Three Data Base Files

The following three figures show the first portion of the three data base files. The entire files are supplied with NEQAIR96. The **spectroscopic.data** file is shown in figure I1, the **excitation.data** file in figure I2, and the **radiation.data** file in figure I3. These data need to be expanded to include additional species, excitation rate coefficients, and radiation systems. Users making such additions, or modifications, are urged to send copies of their files to the STA Research Branch at Ames Research Center.

```

*****
Spectroscopic.data file (fort.2)
for NEQAIR96

Enter as many lines of comments or references as necessary.

Most of the parameters entered are accepted spectroscopic constants. But
for diatomic molecules two optional parameters can be entered that are not
spectroscopic constants. These are:

vdata = the highest vibrational level used to produce we, wexe, etc.
vlimit= the highest vibrational level that is known to exist.

If these parameters are known and entered, they can make the calculation
of the maximum rotational level for each vibrational level before
dissociation occurs somewhat more realistic. They are not needed however,
so enter 0's (zero's) if they are not known.
*****

-----
nstates atomic wt ionpot[cm-1] h0[J/mole]
E- 1 5.4853e-4 0.0 0.0
aaaaaaaaaii rrrrrrrrr rrrrrrrrr rrrrrrrrr Enter species data above this line.
Elec Mult Energy [cm-1]
rrrrrrrrrr rrrrrrrrr Enter state data below this line.
1 2. 0.

-----
nstates atomic wt ionpot[cm-1] h0[J/mole]
Ar 5 39.948 127116.4 0.
aaaaaaaaaii rrrrrrrrr rrrrrrrrr rrrrrrrrr Enter species data above this line.
Elec Mult Energy [cm-1]
rrrrrrrrrr rrrrrrrrr Enter state data below this line.
1 1. 0.
2 5. 93143.8
3 3. 93750.6
4 1. 94553.7
5 3. 95399.9

-----
nstates atomic wt ionpot[cm-1] h0[J/mole]
Ar+ 5 39.947 222847.0 1.520e6
aaaaaaaaaii rrrrrrrrr rrrrrrrrr rrrrrrrrr Enter species data above this line.
Elec Mult Energy [cm-1]
rrrrrrrrrr rrrrrrrrr Enter state data below this line.
1 4. 0.
2 2. 1432.0
3 2. 108822.5
4 8. 132328.2
5 6. 132482.1

-----
nstates atomic wt ionpot[cm-1] h0[J/mole]
C 12 12.011 90878.3 2.996e5
aaaaaaaaaii rrrrrrrrr rrrrrrrrr rrrrrrrrr Enter species data above this line.
Elec Mult Energy [cm-1]
rrrrrrrrrr rrrrrrrrr Enter state data below this line.
1 9. 29.6
2 5. 10193.7
3 1. 21648.4
4 5. 33735.2
5 1. 60373.
6 3. 61982.
7 15. 64091.
8 3. 68858.
9 15. 69772.
10 3. 70744.

```

Figure 11. A portion of the *spectroscopic.data* file for NEQAIR96.

```

*****
This is the excitation.data file (fort.3)
for NEQAIR96

The excitation rates due to electron collisions is expressed as:

      K(l,u) = ro*gu/norm * (Te/10000)**rexp * e(-1.4delE/Te)

The portion of the electron impact excitation rate coefficients (ro) that
depend on the electron orbits are entered after being normalized by:

      norm = p5q5(1/p2-1/q2)4,

where: p and q are the effective principle quantum numbers of the states
involved and the integers (2, 4 and 5) are exponents.

This normalization is removed after the coef's are read in subroutine atomin.
See the work of Gryzinski ("Two-Particle Collisions. II. Coulomb Collisions
in the Laboratory System of Coordinates," Physical Review, Series A,
Vol. 138, 1995, pp. 322-335.), which is reproduced in Eq.2.9a on
page 46 of Chul Park's book, "Nonequilibrium Hypersonic Aerothermodynamics."

*****
Comments and references for atomic N
As many lines as needed.
*****
      Composite atomic energy levels.
N
#   n   ave E   total g   states-->
1   2     0.      4. 2P3 4S
2   2  19228.    10. 2P3 2D
3   2  28840.     6. 2P3 2P
4   3  83337.    12. 3S 4P
5   3  87488.    18. 3S 2P
6   3  95276.    36. 3P 4D 3P 4P 3P 4S
7   3  96793.    18. 3P 2S 3P 2D 3P 2P
8   4 103862.    18. 4S 4P 4S 2P
9   3 104857.    60. 3D 4F 3D 4P 3D 4D
10  3 104902.    30. 3D 2P 3D 2F 3D 2D
11  4 107082.    54. 4P 2S 4P 4D 4P 4P 4P 2D 4P 4S 4P 2P
12  5 110021.    18. 5S 4P 5S 2P
13  4 110315.    90. 4D 2P 4D 4F 4D 4D 4D 2F 4D 4P 4D 2D
14  4 110486.   126. 4F 4D 4F 4F 4F 4G 4F 2D 4F 2F 4F 2G
15  5 111363.    54. 5P 4S 5P 4P 5P 4D 5P 2S 5P 2P 5P 2D
16  5 112851.    90. 5D 2P 5D 4F 5D 4D 5D 2F 5D 4P 5D 2D
17  5 112929.   288. 5F 4D 5F 4F 5F 4G 5F 2D 5F 2F 5F 2G 5G 4F
18  6 114298.    648. 6
19  7 115107.    882. 7
20  8 115631.   1152. 8
21  9 115991.   1458. 9
22 10 116248.   1800. 10
-1  0      0.      0.      0. (terminate entry line)
-----
      Electron impact excitation rate coefficients
      K(l,u) = ro*gu/norm * (Te/10000)**rexp * e(-1.4delE/Te)
1 u ro rexp 1 u ro rexp 1 u ro rexp 1 u ro rexp 1 u ro rexp
1 2 1.1E-08 0.20 1 3 3.5E-09 0.21 1 4 7.1E-09-1.87 1 5 1.0E-30 0.00 1
1 6 4.0E-09 0.82 1 7 1.0E-30 0.00 1 8 1.5E-05-1.93 1 9 1.3E-05-2.06 2
1 10 1.0E-30 0.00 1 11 5.9E-09 0.82 1 12 2.9E-05-1.93 1 13 2.5E-05-2.04 3
1 14 1.0E-30 0.00 1 15 1.0E-30 0.00 1 16 4.7E-05-2.04 1 17 1.0E-30 0.00 4
1 18 1.7E-05-2.09 1 19 1.9E-05-2.09 1 20 2.1E-05-2.09 1 21 2.2E-05-2.09 5
2 3 5.4E-09 0.27 2 4 1.0E-30 0.00 2 5 5.3E-09-1.86 2 6 1.0E-30 0.00 6
2 7 6.8E-09 0.62 2 8 4.5E-06-1.87 2 9 1.0E-30 0.00 2 10 8.0E-06-2.06 7
2 11 3.3E-09 0.79 2 12 9.3E-06-1.88 2 13 8.1E-06-2.04 2 14 1.0E-30 0.00 8
2 15 1.0E-30 0.00 2 16 1.6E-05-2.03 2 17 1.0E-30 0.00 2 18 5.7E-06-2.07 9
2 19 6.3E-06-2.07 2 20 7.0E-06-2.07 2 21 7.6E-06-2.07 2 22 8.1E-06-2.07 10

```

Figure I2. A portion of the excitation.data file for NEQAIR96.

```

*****
                                This is the radiation.data file (fort.4)
                                for NEQAIR96

Free-Free data are not listed here but are in data statements in sub. ffddata.
*****
Comments and references for atomic N
As many lines as needed.
*****
                                Atomic Lines for:
N
(Stark Gam and expn)  gl  gu      Eu      Aul      lambda upper lower QSSul
1.670E-05      0.330  4.0  6.0   88110.0 2.200E+08   1134.98 2P3 4S 2P4 4P 1. 5.
1.670E-05      0.330  4.0  4.0   88153.0 2.500E+08   1134.42 2P3 4S 2P4 4P 1. 5.
1.670E-05      0.330  4.0  2.0   88173.0 2.500E+08   1134.17 2P3 4S 2P4 4P 1. 5.
6.650E-04      0.330  4.0  6.0   83366.0 5.500E+08   1199.55 2P3 4S 3S  4P 1. 4.
7.410E-04      0.330  4.0  4.0   83319.0 5.300E+08   1200.22 2P3 4S 3S  4P 1. 4.
6.650E-04      0.330  4.0  2.0   83286.0 5.500E+08   1200.71 2P3 4S 3S  4P 1. 4.
1.210E-03      0.330  6.0  4.0   86221.0 5.300E+08   1492.62 2P3 2D 3S  2P 2. 5.
1.210E-03      0.330  4.0  2.0   86138.0 5.000E+08   1494.67 2P3 2D 3S  2P 2. 5.
1.210E-03      0.330  4.0  4.0   86221.0 5.800E+07   1492.67 2P3 2D 3S  2P 2. 5.
2.230E-03      0.330  4.0  4.0   86221.0 1.800E+08   1742.73 2P3 2P 3S  2P 3. 5.
2.230E-03      0.330  2.0  2.0   86138.0 1.300E+08   1745.25 2P3 2P 3S  2P 3. 5.
2.230E-03      0.330  4.0  2.0   86138.0 6.500E+07   1745.26 2P3 2P 3S  2P 3. 5.
2.230E-03      0.330  2.0  4.0   86221.0 3.500E+07   1742.72 2P3 2P 3S  2P 3. 5.
0.000E+00      0.000  6.0  6.0   99663.0 4.300E+08   1243.17 2P3 2D 3S' 2D 2. 7.
0.000E+00      0.000  4.0  4.0   99663.0 4.300E+08   1243.30 2P3 2D 3S' 2D 2. 7.
8.400E-04      0.330  6.0  4.0   99663.0 4.500E+07   1243.17 2P3 2D 3S' 2D 2. 7.
0.000E+00      0.000  4.0  6.0   99663.0 3.000E+07   1243.31 2P3 2D 3S' 2D 2. 7.
1.060E-03      0.330  6.0 10.0  99663.0 5.200E+07   1411.94 2P3 2P 3S' 2D 3. 7.
1.150E-01      0.330  6.0  4.0   96752.0 2.100E+06  11564.80 2P4 4P 3P  4S 5. 6.
1.150E-01      0.330  4.0  4.0   96752.0 1.300E+06  11628.00 2P4 4P 3P  4S 5. 6.
1.150E-01      0.330  2.0  4.0   96752.0 6.600E+05  11656.00 2P4 4P 3P  4S 5. 6.
3.430E-03      0.330  6.0  8.0   104883.0 1.100E+08   1167.45 2P3 2D 3D  2F 2.10.
3.430E-03      0.330  4.0  6.0   104811.0 1.300E+08   1168.54 2P3 2D 3D  2F 2.10.
3.430E-03      0.330  6.0  6.0   104811.0 9.500E+06   1168.42 2P3 2D 3D  2F 2.10.
2.600E-01      0.330  6.0  6.0   105144.0 4.300E+07   1163.88 2P3 2D 3D  2D 2.10.
3.670E-02      0.330  4.0  4.0   105121.0 4.300E+07   1164.31 2P3 2D 3D  2D 2.10.
3.670E-03      0.330  6.0  4.0   105121.0 4.800E+06   1164.31 2P3 2D 3D  2D 2.10.
2.910E-01      0.330  4.0  6.0   105144.0 3.200E+06   1163.87 2P3 2D 3D  2D 2.10.
4.100E-03      0.330  4.0  4.0   104615.0 1.100E+08   1319.72 2P3 2P 3D  2P 3.10.
4.100E-03      0.330  2.0  2.0   104655.0 8.500E+07   1319.04 2P3 2P 3D  2P 3.10.
4.100E-03      0.330  4.0  2.0   104655.0 4.200E+07   1319.04 2P3 2P 3D  2P 3.10.
0.000E+00      0.000  2.0  4.0   104615.0 2.200E+07   1319.72 2P3 2P 3D  2P 3.10.
4.650E-03      0.330  4.0  6.0   105144.0 1.300E+08   1310.54 2P3 2P 3D  2D 3.10.
4.650E-03      0.330  2.0  4.0   105121.0 1.100E+08   1310.97 2P3 2P 3D  2D 3.10.
4.650E-03      0.330  4.0  4.0   105121.0 2.300E+07   1310.97 2P3 2P 3D  2D 3.10.
1.290E-01      0.330  6.0  4.0   104227.0 9.500E+07   1176.40 2P3 2D 4S  2P 2. 8.
1.290E-01      0.330  4.0  2.0   104142.0 1.300E+08   1177.70 2P3 2D 4S  2P 2. 8.
1.290E-01      0.330  4.0  4.0   104227.0 1.100E+07   1176.60 2P3 2D 4S  2P 2. 8.
6.390E-03      0.330  4.0  4.0   104227.0 1.500E+07   1326.63 2P3 2P 4S  2P 3. 8.
6.390E-03      0.330  2.0  2.0   104142.0 1.700E+07   1327.96 2P3 2P 4S  2P 3. 8.
6.390E-03      0.330  4.0  2.0   104142.0 8.500E+06   1327.96 2P3 2P 4S  2P 3. 8.
6.390E-03      0.330  2.0  4.0   104227.0 3.000E+06   1326.63 2P3 2P 4S  2P 3. 8.
1.150E-01      0.330  6.0  8.0   106871.0 2.540E+05   5328.70 2P4 4P 4P  4D 5.11.
1.150E-01      0.330  4.0  6.0   106816.0 1.890E+05   5356.77 2P4 4P 4P  4D 5.11.
1.150E-01      0.330  2.0  4.0   106780.0 1.070E+05   5372.66 2P4 4P 4P  4D 5.11.
1.150E-01      0.330  4.0  4.0   106780.0 1.180E+05   5367.10 2P4 4P 4P  4D 5.11.
0.000E+00      0.000  2.0  2.0   106761.0 2.100E+05   5378.30 2P4 4P 4P  4D 5.11.
1.200E-01      0.330  6.0  6.0   107039.0 2.820E+05   5281.18 2P4 4P 4P  4P 5.11.
0.000E+00      0.000  6.0  4.0   106998.0 1.670E+05   5292.90 2P4 4P 4P  4P 5.11.
0.000E+00      0.000  4.0  2.0   106983.0 2.730E+05   5309.20 2P4 4P 4P  4P 5.11.
0.000E+00      0.000  4.0  6.0   107039.0 1.130E+05   5293.50 2P4 4P 4P  4P 5.11.
0.000E+00      0.000  2.0  4.0   106998.0 1.370E+05   5310.60 2P4 4P 4P  4P 5.11.
0.000E+00      0.000  6.0  4.0   107447.0 2.090E+05   5170.00 2P4 4P 4P  4S 5.11.
0.000E+00      0.000  4.0  4.0   107447.0 1.440E+05   5181.50 2P4 4P 4P  4S 5.11.
4.410E-03      0.330 10.0  6.0   110082.0 3.300E+07   1100.70 2P3 2D 5S  2P 2.12.
2.120E-02      0.330  2.0  2.0   110029.0 2.200E+06   1231.70 2P3 2P 5S  2P 3.12.

```

Figure I3. A portion of the radiation.data file for NEQAIR96.

## Appendix J

### Sample Cases

Three sample cases are presented in this appendix:

- Sample Case 1. Uses the line-of-sight and nonBoltzmann options and includes two scans over the calculated spectrum with absorption.
- Sample Case 2. Uses the stagnation point and Boltzmann options with the spherical cap model option for calculating the radiative heating rate at the stagnation point of an entry vehicle. The spectra are printed in the plot file as a function of wavelength in nanometers [nm] and as a function of wavenumbers [ $\text{cm}^{-1}$ ].
- Sample Case 3. Uses the shock tube and equilibrium options. It includes two wavelength regions, an incident spectrum for region 2, and uses Voigt line shapes calculated by the code.

#### Sample Case 1

The **Input** file for sample case 1 is shown in figure J1. The region data are included as a part of the **Input** file. Portions of the **los.data**, **scan.data**, and **Output** files are shown in figures J2–J4. The complete files are included in the NEQAIR96 package sent to Users. The slit and instrument functions used are printed in the **Output** file. The first scan uses a Gaussian profile with a width of 10.0 Angstroms and the other is a linear segment slit selected to mimic the Gaussian slit. The instrument functions each are entered with only three lines including the line of 0.0's to terminate the entry of data, although they can contain up to 5000 data points. The instrument function in this case is set to 1.0 for all wavelengths. This ensures that the areas under the original spectrum and the scan spectrum are equal.

The calculated spectra for this case are shown in figures J5–J7. Figure J5 shows the spectrum from 3000 to 5000 Angstroms and figures J6 and J7 show two portions of this spectrum in greater detail. The scanned spectra are not easy to see in figure J5 but are easily seen in figures J6 and J7. The two scans are nearly identical and exactly overlay in these figures. The more detailed figures show the smoothing effect of scanning a spectrum whose resolution is 2.0 Angstroms with slit functions whose widths are 10.0 Angstroms.

The resolution of 2.0 Angstroms for the unscanned spectrum comes from the **Input** file where:

1. The spectral range in Line 11 is entered as 3000.0 to 5000.0 Angstroms.
2. The number of spectral intervals is 10,000 (spectral interval of 0.2 Angstrom).
3. Gaussian line profile with a line width at half height of 10 spectral intervals (lwidth = 2).

## Sample Case 2

The **Input** file for sample case 2 is shown in figure J8, which also includes the region data. The **los.data** file is the same as that for sample case 1 shown in figure J2. The **Output** file is shown in figure J9. The complete files are included in the NEQAIR96 package sent to Users.

Spectra at the stagnation point, from the direction of the stagnation streamline (line-of-sight), are shown in figures J10–J12. Figure J10 shows two spectra, one with and one without absorption, as a function of wavelength [nm], and figure J11 shows the spectrum with absorption as a function of wavenumber [ $\text{cm}^{-1}$ ]. The difference between the two spectra in figure J10 is small. The detailed plot in figure J12 shows the effect of absorption in the strong atomic oxygen lines near 777 nm. The continuum underlying the atomic lines is produced by large numbers of weak rotational lines and the bound-free and free-free continua.

## Sample Case 3

The **Input** file for sample case 3 is shown in figure J13, which does not include the region data. The **region.data** file is shown in figure J14, and the **Output** file is shown in figure J15. The equilibrium option is selected, so an externally derived **los.data** file is not needed. The equilibrium gas properties in the free stream ahead of the shock wave, and the properties behind the shock wave, are printed in the **Output** file. The properties behind the shock wave are used as a single layer **los.data** file. This file is written to tape unit 20 and shown in figure J16. Two regions are specified in the **region.data** file, and region 2 includes an incident spectrum. The complete files are included in the NEQAIR96 package sent to Users.

This case only calculates the three atomic oxygen lines near 1300 Angstroms and spreads them over the entire spectral region from 1298 to 1310 Angstroms by entering a value of 0 (zero) for range in the **region.data** file. The Voigt line shape is calculated by the code to produce realistic line shapes. This option was selected by entering 1 (one) for lwidth in the **region.data** file.

The calculated spectra, averaged over the time that the gates are open, are shown in figures J17–J20. Figures J17 and J18 are for region 1, and figures J19 and J20 are for region 2. The two spectral regions are identical, except that region 2 includes an incident spectrum. Also, the widths of the timing gates are slightly different in the two regions, although both gates cover the major portions of the three lines. The Planck function or Black Body spectrum for the equilibrium temperature calculated is also shown in the figures.

Figure J18 is a more detailed view of the line at 1302 Angstroms without an incident spectrum. The strong absorption in this line is evident from the figure. The shape of the line near its peak illustrates how the line broadens as the Black Body limit is approached.

The incident spectrum in region 2 can be seen in figures J19 and J20 in the space between the lines, where the absorption is small. Notice that the spectrum with absorption in figure J20 is also approaching the black body limit, as in figure J18, but in this case the Black Body limit is being approached from above because of the strong incident spectrum.

The shock tube option prints the spectral regions and timing gates for each region, the time averaged radiative heating rate  $[W/cm^2-sr]$  over each gate, and the effective emission  $[W/cm^3-sr]$ . The effective emission  $[W/cm^3-sr]$  is found by dividing the time-averaged value by the shock tube width.

```

*****
Sample Case 1. Input file for NEQAIR96

Illustrates the line-of-sight option and includes two
scans over the calculated spectra.
aaaaaaaaaaaaaaaaaaaaaaaaaaaaaaaaaaaaaaaaaaaaaaaaaaaaa <- 1st format line
123456789 123456789 123456789 123456789 123456789
An unlimited number of comment lines can go here.
All lines entered AFTER line of ***'s above, and BEFORE the first format
line (line of aaa's above) will be printed as heading lines in the Output
file. Format for the heading lines is a60.

Enter data ABOVE the format lines shown below.
Line0
*****
SPECTRUM      :Dont Create 0;   Create Only 0;   Create and Scan X;   Scan Only 0
Line1          a                   a                   a                   a
-----
PLOT UNITS    : Angstroms X;   NanoMeters 0;   Wave Numbers 0;
Line2          a                   a                   a
-----
PLOT FORMAT   :Plot File(s) are Formatted X;   Unformatted 0
Line3          a                   a
-----
PRINT OUT     : LOS Data 0; Spectros Data 0;   Extra Plot at Grid # jx= 0;
Line4          a                   a                   iii
-----
KIND OF FLOW  :nonBoltzmann X; d= 1.0; Boltzmann 0 Equilibrium 0; BlackBody 0
Line5          a   rrrrrrr   a                   a   a
-----
EQUILIBRIUM   : Temp= 0.0 K Rho= 0.000e-0 gm/cm3 LOSlength= 0.0 cm
Line6          rrrrrrr   rrrrrrrrrrrrr   rrrrrrr
Species Molfrac :For a known condition where Sum Molfrac=1.0
0.0 :end species entry with blank and 0.0
aaaaaaa rrrrrrrrrrrrr:left justify species (enter above this line)
-----
TYPE OF GEOM.:Line-of-Sight X; Stag Point 0; Shock Tube 0;
Line7          a                   a                   a
-----
FOR STAG PT. :Infinite Slab 0; Sphere. Cap 0; Rnose= 0.0 cm; Shock Div= 0.0
Line8          a                   a   rrrrrrr   rrrrrrr
-----
FOR SHOCK T. :Stwidth= 0.0cm; VS= 0.0 km/s; Rho1= 0.000e-0gm/cc; Temp1= 0.0K
Line9          rrrrrr   rrrrrrr   rrrrrrrrrrr   rrrrrrr
-----

```

Figure J1(a). Input file for sample case 1.

```

SYSTEMS      :Spectral Systems in Spectrum
Line10
      :Atomic Systems
      Escape Factors= Calculated X or 0.0
                        a rrrrr
Atom    smf:b-b      smf:b-f      smf:f-f
N        1.0          1.0          1.0
O        0.0          1.0          1.0
C        0.0          1.0          1.0
H        0.0          0.0          0.0
He       0.0          0.0          0.0
         0.0          0.0          0.0 :End with blank and 0.0's.
aaaaaaa rrrrr      rrrrr      rrrrr

      :Diatomic Electronic Transition Systems
      IPEAK= -9; Keep vib bands; Ivv>Imax*10**IPEAK
      iiii

      Save      Major
      Rot EHL  One Band  SpinMult  Branches  vvExtend  Nmax
Diatomic  smf Files  YN (vu,vl)  Use Real  Only!      [Ang's]
-----
1 N2+ 1-   1.0  X      0 ( 0, 0)  1 2      X          0.0      0
2 N2 1+   0.0  X      0 ( 0, 0)  1 3      X          0.0      0
3 N2 2+   0.0  X      0 ( 0, 0)  1 3      X          0.0      0
4 N2 BH2  0.0  X      0 ( 0, 0)  1 1      X          0.0      0
5 NO beta 0.0  X      0 ( 0, 0)  1 2      X          0.0      0
6 NO gam  0.0  X      0 ( 0, 0)  1 2      X          0.0      0
7 NO del  0.0  X      0 ( 0, 0)  1 2      X          0.0      0
8 NO eps  0.0  X      0 ( 0, 0)  1 2      X          0.0      0
9 NO bp   0.0  X      0 ( 0, 0)  1 2      X          0.0      0
10 NO gp  0.0  X      0 ( 0, 0)  1 2      X          0.0      0
11 O2 SR  0.0  X      0 ( 0, 0)  1 3      X          0.0      0
12 CN VIO 0.0  X      0 ( 0, 0)  1 2      X          0.0      0
13 CN RED 0.0  X      0 ( 0, 0)  1 2      X          0.0      0
14 CO 4+  0.0  X      0 ( 0, 0)  1 1      X          0.0      0
15 C2 Swan 0.0  X      0 ( 0, 0)  1 3      X          0.0      0
16 OH A-X  0.0  X      0 ( 0, 0)  1 2      X          0.0      0
17 H2 B-X  0.0  X      0 ( 0, 0)  1 1      X          0.0      0
18 H2 C-X  0.0  X      0 ( 0, 0)  1 1      X          0.0      0
19 H2 B'-X 0.0  X      0 ( 0, 0)  1 1      X          0.0      0
         0.0  0      0 ( 0, 0)  0 0      0          0.0      0:End Line
aaaaaaa rrrrr  a      a ii ii  i i      a      rrrrr      iii

      :Diatomic Infra-Red Transition Systems

      Save      Major
      Rot EHL  One Band  SpinMult  Branches
Diatomic  smf Files  YN (vu, vl)  Use Real  Only!
-----
1 NO      0.0  X      0 ( 0, 0)  1 2      X
2 CN      0.0  X      0 ( 0, 0)  1 2      X
3 CO      0.0  X      0 ( 0, 0)  1 1      X
4 OH      0.0  X      0 ( 0, 0)  1 2      X
5 NH      0.0  X      0 ( 0, 0)  1 3      X
6 CH      0.0  X      0 ( 0, 0)  1 2      X
         0.0  0      0 ( 0, 0)  0 0      0:End Line
aaaaaaa rrrrr  a      a ii ii  i i      a

Actual spin mult. does not need to be entered, it is informational only.
Bands with origins from w1-vvExtend to w2+vvExtend of the wavelength range
w1-w2 are included. Enter vvExtend=0.0 to include all bands.
Nmax limits the number of rotational lines; enter 0(zero)to keep all rot lines.
-----

```

Figure J1(b). Input file for sample case 1 (continued).

```

REGION DATA:      Lines11-12      regionfile = 5;
If regionfile=5, data follow; else on unit # =regionfile. iii
*****
                        template.region file

                        Template of Region file for NEQAIR96

An unlimited number of comment lines can go here.

Enter Region data ABOVE the data format lines in this file.

To enter an incident spectrum for a Region enter something other
than zero in the "check location" after INCIDENT SPECTRUM, and ABOVE
the 1st format line as shown below, and enter the incident spectrum
values above the 3rd format line.

If an incident spectrum is not needed, the incident spectrum lines
can be removed or left in. If removed, remove all lines after the
1st format line and before the line of ---'s, including the blank
line immediately after the 2nd format line.

The line of ---'s after the 3rd format line, and all of the timing gate
lines can be removed, except when timing gates are needed for a shock
tube flow case.

The line of +++'s must be retained for each region.

End region input with anything but 'REGION' in first 6 characters of
1st data line.

*****
REGION 1      :10 regions allowed.  INCIDENT SPECTRUM 0;      <- 1st data line.
aaaaaa                        a      <- 1st format line.
Line 11
    w1 [A]    w2 [A]    narray    range    shape    wg [A]    w1 [A]
    3000.0    5000.0    10000     3        2        0.0      0.0
    rrrrrrrr rrrrrrrr iiiiiiiii iiiiiiiii iiiiiiiii rrrrrrrr rrrrrrrr <- 2nd.

        Wavelength    Specific Intensity    Incident Spectrum, if needed
            [A]          [W/cm2-micron-sr]
            0.0          0.0      :End with 0.0's as shown here.
    rrrrrrrr rrrrrrrrrrrrrr      (10x,e10.0,e15.0)      <- 3rd.
-----
Line 12      :Shock tube timing gates, as needed.  10 gates allowed all regions.
            Enter gates for region after next line.  End entry with all 0.0's.
tstart [s] topen [s] lam1 [A] lam2 [A] planckT[K]
    0.0      0.0      0.0      0.0      0.0
    rrrrrrrr rrrrrrrr rrrrrrrr rrrrrrrr rrrrrrrr (5e10.0)      <- 4th.
*****
            :Repeat REGION to +++'s line for new region, or end as noted above.
-----
LINE-of-SIGHT DATA: Line13      losfile      = 90;
If losfile =5, data follow; else on unit # =losfile.  iii
-----
SCAN SPECTRA DATA: Line14      scanfile      = 95;
If scanfile =5, data follow; else on unit # =scanfile.  iii
-----

```

*Figure J1(c). Input file for sample case 1 (concluded).*

```

*****
                      LOS file for Sample Cases 1 and 2

Enter Data AFTER the data-format lines!

(1) Enter species in any order; limited to atoms, diatomics, triatomics,
    atomic ions, diatomic ions, and electrons. Left-justify the species
    symbols in the fields. Dimensioned up to 25 species. End entry
    with a blank line.

(2) Properties entered at each grid point along line-of-sight. The
    properties apply to the layer between the grid point and the
    previous grid point. Thus, the properties at the first grid point
    are not used. This grid point only establishes the origin of the
    line-of-sight.

(3) Enter species number densities [cm-3] in the same order that the species
    symbols are entered. End data entry at each grid point with a blank
    line.

(4) End line-of-sight data entry, with a line of 0's as shown.

*****
    aaaaaaaa      aaaaaaaa      aaaaaaaa      aaaaaaaa      (2x, (7x,a8))
    Ar            C            N            O            :Species Symbols.
    C2            N2            O2            CN
    CO            NO            CO2           Ar+
    C+            N+            O+            N2+
    O2+           NO+           E-

-----
no.  x,cm  total partcc  t      tr      tv      te (i5,f8.3,
iiii rrrrrr rrrrrrrrrrrr rrrrrrrr rrrrrrrr rrrrrrrr rrrrrrrrrr15.6,4f10.1
rrrrrrrrrrrr rrrrrrrrrrrr rrrrrrrrrrrr rrrrrrrrrrrr (6x,4e15.6)
Include these 9 lines (from --- to --- lines) for first grid point only!!
End each grid point entry with a blank line.
End data file with a line of zero's as shown on the next line.
0      0.0      0.0      0.0      0.0      0.0      0.0

-----
1  0.000  2.076137E+16  50134.5  50134.5  1670.3  1670.3
    1.862807E+14  6.641611E+07  6.203195E+13  1.605643E+14
    1.971826E+02  1.625456E+16  4.078477E+15  4.917564E+07
    3.635425E+10  1.286579E+13  6.552627E+12  9.064549E+03
    5.974110E-03  2.718353E+08  5.108293E+07  5.974110E-03
    3.200198E+08  5.974110E-03  6.429471E+08

2  0.054  2.121777E+16  48934.0  48934.0  3466.5  3466.5
    1.888891E+14  1.626522E+08  1.244391E+14  5.961418E+14
    4.605673E+01  1.636908E+16  3.897452E+15  9.589355E+07
    1.368933E+11  3.501815E+13  6.534951E+12  1.225127E+04
    7.255302E+02  6.034417E-03  6.034417E-03  1.396579E+10
    2.448981E+10  1.649942E+09  4.010555E+10

38  8.800  1.200292E+17  10061.7  10061.7  10064.5  10064.5
    5.030145E+14  9.735898E+12  8.261776E+16  2.274643E+16
    4.572317E+04  4.708609E+13  2.761956E+10  2.361691E+09
    3.828541E+09  1.604640E+12  1.135310E+03  2.485872E+13
    8.992013E+12  5.945074E+15  1.066582E+15  1.928016E+12
    1.346651E+10  4.310707E+12  7.051759E+15

39  9.957  1.200292E+17  10061.7  10061.7  10064.5  10064.5
    5.030179E+14  9.735879E+12  8.261774E+16  2.274647E+16
    4.572261E+04  4.708604E+13  2.761958E+10  2.361679E+09
    3.828481E+09  1.604636E+12  1.135972E+03  2.485549E+13
    8.992034E+12  5.945116E+15  1.066547E+15  1.928011E+12
    1.346653E+10  4.310711E+12  7.051762E+15

0      0.0      0.0      0.0      0.0      0.0      0.0

```

Figure J2. Los.data file for sample cases 1 and 2.

```

*****
Scan file for Sample Case 1 for NEQAIR96

Two scans: 1. 10 Angstrom wide Gaussian slit.
           2. 10 Angstrom wide Linear Segments slit that mimics
              the 10 Angstrom wide Gaussian slit.
Enter Data ABOVE the data format lines!

*****
SCAN NO. 1. Enter "SCAN NO." for new scan or 8 blanks to end scans.
aaaaaaaa                                     <- 1st format line.
Voigt                                     :Enter Cap V in first character for Voigt slit function.
      1 :Enter Type Slit Function, and Region or Gate Number.
aaaaaaaaaaaaaaaa iiii (a15,i5)           <- 2nd format line.
-----
Enter Slit Parameters. (Next 2 lines are each the 2nd format line.)
10.0      0.0      3
rrrrrrrrrr rrrrrrrrr iiii Voigt Slit : widthg[A], widthl[A], range.
rrrrrrrrrr rrrrrrrrr aaaa Linear slit: lam[A], height, plus "line" at line
format(5x,2e10.0,a5)                center point; " end" at last point.
-----
Enter Spectral Interval for scan and scan step [A].
3100.0    4900.0    1.0
rrrrrrrrrr rrrrrrrrrrr rrrrrrrrrrr (3e10.0) <- 3rd format line.
-----
Enter Instrument Function. Wavelength [A] and Instrument Calibration.
(At least 2 lines must be entered, including the line of 0.0's to end entry.)
1500.0      1.0
5500.0      1.0
0.0          0.0 : Enter 0.0's to end instrument function.
rrrrrrrrrr rrrrrrrrrrr (2e10.0) <- 4th format line.
*****
SCAN NO. 2. Enter "SCAN NO." for new scan or 8 blanks to end scans.
aaaaaaaa                                     <- 1st format line.
Linear Segment :Enter Cap V in first character for Voigt slit function.
      1 :Enter Type Slit Function, and Region or Gate Number.
aaaaaaaaaaaaaaaa iiii (a15,i5)           <- 2nd format line.
-----
Enter Slit Parameters. (Next 2 lines are each the 2nd format line.)
1      0.0      0.00000
2      0.4      0.00001
3      0.8      0.00001

52     20.4     0.98242
53     20.8     0.99557
54     21.2     1.00000 line
55     21.6     0.99557
56     22.0     0.98242

106     42.0     0.00001
107     42.4     0.00000 end
rrrrrrrrrr rrrrrrrrrrr iiii Voigt Slit : widthg[A], widthl[A], range.
rrrrrrrrrr rrrrrrrrrrr aaaa Linear slit: lam[A], height, plus "line" at line
format(5x,2e10.0,a5)                center point; " end" at last point.
-----
Enter Spectral Interval for scan and scan step [A].
3100.0    4900.0    1.0
rrrrrrrrrr rrrrrrrrrrr rrrrrrrrrrr (3e10.0) <- 3rd format line.
-----
Enter Instrument Function. Wavelength [A] and Instrument Calibration.
(At least 2 lines must be entered, including the line of 0.0's to end entry.)
1500.0      1.0
5500.0      1.0
0.0          0.0 : Enter 0.0's to end instrument function.
rrrrrrrrrr rrrrrrrrrrr (2e10.0) <- 4th format line.
*****
:Enter SCAN NO. for new slit, or 8 spaces to end entry.

```

Figure J3. Scan.data file for sample case 1.

Sample Case 1. Output file for NEQAIR96

Illustrates the line-of-sight option and includes two scans over the calculated spectra.

STANDARD OUTPUT FOR NEQAIR

Line 1; A Spectrum was Created AND Scanned.  
 Line 2; Spectra Files are Printed versus: Angstroms.  
 Line 3; Spectral Plot Files are FORMATTED.  
 Line 4; Spectrum Plotted for Last Field Pt.  
 Line 5; Radiation is for Non Boltzmann Excitation.  
 Line 6; NOT Used in this Case (Equilibrium).  
 Line 7; This is a Line-of-Sight (LOS) Geometry Case.  
 Lines 8-9; Not used in this case (Stag Pt and Shock Tube).  
 Line 10; Spectral Systems and Parameters

Atomic Systems

Line 10; All b-b atomic Escape Factors are calculated.

	Atom	smf:b-b	smf:b-f	smf:f-f
1	N	1.00	1.00	1.00
2	O	0.00	1.00	1.00
3	C	0.00	1.00	1.00

Diatomic Electronic Transition Systems

Line 10; IPEAK for diatomic bands = -9

Diatomic	Save Rot EHL smf Files	One Band YN (vu, vl)	SpinMult Use Real	Major Branches		Nmax
				Only!	vvExtend [Angstrom]	
1 N2+ 1-	1.00 X	0 ( 0, 0)	1 2	X	0.0	0

Line 11; Wavelength Regions; and Incident Spectra as Needed.  
 Line 12; NOT used in this case (Timing Gates).

Spectral Regions

region	w1	w2	narray	dellam	range	lshape	widthg	widthl
1	3000.000	5000.000	10001	0.2000	3	2	2.0000	0.0000

Line 13; The Line-of-Sight Data are NOT Printed for this case.  
 Line-of-Sight Data are on Unit 90.  
 Line 14; Scan Data are on Unit 95.  
 Scan Data are Reproduced Below.

Figure J4(a). Output file for sample case 1.

Heat flux per sr along the central streamline

jx	x(cm)	power(w/cm2-sr)	powerthin(w/cm2-sr)
1	0.0000	0.0000E+00	0.0000E+00
2	0.0540	1.3011E-08	1.3011E-08
3	0.1110	1.3013E-08	1.3013E-08
4	0.1700	1.5775E-04	1.5775E-04
5	0.2330	1.7360E-03	1.7360E-03
6	0.2980	2.3919E-02	2.3919E-02
7	0.3660	1.3225E-01	1.3225E-01
8	0.4360	2.5558E-01	2.5558E-01
29	2.8530	7.6006E-01	7.6006E-01
30	3.1710	7.7924E-01	7.7924E-01
31	3.5450	8.0181E-01	8.0181E-01
32	3.9850	8.2836E-01	8.2836E-01
33	4.5010	8.5950E-01	8.5951E-01
34	5.1080	8.9612E-01	8.9613E-01
35	5.8210	9.3913E-01	9.3915E-01
36	6.6590	9.8968E-01	9.8970E-01
37	7.6440	1.0491E+00	1.0491E+00
38	8.8000	1.1188E+00	1.1189E+00
39	9.9570	1.1886E+00	1.1887E+00

Spectral Power along flow for region 1 from 3000.000 to 5000.000 Angstroms.

	x (cm)	ttran	trot	tvib	telec	particle density (cm-3)	emission (w/cm3-sr)	infinite slab opt-thin-flux (w/cm2)
1	0.000						0.000E+00	0.000E+00
2	0.054	48934.	48934.	3467.	3467.	2.122E+16	2.410E-07	8.178E-08
3	0.111	47082.	47082.	5343.	5343.	2.211E+16	2.756E-11	8.179E-08
4	0.170	44166.	44166.	7515.	7515.	2.374E+16	2.675E-03	9.916E-04
5	0.233	39546.	39546.	9540.	9540.	2.685E+16	2.506E-02	1.091E-02
6	0.298	32054.	32054.	12832.	12832.	3.384E+16	3.414E-01	1.503E-01
7	0.366	24583.	24583.	14554.	14554.	4.548E+16	1.594E+00	8.313E-01
8	0.436	20666.	20666.	12825.	12825.	5.492E+16	1.763E+00	1.606E+00
29	2.853	10071.	10071.	10066.	10066.	1.199E+17	5.770E-02	4.756E+00
30	3.171	10064.	10064.	10065.	10065.	1.200E+17	5.773E-02	4.872E+00
31	3.545	10062.	10062.	10065.	10065.	1.200E+17	5.776E-02	5.008E+00
32	3.985	10061.	10061.	10065.	10065.	1.200E+17	5.776E-02	5.167E+00
33	4.501	10061.	10061.	10065.	10065.	1.200E+17	5.776E-02	5.355E+00
34	5.108	10061.	10061.	10065.	10065.	1.200E+17	5.775E-02	5.575E+00
35	5.821	10062.	10062.	10065.	10065.	1.200E+17	5.775E-02	5.833E+00
36	6.659	10062.	10062.	10065.	10065.	1.200E+17	5.774E-02	6.138E+00
37	7.644	10062.	10062.	10065.	10065.	1.200E+17	5.774E-02	6.495E+00
38	8.800	10062.	10062.	10065.	10065.	1.200E+17	5.774E-02	6.914E+00
39	9.957	10062.	10062.	10065.	10065.	1.200E+17	5.774E-02	7.334E+00

Figure J4(b). Output file for sample case 1 (continued).

```

-----
Spectral Scan Data

SCAN NUMBER  1
-----

Type Bandpass = Voigt                      Region  1.

Line-of-Sight Scan.
Input  Spectrum on fort.21.
Output Spectrum on fort.31.

widthg  widthl  widthv  range
10.000  0.000  10.000   3

scanstart  scanend  scanstep
3100.00    4900.00    1.00

calibration: wavelength    factor
1  1500.00    1.00000E+00
2  5500.00    1.00000E+00
-----

SCAN NUMBER  2
-----

Type Bandpass = Linear Segment            Region  1.

Line-of-Sight Scan.
Input  Spectrum on fort.21.
Output Spectrum on fort.31.

Relative Central Wavelength = 21.20 Ang
Bandpass Effective Width   = 10.65 Ang

Bandpass: Relative Wavelength  Height  Center
1  0.00000  0.00000
2  0.40000  0.00001

53 20.80000  0.99557
54 21.20000  1.00000  Band Center
55 21.60000  0.99557
56 22.00000  0.98242

107 42.40000  0.00000

scanstart  scanend  scanstep
3100.00    4900.00    1.00

calibration: wavelength    factor
1  1500.00    1.00000E+00
2  5500.00    1.00000E+00
-----

Total lines calculated                = 1170400.
Total lines spread into spectrum      = 976752.

Total run time                        = 30.618 seconds.
Time to cal Rot Energys and HL (EHL) files = 0.000 seconds.
Time to calculate and spread rotational lines = 4.992 seconds.
Time to spread rotational lines        = 4.014 seconds.

```

*Figure J4(c). Output file for sample case 1 (concluded).*

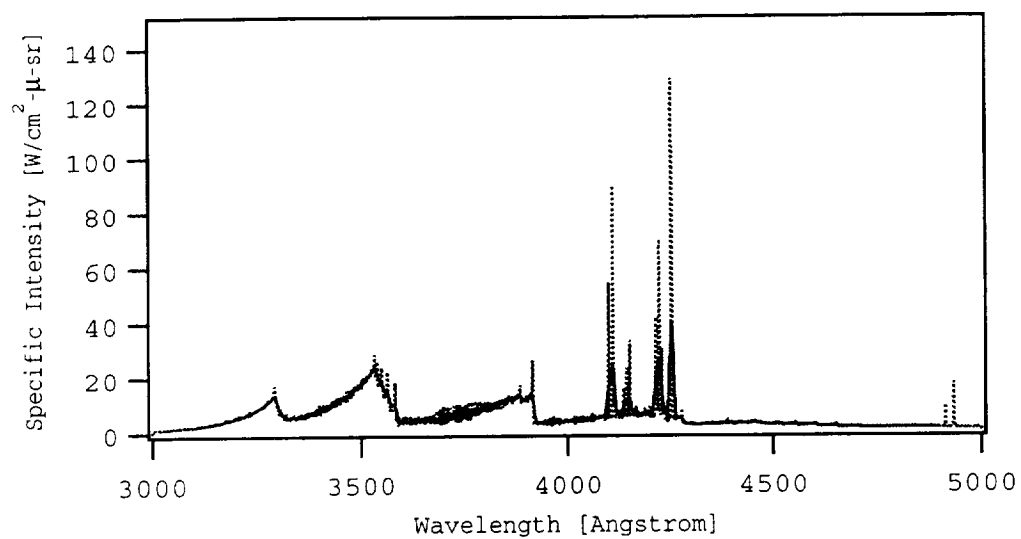


Figure J5. Calculated and scanned spectra from sample case 1.

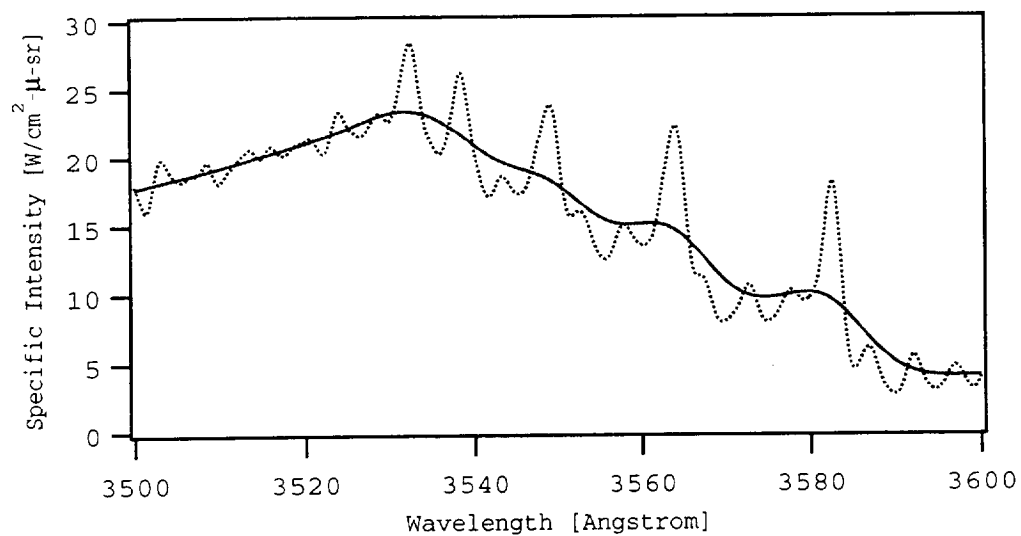
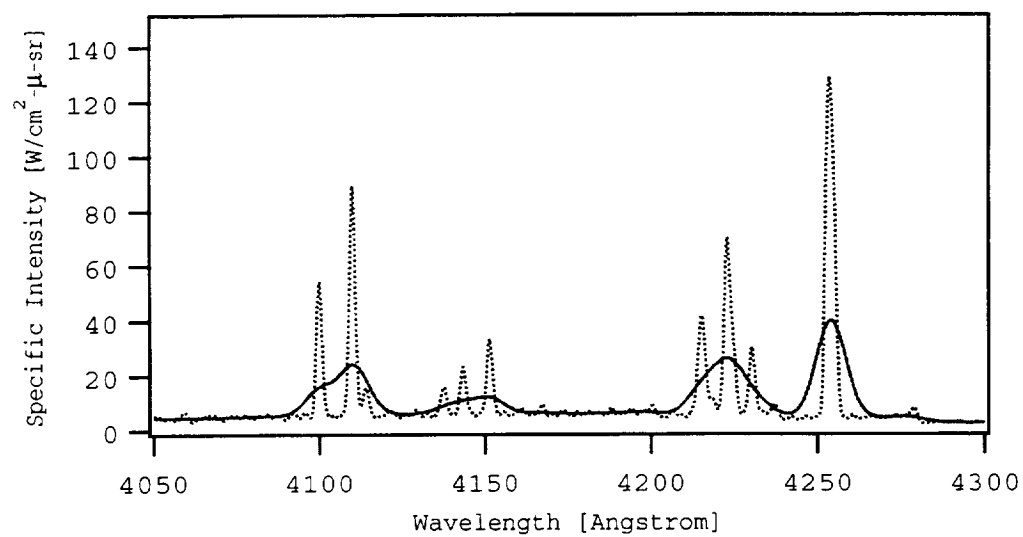


Figure J6. Calculated and scanned spectra of the  $\Delta v = 1$  sequence of  $N_2^+(1-)$  from sample case 1.



*Figure J7. Calculated and scanned spectra of atomic N lines from sample case 1.*

```

*****
Sample Case 2. Input file for NEQAIR96

Illustrates the stagnation point option and the spherical
cap model option for calculating the radiative heating rate
at the stagnation point. Two spectra are written to the
Plot file (on tape unit 21, fort.21) one in terms of
wavelength [nm] and the other in terms of wavenumber [cm-1].
aaaaaaaaaaaaaaaaaaaaaaaaaaaaaaaaaaaaaaaaaaaaaaaaaaaaaaa <- 1st format line
123456789 123456789 123456789 123456789 123456789 123456789
template.input

Template of Input file for NEQAIR(96)

An unlimited number of comment lines can go here.

All lines entered AFTER line of ***'s above, and BEFORE the first format
line (line of aaa's above) will be printed as heading lines in the Output
file. Format for the heading lines is a60.

Enter data ABOVE the format lines shown below.

Line0
*****
SPECTRUM      :Dont Create 0;   Create Only X;   Create and Scan 0;   Scan Only 0
Line1          a                a                a                a
-----
PLOT UNITS    : Angstroms 0;   NanoMeters X;   Wave Numbers X;
Line2          a                a                a
-----
PLOT FORMAT   :Plot File(s) are Formatted X;   Unformatted 0
Line3          a                a
-----
PRINT OUT     : LOS Data 0; Spectros Data 0;   Extra Plot at Grid # jx= 0;
Line4          a                a                iii
-----
KIND OF FLOW  :nonBoltzmann 0; d= 0.0; Boltzmann X Equilibrium 0; BlackBody 0
Line5          a      rrrrrrr      a                a                a
-----
EQUILIBRIUM   : Temp= 0.0 K Rho= 0.000e-0 gm/cm3 LOSlength= 0.0 cm
Line6          rrrrrrr      rrrrrrrrrrrrr      rrrrrrr
Species Molfrac :For a known condition where Sum Molfrac=1.0
0.0 :end species entry with blank and 0.0
aaaaaaa rrrrrrrrrrrrr:left justify species (enter above this line)
-----
TYPE OF GEOM.:Line-of-Sight 0; Stag Point X; Shock Tube 0;
Line7          a                a                a
-----
FOR STAG PT. :Infinite Slab 0; Sphere. Cap X; Rnose= 60.0 cm; Shock Div= 0.0
Line8          a                a      rrrrrrr      rrrrrrr
-----
FOR SHOCK T. :STwidth= 0.0cm; VS= 0.0 km/s; Rho1= 0.000e-0gm/cc; Temp1= 0.0K
Line9          rrrrrr      rrrrrr      rrrrrrrrrrrrr      rrrrrrr
-----

```

Figure J8(a). Input file for sample case 2.

```

SYSTEMS      :Spectral Systems in Spectrum
Line10
      :Atomic Systems
      Escape Factors= Calculated X or 0.0
                        a rrrrr
Atom    smf:b-b      smf:b-f      smf:f-f
N        0.0          1.0          1.0
O        1.0          1.0          1.0
C        0.0          1.0          1.0
H        0.0          0.0          0.0
He       0.0          0.0          0.0
        0.0          0.0          0.0 :End with blank and 0.0's.
aaaaaaa rrrrr      rrrrr      rrrrr

      :Diatomic Electronic Transition Systems
      IPEAK= -9; Keep vib bands; Ivv>Imax*10**IPEAK
      iiii

      Save      Major
      Rot EHL One Band SpinMult Branches vvExtend Nmax
      Diatomic smf Files YN (vu,vl) Use Real Only! [Ang's]
-----
1 N2+ 1-      1.0 X 0 ( 0, 0) 1 2 X 0.0 0
2 N2 1+      0.0 X 0 ( 0, 0) 1 3 X 0.0 0
3 N2 2+      1.0 X 0 ( 0, 0) 1 3 X 0.0 0
4 N2 BH2     0.0 X 0 ( 0, 0) 1 1 X 0.0 0
5 NO beta    0.0 X 0 ( 0, 0) 1 2 X 0.0 0
6 NO gam     0.0 X 0 ( 0, 0) 1 2 X 0.0 0
7 NO del     0.0 X 0 ( 0, 0) 1 2 X 0.0 0
8 NO eps     0.0 X 0 ( 0, 0) 1 2 X 0.0 0
9 NO bp      0.0 X 0 ( 0, 0) 1 2 X 0.0 0
10 NO gp     0.0 X 0 ( 0, 0) 1 2 X 0.0 0
11 O2 SR     0.0 X 0 ( 0, 0) 1 3 X 0.0 0
12 CN VIO    1.0 X 0 ( 0, 0) 1 2 X 0.0 0
13 CN RED    0.0 X 0 ( 0, 0) 1 2 X 0.0 0
14 CO 4+     0.0 X 0 ( 0, 0) 1 1 X 0.0 0
15 C2 Swan   0.0 X 0 ( 0, 0) 1 3 X 0.0 0
16 OH A-X    0.0 X 0 ( 0, 0) 1 2 X 0.0 0
17 H2 B-X    0.0 X 0 ( 0, 0) 1 1 X 0.0 0
18 H2 C-X    0.0 X 0 ( 0, 0) 1 1 X 0.0 0
19 H2 B'-X   0.0 X 0 ( 0, 0) 1 1 X 0.0 0
        0.0 0 0 ( 0, 0) 0 0 0 0.0 0:End Line
aaaaaaa rrrrr a a ii ii i i a rrrrrr iii

      :Diatomic Infra-Red Transition Systems

      Save      Major
      Rot EHL One Band SpinMult Branches
      Diatomic smf Files YN (vu, vl) Use Real Only!
-----
1 NO      0.0 X 0 ( 0, 0) 1 2 X
2 CN      0.0 X 0 ( 0, 0) 1 2 X
3 CO      0.0 X 0 ( 0, 0) 1 1 X
4 OH      0.0 X 0 ( 0, 0) 1 2 X
5 NH      0.0 X 0 ( 0, 0) 1 3 X
6 CH      0.0 X 0 ( 0, 0) 1 2 X
        0.0 0 0 ( 0, 0) 0 0 0:End Line
aaaaaaa rrrrr a a ii ii i i a

```

Actual spin mult. does not need to be entered, it is informational only.  
Bands with origins from w1-vvExtend to w2+vvExtend of the wavelength range  
w1-w2 are included. Enter vvExtend=0.0 to include all bands.  
Nmax limits the number of rotational lines; enter 0(zero) to keep all rot lines.

Figure J8(b). Input file for sample case 2 (continued).

```

REGION DATA:      Lines11-12      regionfile = 5;
If regionfile=5, data follow; else on unit # =regionfile. iii
*****
                        template.region file

                        Template of Region file for NEQAIR96

An unlimited number of comment lines can go here.

Enter Region data ABOVE the data format lines in this file.

To enter an incident spectrum for a Region enter something other
than zero in the "check location" after INCIDENT SPECTRUM, and ABOVE
the 1st format line as shown below, and enter the incident spectrum
values above the 3rd format line.

If an incident spectrum is not needed, the incident spectrum lines
can be removed or left in. If removed, remove all lines after the
1st format line and before the line of ---'s, including the blank
line immediately after the 2nd format line.

The line of ---'s after the 3rd format line, and all of the timing gate
lines can be removed, except when timing gates are needed for a shock
tube flow case.

The line of +++'s must be retained for each region.

End region input with anything but 'REGION' in first 6 characters of
1st data line.

*****
REGION 1      :10 regions allowed.  INCIDENT SPECTRUM 0;      <- 1st data line.
aaaaaa                        a      <- 1st format line.
Line 11
      w1 [A]    w2 [A]    narray    range    shape    wg [A]    wl [A]
      5000.0   11000.0   12000      3        2        0.0      0.0
      rrrrrrrr rrrrrrrr iiiiiiiiii iiiiiiiiii iiiiiiiiii rrrrrrrr rrrrrrrr <- 2nd.

      Wavelength    Specific Intensity    Incident Spectrum, if needed
      [A]            [W/cm2-micron-sr]
      0.0            0.0      :End with 0.0's as shown here.
      rrrrrrrr rrrrrrrrrrrr      (10x,e10.0,e15.0)      <- 3rd.
-----
Line 12      :Shock tube timing gates, as needed.  10 gates allowed all regions.
      Enter gates for region after next line.  End entry with all 0.0's.
tstart [s] topen [s] lam1 [A] lam2 [A] planckT[K]
      0.0      0.0      0.0      0.0      0.0
      rrrrrrrr rrrrrrrr rrrrrrrr rrrrrrrr rrrrrrrr (5e10.0)      <- 4th.
*****
      :Repeat REGION to +++'s line for new region, or end as noted above.
-----
LINE-of-SIGHT DATA: Line13      losfile    = 90;
If losfile =5, data follow; else on unit # =losfile.    iii
-----
SCAN SPECTRA DATA: Line14      scanfile    = 0;
If scanfile =5, data follow; else on unit # =scanfile.    iii
-----

```

Figure J8(c). Input file for sample case 2 (concluded).

Sample Case 2. Output file for NEQAIR96

Illustrates the stagnation point option and the spherical cap model option for calculating the radiative heating rate at the stagnation point. Two spectra are written to the Plot file (on tape unit 21, fort.21) one in terms of wavelength [nm] and the other in terms of wavenumber [cm-1].

STANDARD OUTPUT FOR NEQAIR

Line 1; A Spectrum was Created but NOT Scanned.  
 Line 2; Spectra Files are Printed versus: Nanometers.  
 Line 2; Spectra Files are Printed versus: Wavenumbers.  
 Line 3; Spectral Plot Files are FORMATTED.  
 Line 4; Spectrum Plotted for Last Field Pt.  
 Line 5; Radiation is for Boltzmann Excitation.  
 Line 6; NOT Used in this Case (Equilibrium).  
 Line 7; This is a Stagnation Point Geometry Case.  
 Line 8; The Stagnation Point Flow is Modeled as a Spherical Cap.  
 Line 8; Rnose = 60.00 cm. Shock Divergence = 0.00 cm/radian.  
 Line 9; NOT used in this case; for Shock Tube Flow.  
 Line 10; Spectral Systems and Parameters

Atomic Systems

	Atom	smf:b-b	smf:b-f	smf:f-f
1	N	0.00	1.00	1.00
2	O	1.00	1.00	1.00
3	C	0.00	1.00	1.00

Diatomic Electronic Transition Systems

Line 10; IPEAK for diatomic bands = -9

Diatomic		smf	Save Rot EHL Files	One Band YN (vu, vl)	SpinMult Use Real	Major		Nmax
						Branches Only!	vvExtend [Angstrom]	
1	N2+ 1-	1.00	X	0 ( 0, 0)	1 2	X	0.0	0
2	N2 2+	1.00	X	0 ( 0, 0)	1 3	X	0.0	0
3	CN VIO	1.00	X	0 ( 0, 0)	1 2	X	0.0	0

Line 11; Wavelength Regions; and Incident Spectra as Needed.  
 Line 12; NOT used in this case (Timing Gates).

Spectral Regions

region	w1	w2	narray	dellam	range	lshape	widthg	widthl
1	5000.000	11000.000	12001	0.5000	3	2	5.0000	0.0000

Line 13; The Line-of-Sight Data are NOT Printed for this case.  
 Line-of-Sight Data are on Unit 90.  
 Line 14; Scanning Data are NOT Used in this Case.

Figure J9(a). Output file for sample case 2.

Heat flux per sr along the central streamline			
jx	x(cm)	power(w/cm2-sr)	powerthin(w/cm2-sr)
1	0.0000	0.0000E+00	0.0000E+00
2	0.0540	4.3700E-11	4.3700E-11
3	0.1110	9.2353E-09	9.2353E-09
4	0.1700	1.7401E-05	1.7401E-05
5	0.2330	1.0752E-03	1.0752E-03
6	0.2980	6.0620E-02	6.0671E-02
7	0.3660	3.8718E-01	3.8874E-01
8	0.4360	5.0950E-01	5.1253E-01
9	0.5100	5.6124E-01	5.6518E-01
10	0.5860	5.8965E-01	5.9422E-01
11	0.6650	6.0921E-01	6.1426E-01
12	0.7470	6.2527E-01	6.3075E-01
13	0.8310	6.3976E-01	6.4566E-01
14	0.9180	6.5411E-01	6.6044E-01
15	1.0080	6.6885E-01	6.7563E-01
16	1.1010	6.8472E-01	6.9200E-01
17	1.1970	7.0166E-01	7.0949E-01
18	1.2950	7.2040E-01	7.2884E-01
19	1.3960	7.3991E-01	7.4901E-01
20	1.4600	7.5245E-01	7.6198E-01
21	1.5340	7.6734E-01	7.7739E-01
22	1.6220	7.8563E-01	7.9632E-01
23	1.7250	8.0776E-01	8.1922E-01
24	1.8460	8.3461E-01	8.4702E-01
25	1.9880	8.6716E-01	8.8071E-01
26	2.1550	9.0644E-01	9.2138E-01
27	2.3510	9.5314E-01	9.6980E-01
28	2.5820	1.0083E+00	1.0271E+00
29	2.8530	1.0730E+00	1.0944E+00
30	3.1710	1.1488E+00	1.1734E+00
31	3.5450	1.2377E+00	1.2664E+00
32	3.9850	1.3419E+00	1.3757E+00
33	4.5010	1.4636E+00	1.5039E+00
34	5.1080	1.6062E+00	1.6547E+00
35	5.8210	1.7727E+00	1.8318E+00
36	6.6590	1.9672E+00	2.0400E+00
37	7.6440	2.1941E+00	2.2847E+00
38	8.8000	2.4582E+00	2.5718E+00
39	9.9570	2.7201E+00	2.8593E+00
Radiative heating rate for shock layer, $rs=r+\delta(1+c*\phi)$			
Effective Nose Radius = 60.0 cm			
Shock Standoff Dist, Delta = 10.0 cm			
c = Shock Divergence = 0.00 cm/radian			
Total radiative heating rate at the surface point = 1.2316740E+01 watts/cm2			
The integral of the heating flux with theta is:			
Theta(degrees)	Power(watts/cm2)		
0.00	0.0000000E+00		
10.00	2.6032555E-01		
20.00	1.0247036E+00		
30.00	2.2594906E+00		
40.00	3.8948628E+00		
50.00	5.8359706E+00		
60.00	7.9335765E+00		
70.00	9.9740826E+00		
80.00	1.1611832E+01		
90.00	1.2316740E+01		

Figure J9(b). Output file for sample case 2 (continued).

Spectral Power along flow for region 1 from 5000.000 to 11000.000 Angstroms.								
	x (cm)	ttran	trot	tvib	telec	particle density (cm-3)	emission (w/cm3-sr)	infinite slab opt-thin-flux (w/cm2)
1	0.000						0.000E+00	0.000E+00
2	0.054	48934.	48934.	3467.	3467.	2.122E+16	8.117E-10	2.754E-10
3	0.111	47082.	47082.	5343.	5343.	2.211E+16	1.613E-07	5.805E-08
4	0.170	44166.	44166.	7515.	7515.	2.374E+16	2.949E-04	1.094E-04
5	0.233	39546.	39546.	9540.	9540.	2.685E+16	1.680E-02	6.758E-03
6	0.298	32054.	32054.	12832.	12832.	3.384E+16	9.172E-01	3.814E-01
7	0.366	24583.	24583.	14554.	14554.	4.548E+16	4.826E+00	2.443E+00
8	0.436	20666.	20666.	12825.	12825.	5.492E+16	1.769E+00	3.222E+00
9	0.510	18470.	18470.	11654.	11654.	6.198E+16	7.116E-01	3.552E+00
10	0.586	16976.	16976.	10967.	10967.	6.806E+16	3.819E-01	3.735E+00
11	0.665	15924.	15924.	10559.	10559.	7.255E+16	2.534E-01	3.861E+00
12	0.747	15242.	15242.	10326.	10326.	7.673E+16	2.006E-01	3.964E+00
13	0.831	14695.	14695.	10200.	10200.	7.998E+16	1.768E-01	4.057E+00
14	0.918	14259.	14259.	10141.	10141.	8.326E+16	1.691E-01	4.150E+00
15	1.008	13826.	13826.	10119.	10119.	8.573E+16	1.677E-01	4.244E+00
16	1.101	13466.	13466.	10128.	10128.	8.907E+16	1.747E-01	4.347E+00
17	1.197	13068.	13068.	10140.	10140.	9.139E+16	1.804E-01	4.455E+00
18	1.295	12724.	12724.	10180.	10180.	9.474E+16	1.951E-01	4.575E+00
19	1.396	12179.	12179.	10157.	10157.	9.858E+16	1.966E-01	4.700E+00
20	1.460	11989.	11989.	10150.	10150.	1.006E+17	1.990E-01	4.780E+00
21	1.534	11712.	11712.	10149.	10149.	1.031E+17	2.038E-01	4.875E+00
22	1.622	11395.	11395.	10145.	10145.	1.061E+17	2.095E-01	4.991E+00
23	1.725	11049.	11049.	10134.	10134.	1.094E+17	2.152E-01	5.130E+00
24	1.846	10705.	10705.	10114.	10114.	1.130E+17	2.208E-01	5.298E+00
25	1.988	10409.	10409.	10093.	10093.	1.161E+17	2.266E-01	5.500E+00
26	2.155	10208.	10208.	10077.	10077.	1.184E+17	2.315E-01	5.743E+00
27	2.351	10111.	10111.	10069.	10069.	1.195E+17	2.342E-01	6.031E+00
28	2.582	10080.	10080.	10066.	10066.	1.198E+17	2.350E-01	6.373E+00
29	2.853	10071.	10071.	10066.	10066.	1.199E+17	2.352E-01	6.773E+00
30	3.171	10064.	10064.	10065.	10065.	1.200E+17	2.354E-01	7.243E+00
31	3.545	10062.	10062.	10065.	10065.	1.200E+17	2.354E-01	7.797E+00
32	3.985	10061.	10061.	10065.	10065.	1.200E+17	2.353E-01	8.447E+00
33	4.501	10061.	10061.	10065.	10065.	1.200E+17	2.353E-01	9.210E+00
34	5.108	10061.	10061.	10065.	10065.	1.200E+17	2.353E-01	1.011E+01
35	5.821	10062.	10062.	10065.	10065.	1.200E+17	2.353E-01	1.116E+01
36	6.659	10062.	10062.	10065.	10065.	1.200E+17	2.353E-01	1.240E+01
37	7.644	10062.	10062.	10065.	10065.	1.200E+17	2.353E-01	1.386E+01
38	8.800	10062.	10062.	10065.	10065.	1.200E+17	2.353E-01	1.557E+01
39	9.957	10062.	10062.	10065.	10065.	1.200E+17	2.353E-01	1.728E+01
-----								
Total lines calculated						=	1495424.	
Total lines spread into spectrum						=	1052040.	
Total run time						=	25.272 seconds.	
Time to cal Rot Energys and HL (EHL) files						=	0.000 seconds.	
Time to calculate and spread rotational lines						=	6.022 seconds.	
Time to spread rotational lines						=	4.461 seconds.	

Figure J9(c). Output file for sample case 2 (concluded).

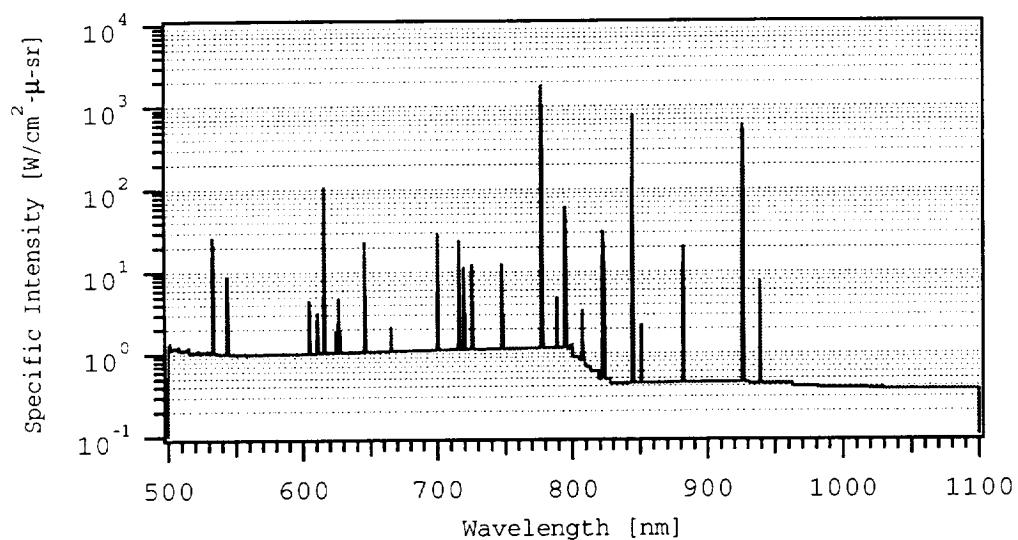


Figure J10. Calculated spectra of atomic O lines and background radiation, with and without absorption, from sample case 2.

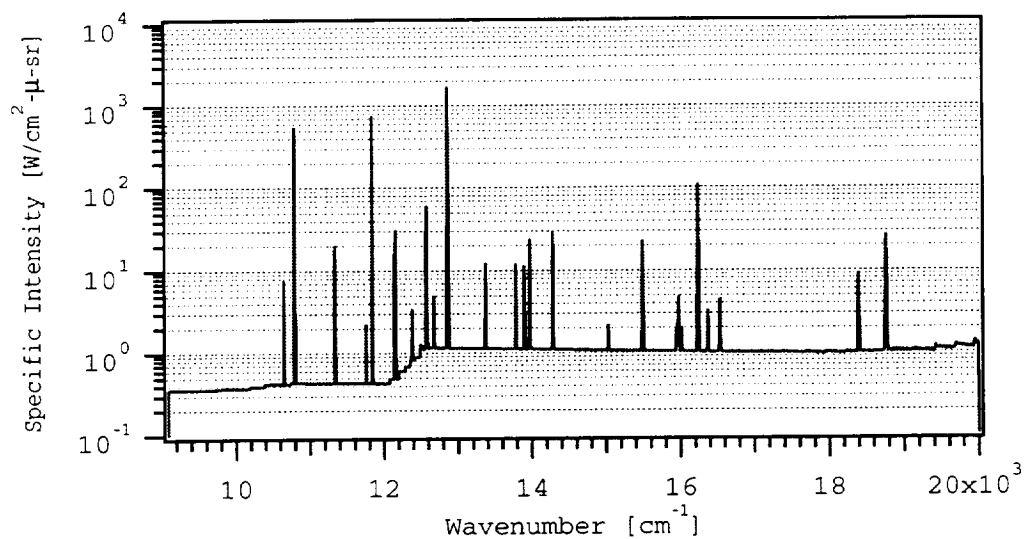
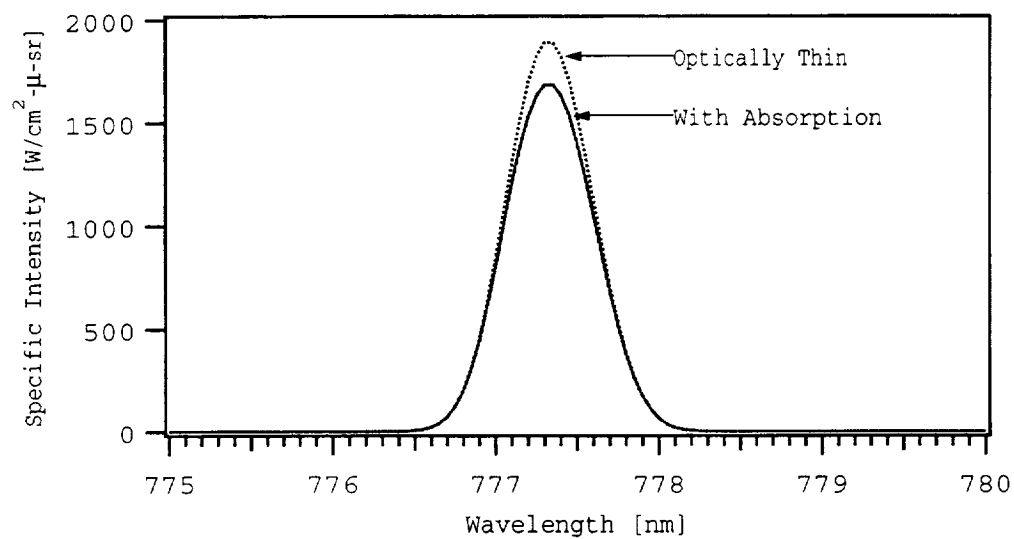


Figure J11. Calculated spectrum of atomic O lines and background radiation, with absorption, vs. wavenumbers, from sample case 2.



*Figure J12. Calculated spectra of the 3 atomic O lines and background radiation near 777 nm, with and without absorption, from sample case 2.*

```

*****
Sample Case 3 for NEQAIR96

Illustrates the shock tube and equilibrium flow options.
Includes two regions. An incident spectrum is included in
region 2 and the Voigt line shapes are calculated.
aaaaaaaaaaaaaaaaaaaaaaaaaaaaaaaaaaaaaaaaaaaaaaaaaaaaaa <- 1st format line
123456789 123456789 123456789 123456789 123456789 123456789
template.input

Template of Input file for NEQAIR(96)

An unlimited number of comment lines can go here.

All lines entered AFTER line of ***'s above, and BEFORE the first format
line (line of aaa's above) will be printed as heading lines in the Output
file. Format for the heading lines is a60.

Enter data ABOVE the format lines shown below.

Line0
*****
SPECTRUM      :Dont Create 0;   Create Only X;   Create and Scan 0;   Scan Only 0
Line1          a                a                a                a
-----
PLOT UNITS    : Angstroms X;   NanoMeters 0;   Wave Numbers 0;
Line2          a                a                a
-----
PLOT FORMAT   :Plot File(s) are Formatted X;   Unfortmatted 0
Line3          a                a
-----
PRINT OUT     :  LOS Data 0; Spectros Data 0;   Extra Plot at Grid # jx= 0;
Line4          a                a                iii
-----
KIND OF FLOW  :nonBoltzmann 0; d= 0.0; Boltzmann 0 Equilibrium X; BlackBody 0
Line5          a      rrrrrrr      a                a                a
-----
EQUILIBRIUM   : Temp= 0.0 K Rho= 0.000e-0 gm/cm3 LOSlength= 5.0 cm
Line6          rrrrrrr      rrrrrrrrrrrrr      rrrrrr
Species Molfrac :For a known condition where Sum Molfrac=1.0
O2        0.1
Ar        0.9
          0.0 :end species entry with blank and 0.0
aaaaaaa rrrrrrrrr :left justify species (enter above this line)
-----
TYPE OF GEOM.:Line-of-Sight 0; Stag Point 0; Shock Tube X;
Line7          a                a                a
-----
FOR STAG PT. :Infinite Slab 0; Sphere. Cap 0; Rnose= 0.0 cm; Shock Div= 0.0
Line8          a                a      rrrrrr      rrrrrr
-----
FOR SHOCK T. :STwidth= 10.0cm; VS= 8.0 km/s; Rho1= 2.16e-10gm/cc; Temp1= 300.0K
Line9          rrrrr      rrrrrr      rrrrrrrrr      rrrrrr
-----

```

Figure J13(a). Input file for sample case 3.

```

SYSTEMS      :Spectral Systems in Spectrum
Line10
      :Atomic Systems
      Escape Factors= Calculated X or 0.0
                        a rrrrr
Atom      smf:b-b      smf:b-f      smf:f-f
N          0.0          0.0          0.0
O          1.0          0.0          0.0
C          0.0          0.0          0.0
H          0.0          0.0          0.0
He         0.0          0.0          0.0
          0.0          0.0          0.0 :End with blank and 0.0's.
aaaaaaa rrrrr      rrrrr      rrrrr

      :Diatomic Electronic Transition Systems
      IPEAK= -9; Keep vib bands; Ivv>Imax*10**IPEAK
      iiii
      Save
      Rot EHL One Band SpinMult Major
Diatomic  smf Files YN (vu,vl) Use Real Branches vvExtend Nmax
              [Ang's]
-----
1 N2+ 1- 0.0 X 0 ( 0, 0) 1 2 X 0.0 0
2 N2 1+ 0.0 X 0 ( 0, 0) 1 3 X 0.0 0
3 N2 2+ 0.0 X 0 ( 0, 0) 1 3 X 0.0 0
4 N2 BH2 0.0 X 0 ( 0, 0) 1 1 X 0.0 0
5 NO beta 0.0 X 0 ( 0, 0) 1 2 X 0.0 0
6 NO gam 0.0 X 0 ( 0, 0) 1 2 X 0.0 0
7 NO del 0.0 X 0 ( 0, 0) 1 2 X 0.0 0
8 NO eps 0.0 X 0 ( 0, 0) 1 2 X 0.0 0
9 NO bp 0.0 X 0 ( 0, 0) 1 2 X 0.0 0
10 NO gp 0.0 X 0 ( 0, 0) 1 2 X 0.0 0
11 O2 SR 0.0 X 0 ( 0, 0) 1 3 X 0.0 0
12 CN VIO 0.0 X 0 ( 0, 0) 1 2 X 0.0 0
13 CN RED 0.0 X 0 ( 0, 0) 1 2 X 0.0 0
14 CO 4+ 0.0 X 0 ( 0, 0) 1 1 X 0.0 0
15 C2 Swan 0.0 X 0 ( 0, 0) 1 3 X 0.0 0
16 OH A-X 0.0 X 0 ( 0, 0) 1 2 X 0.0 0
17 H2 B-X 0.0 X 0 ( 0, 0) 1 1 X 0.0 0
18 H2 C-X 0.0 X 0 ( 0, 0) 1 1 X 0.0 0
19 H2 B'-X 0.0 X 0 ( 0, 0) 1 1 X 0.0 0
          0.0 0 0 ( 0, 0) 0 0 0 0.0 0:End Line
aaaaaaa rrrrr a a ii ii i i a rrrrrr iii

      :Diatomic Infra-Red Transition Systems
      Save
      Rot EHL One Band SpinMult Major
Diatomic  smf Files YN (vu, vl) Use Real Branches
              Only!
-----
1 NO 0.0 X 0 ( 0, 0) 1 2 X
2 CN 0.0 X 0 ( 0, 0) 1 2 X
3 CO 0.0 X 0 ( 0, 0) 1 1 X
4 OH 0.0 X 0 ( 0, 0) 1 2 X
5 NH 0.0 X 0 ( 0, 0) 1 3 X
6 CH 0.0 X 0 ( 0, 0) 1 2 X
          0.0 0 0 ( 0, 0) 0 0 0:End Line
aaaaaaa rrrrr a a ii ii i i a

Actual spin mult. does not need to be entered, it is informational only.
Bands with origins from w1-vvExtend to w2+vvExtend of the wavelength range
w1-w2 are included. Enter vvExtend=0.0 to include all bands.
Nmax limits the number of rotational lines; enter 0(zero)to keep all rot lines.
-----
REGION DATA: Lines11-12 regionfile = 85;
If regionfile=5, data follow; else on unit # =regionfile. iii
-----
LINE-of-SIGHT DATA: Line13 losfile = 0;
If losfile =5, data follow; else on unit # =losfile. iii
-----
SCAN SPECTRA DATA: Line14 scanfile = 0;
If scanfile =5, data follow; else on unit # =scanfile. iii
-----

```

Figure J13(b). Input file for sample case 3 (concluded).

```

*****
template.region file

An unlimited number of comment lines can go here.

Enter Region data ABOVE the data format lines in this file.

To enter an incident spectrum for a Region enter something other
than zero in the "check location" after INCIDENT SPECTRUM, and ABOVE
the 1st format line as shown below, and enter the incident spectrum
values above the 3rd format line.

If an incident spectrum is not needed, the incident spectrum lines
can be removed or left in. If removed, remove all lines after the
1st format line and before the line of ---'s, including the blank
line immediately after the 2nd format line.

The line of ---'s after the 3rd format line, and all of the timing gate
lines can be removed, except when timing gates are needed for a shock
tube flow case.

The line of +++'s must be retained for each region.

End region input with anything but 'REGION' in first 6 characters of
1st data line.

*****
REGION 1      :10 regions allowed. INCIDENT SPECTRUM 0;      <- 1st data line.
aaaaaa      a      <- 1st format line.
Line 11
  w1 [A]    w2 [A]    narray    range    shape    wg [A]    w1 [A]
  1298.0    1310.0    12000     0        1        0.0      0.0
  rrrrrrrr rrrrrrrr iiiiiiii iiiiiiii iiiiiiii rrrrrrrr rrrrrrrr <- 2nd.

      Wavelength    Specific Intensity    Incident Spectrum, if needed
      [A]           [W/cm2-micron-sr]
      0.0           0.0 :End with 0.0's as shown here.
      rrrrrrrr rrrrrrrrrrrrrr (10x,e10.0,e15.0) <- 3rd.
-----
Line 12      :Shock tube timing gates, as needed. 10 gates allowed all regions.
              Enter gates for region after next line. End entry with all 0.0's.
tstart [s] topen [s] lam1 [A] lam2 [A] planckT[K]
  1.0e-7    1.0e-7    1298.0    1310.0    0.0
  0.0       0.0       0.0       0.0       0.0
  rrrrrrrr rrrrrrrr rrrrrrrr rrrrrrrr rrrrrrrr (5e10.0) <- 4th.
*****
REGION 2      :10 regions allowed. INCIDENT SPECTRUM X;      <- 1st data line.
aaaaaa      a      <- 1st format line.
Line 11
  w1 [A]    w2 [A]    narray    range    shape    wg [A]    w1 [A]
  1298.0    1310.0    12000     0        1        0.0      0.0
  rrrrrrrr rrrrrrrr iiiiiiii iiiiiiii iiiiiiii rrrrrrrr rrrrrrrr <- 2nd.

      Wavelength    Specific Intensity    Incident Spectrum, if needed
      [A]           [W/cm2-micron-sr]
      1200.0         100.0
      1400.0        10000.0
      0.0            0.0 :End with 0.0's as shown here.
      rrrrrrrr rrrrrrrrrrrrrr (10x,e10.0,e15.0) <- 3rd.
-----
Line 12      :Shock tube timing gates, as needed. 10 gates allowed all regions.
              Enter gates for region after next line. End entry with all 0.0's.
tstart [s] topen [s] lam1 [A] lam2 [A] planckT[K]
  1.0e-7    5.0e-8    1300.0    1307.0    0.0
  0.0       0.0       0.0       0.0       0.0
  rrrrrrrr rrrrrrrr rrrrrrrr rrrrrrrr rrrrrrrr (5e10.0) <- 4th.
*****
:Repeat REGION to +++'s line for new region, or end as noted above.

```

Figure J14. Region.data file for sample case 3.

Sample Case 3 Output for NEQAIR96

Illustrates the shock tube and equilibrium flow options.  
Includes two regions. An incident spectrum is included in  
region 2 and the Voigt line shapes are calculated.

STANDARD OUTPUT FOR NEQAIR

Line 1; A Spectrum was Created but NOT Scanned.  
Line 2; Spectra Files are Printed versus: Angstroms.  
Line 3; Spectral Plot Files are FORMATTED.  
Line 4; Spectrum Plotted for Last Field Pt.  
Line 5; Radiation is for Equilibrium Excitation.  
Line 6; LOSlength = 5.000 cm.  
Line 6; Equilibrium; Mole Frac. Entered  
Line 7; This is a Shock Tube Geometry Case.  
Line 8; For Stagnation Pt. Flow; NOT Used in this Case.  
Line 9; Shock Tube Width = 10.00 cm.  
Line 9; Shock Velocity = 8.000E+00 km/s.  
Line 9; Rho1 = 2.160E-10 gm/cm3.  
Line 9; Temp1 = 300.00 K

Species Mol Fraction; for Equil Calculation.  
O2 0.1000  
A 0.9000

Line 10; Spectral Systems and Parameters

Atomic Systems

Atom	smf:b-b	smf:b-f	smf:f-f
1 O	1.00	0.00	0.00

Line 11; Wavelength Regions; and Incident Spectra as Needed.  
Line 12; Shock Tube Timing Gates as Needed.

Spectral Regions

region	w1	w2	narray	dellam	range	lshape	widthg	widthl
1	1298.000	1310.000	12001	0.0010	0	1	Line Width Cal. by Code.	

shock tube gates

gate	t1(sec)	gate(sec)	lam1(Ang)	lam2(Ang)	planckT
1	1.000E-07	1.000E-07	1298.000	1310.000	0.0

region	w1	w2	narray	dellam	range	lshape	widthg	widthl
2	1298.000	1310.000	12001	0.0010	0	1	Line Width Cal. by Code.	

incident spectrum

	wavelength	watts/cm2-micron-sr
1	1200.0000	1.00000E+02
2	1400.0000	1.00000E+04

shock tube gates

gate	t1(sec)	gate(sec)	lam1(Ang)	lam2(Ang)	planckT
2	1.000E-07	5.000E-08	1300.000	1307.000	0.0

Figure J15(a). Output file for sample case 3.

```

Free-Stream Starting Gas Mixture and Gas Properties

species      mole fraction  atomic or mol wt.

1  O2        0.100000000    32.0000
2  Ar        0.900000000    39.9480

average molecular weight = 39.1532
rho = 2.16000E-07 kg/m3
temp = 300.0 K

```

---

```

Equilibrium Conditions and Species Concentrations

Free-Stream Conditions

rho = 2.16000E-07 kg/m3
temp = 300.0 K
p = 1.37605E-02 N/m2
specific enthalpy, h = 1.75280E+05 J/kg
specific energy, e = 1.11574E+05 J/kg
v = 8.0000 km/sec

```

---

```

mole/kg      mole/mole      part/cm3

1  Ar        2.29866E+01    9.00000E-01    2.99006E+12
2  O         4.15915E-37      1.62844E-38    5.41015E-26
3  O2        2.55407E+00          1.00000E-01    3.32229E+11
4  Ar+       3.47292-158        1.35976-159    4.51751-147
5  O+        8.75645-161        3.42843-162    1.13902-149
6  O++       7.66522-645        3.00118-646    9.97077-634
7  O+++      1.00000-1000        3.91532-1002    1.30078-989
8  O2+       8.97142E-98        3.51260E-99    1.16699E-86
9  E-        8.97142E-98        3.51260E-99    1.16699E-86

```

---

```

Behind Normal Shock Wave with Vs = 8.0000 km/sec

rho = 5.31360E-06 kg/m3
temp = 8439.7 K
p = 1.32762E+01 N/m2
specific enthalpy, h = 1.86631E+07 J/kg
specific energy, e = 1.61646E+07 J/kg

```

---

```

mole/kg      mole/mole      part/cm3

1  Ar        1.72005E+01    4.83069E-01    5.50403E+13
2  O         3.38234E+00          9.49917E-02    1.08232E+13
3  O2        5.81084E-09          1.63195E-10    1.85942E+04
4  Ar+       5.78613E+00          1.62501E-01    1.85152E+13
5  O+        1.72580E+00          4.84684E-02    5.52242E+12
6  O++       6.48705E-13          1.82186E-14    2.07581E+00
7  O+++      7.55496E-38          2.12178E-39    2.41753E-25
8  O2+       4.40780E-08          1.23791E-09    1.41046E+05
9  E-        7.51193E+00          2.10970E-01    2.40376E+13

```

---

```

Line 14; Scanning Data are NOT used in this Case.

```

Figure J15(b). Output file for sample case 3 (continued).

```

Shock Tube Calculation

      Region 1 Gate 1
      (plot file for spectrum is fort.21)

gate width =      0.100 micro sec; from      0.100 to      0.200 micro sec.
wavelength range from 1298.000 to 1310.000 Angstroms

      x      time      delta t      Emission
      (cm)      (micro sec) (micro sec) (w/cm3-sr)

      1      0.000      0.000      0.000
      2      5.000      6.515      0.100      5.476E-04

Average radiant power over the gate is:
      With incident spectrum = 3.464E-03 W/cm2-sr
      Without incident spectrum = 3.464E-03 W/cm2-sr
      Optically thin = 5.473E-03 W/cm2-sr

Effective emission over gate and shock tube width = 3.464E-04 W/cm3-sr
-----

Shock Tube Calculation, wavelength region 1, 1298.000 to 1310.000 Angstroms

      x      ttran      trot      tvib      telec      rho      time-from-shock      emission
      (cm)      (micro sec) (micro sec) (micro sec) (w/cm3-sr)

      1      0.000      6.51E+00      0.000E+00
      2      5.000      8440.      8440.      8440.      8440.      5.31E-09      6.51E+00      5.476E-04
-----

Shock Tube Calculation

      Region 2 Gate 2
      (plot file for spectrum is fort.22)

gate width =      0.050 micro sec; from      0.100 to      0.150 micro sec.
wavelength range from 1300.000 to 1307.000 Angstroms

      x      time      delta t      Emission
      (cm)      (micro sec) (micro sec) (w/cm3-sr)

      1      0.000      0.000      0.000
      2      5.000      6.515      0.050      5.476E-04

Average radiant power over the gate is:
      With incident spectrum = 3.632E+00 W/cm2-sr
      Without incident spectrum = 3.464E-03 W/cm2-sr
      Optically thin = 5.473E-03 W/cm2-sr

Effective emission over gate and shock tube width = 3.632E-01 W/cm3-sr
-----

Shock Tube Calculation, wavelength region 2, 1298.000 to 1310.000 Angstroms

      x      ttran      trot      tvib      telec      rho      time-from-shock      emission
      (cm)      (micro sec) (micro sec) (micro sec) (w/cm3-sr)

      1      0.000      6.51E+00      0.000E+00
      2      5.000      8440.      8440.      8440.      8440.      5.31E-09      6.51E+00      5.476E-04
-----

Total lines calculated = 6.
Total lines spread into spectrum = 6.
-----

Total run time = 17.801 seconds.
Time to cal Rot Energys and HL (EHL) files = 0.000 seconds.
Time to calculate and spread rotational lines = 0.000 seconds.
Time to spread rotational lines = 0.000 seconds.

```

Figure J15(c). Output file for sample case 3 (concluded).

```

*****
                                LOS file from Equilibrium Calculation.

An unlimited number of comment lines can go here.

Enter Data AFTER the data-format lines!

(1) Enter species in any order; limited to atoms, diatomics, triatomics,
    atomic ions, diatomic ions, and electrons. Left-justify the species
    symbols in the fields. End entry with a blank line.

(2) Properties entered at each grid point along line-of-sight. The
    properties apply to the layer between the grid point and the
    previous grid point. Thus, the properties at the first grid point
    are not used. This grid point only establishes the origin of the
    line-of-sight.

(3) Enter species number densities [cm-3] in the same order that the species
    symbols are entered. End data entry at each grid point with a blank
    line.

(4) End line-of-sight data entry, with a line of zeros as shown.
*****
    aaaaaaaa      aaaaaaaa      aaaaaaaa      aaaaaaaa      (2x, (7x,a8))
    Ar            O            O2           Ar+
    O+           O++          O+++         O2+
    E-
                                           :Species symbols.
-----
no.  x,cm  total partcc      t      tr      tv      te (i5,e8.0,
iiii rrrrrr rrrrrrrrrrrrr rrrrrrrr rrrrrrrr rrrrrrrr rrrrrrrr e15.0,4e10)
rrrrrrrrrrrr rrrrrrrrrrrrr rrrrrrrrrrrr rrrrrrrrrrrr (6x,4e15.7)
Include these 9 lines (from --- to --- lines)for first grid point only!!
End each grid point entry with a blank line.
End data file with a line of zeros as shown on the next line.
0      0.0      0.0      0.0      0.0      0.0      0.0
-----
1  0.000  1.1394580E+14    8439.2    8439.2    8439.2    8439.2
   5.5062576E+13  1.0827816E+13  3.7406848E+04  1.8506777E+13
   5.5209280E+12  2.0704641E+00  2.4021279E-25  2.8315506E+05
   2.4027705E+13
2  5.000  1.1394580E+14    8439.2    8439.2    8439.2    8439.2
   5.5062576E+13  1.0827816E+13  3.7406848E+04  1.8506777E+13
   5.5209280E+12  2.0704641E+00  2.4021279E-25  2.8315506E+05
   2.4027705E+13
0      0.0      0.0      0.0      0.0      0.0      0.0

```

Figure J16. One layer equilibrium *los.data* file produced by sample case 3.

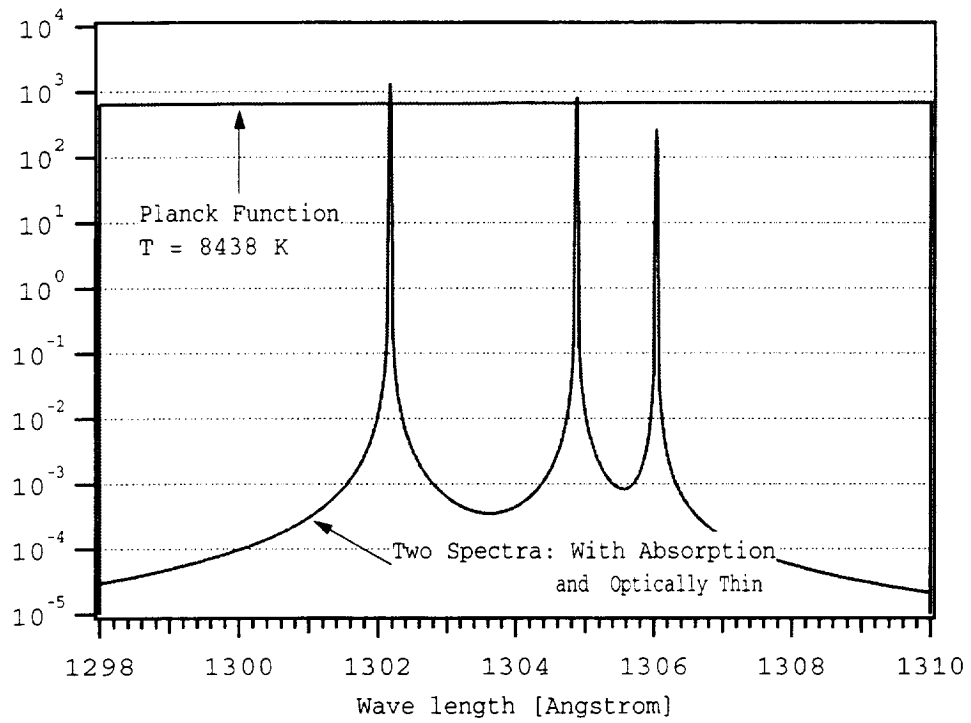


Figure J17. Region 1 spectra for sample case 3.

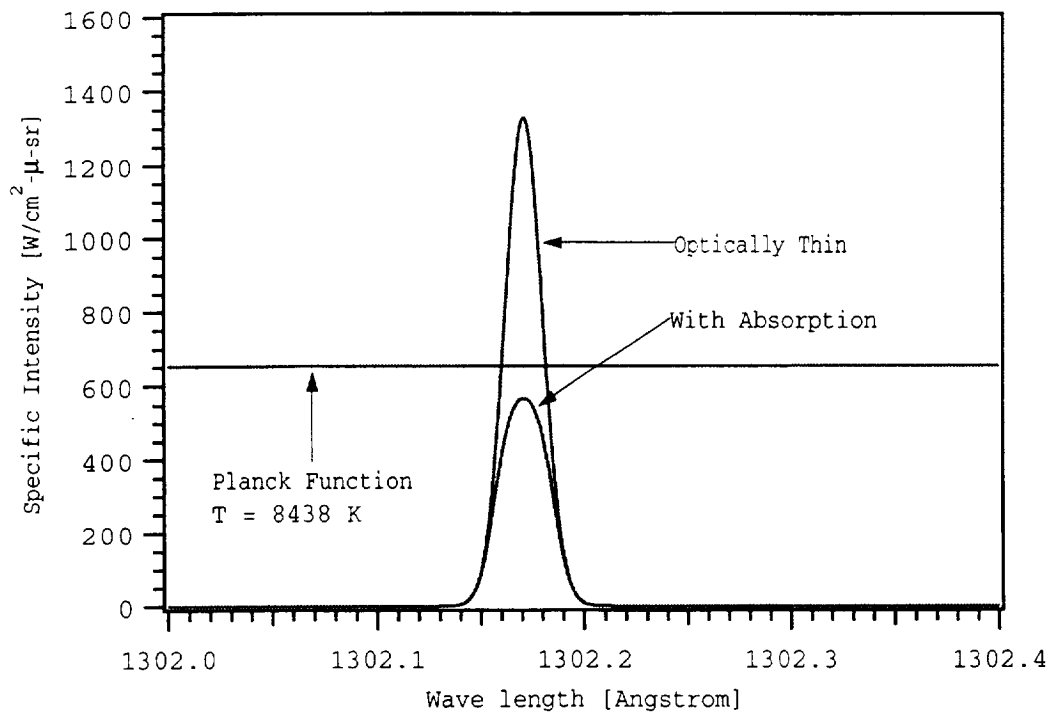


Figure J18. Region 1 detail spectra for sample case 3.

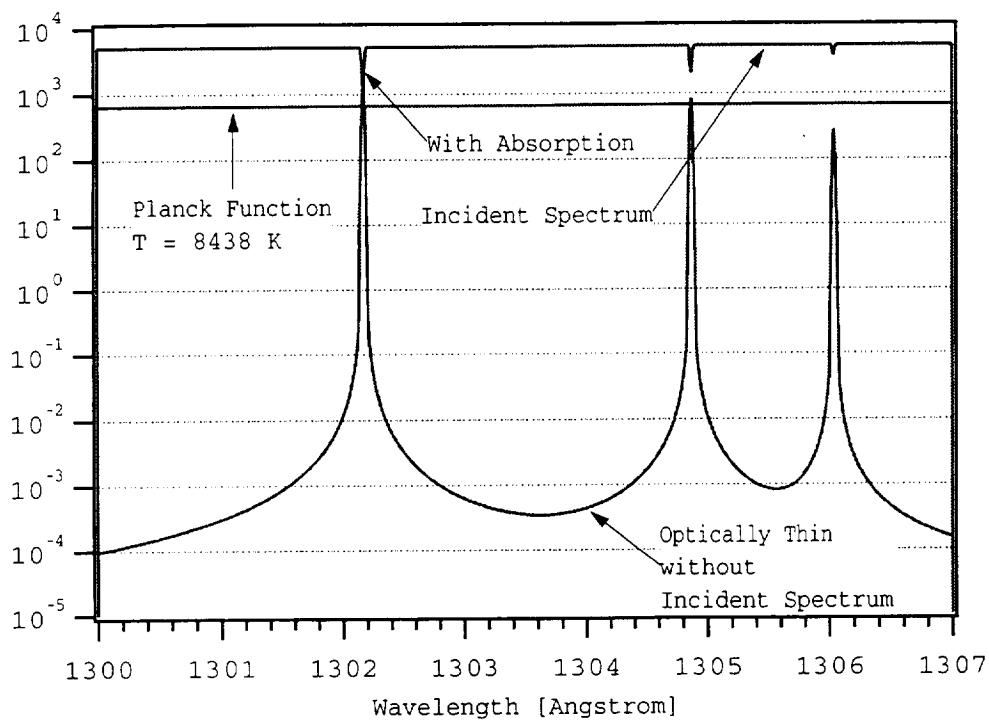


Figure J19. Region 2 spectra for sample case 3.

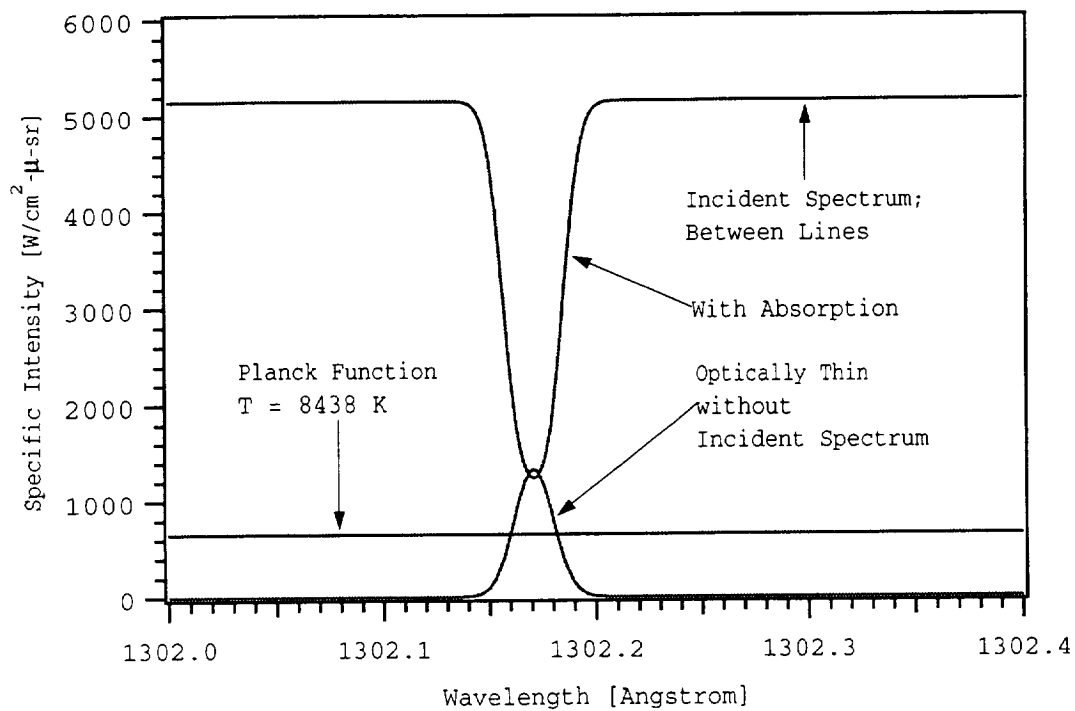


Figure J20. Region 2 detail spectra for sample case 3.



## References

1. Park, Chul: Nonequilibrium Air Radiation (NEQAIR) Program: User's Manual. NASA TM-86707, July 1985.
2. Whiting, E. E.; Arnold, J. O.; and Lyle, G. C.: A Computer Program for a Line-by-Line Calculation of Spectra from Diatomic Molecules and Atoms Assuming a Voigt Line Profile. NASA TN D-5088, March 1969.
3. Whiting, E. E.; Arnold, J. O.; Page, W. A.; and Reynolds, R. M.: Composition of the Earth's Atmosphere by Shock-Layer Radiometry during the PAET Entry Probe Experiment. JQSRT, vol. 13, 1973. p. 837.
4. Babikian, D. S.; Palumbo, G.; Craig, R. A.; Park, C.; Palmer, G.; and Sharma, S. P.: Measured and Calculated Spectral Radiation from a Blunt Body Shock Layer in an Arc-Jet Wind Tunnel. AIAA Paper 94-0086, Jan. 1994.
5. Whiting, E. E.; and Park, C.: Radiative Heating at the Stagnation Point of the AFE Vehicle. NASA TM-102829, Nov. 1990.
6. Terrazas-Salinas, I.; Park, C.; Strawa, A. W.; Gopal, N. K. J. M.; and Taunk, J. S.: Spectral Measurements in the Arc Column of an Arcjet Wind Tunnel. AIAA Paper 94-2595, June 1994.
7. Babikian, D. S.; Gopaul, N. K. J. M.; and Park, C.: Measurement and Analysis of the Nitric Oxide Radiation in an Arcjet Flow: J. Thermophysics and Heat Transfer, vol. 8, Dec. 1994, p. 737.
8. Babikian, D. S.; Park, C.; and Raiche, G. A.: Spectroscopic Determination of the Enthalpy in an Arcjet Wind Tunnel. AIAA Paper 95-0712, Jan. 1995.
9. Sharma, S. P.; and Whiting, E. E.: Modeling of Nonequilibrium Radiation Phenomena: An Assessment. AIAA Paper 94-0253, Jan. 1994.
10. Partridge, H.; and Schwenke, D. W.: The Determination of an Accurate Isotope Dependent Potential Energy Surface for Water from Extensive *ab initio* Calculations and Experimental Data. Submitted to J. Phy. Chem., Oct. 1996.
11. Dirac, P. A. M.: The Principles of Quantum Mechanics. Fourth Ed., Oxford at the Clarendon Press, 1958 (First Ed., 1930).
12. Condon, E. U.; and Shortley, G. H.: The Theory of Atomic Spectra. Reprinted, Cambridge at the University Press, 1967 (First Ed., 1935).

13. Kovács, István: Rotational Structure in the Spectra of Diatomic Molecules. Adam Hilger Ltd., London, 1969.
14. Herzberg, Gerhard: Molecular Spectra and Molecular Structure. I. Spectra of Diatomic Molecules. Second ed., Van Nostrand Co., New York, 1950.
15. Huber, K. P.; and Herzberg, G.; Molecular Spectra and Molecular Structure. IV. Constants of Diatomic Molecules. Van Nostrand Reinhold Co., New York, 1979.
16. Dunham, J. L.: Energy Levels of a Rotating Vibrator. *Physic. Rev.*, vol. 41, 1932, p. 721.
17. Hönl, H.; and London, F.: The Intensities of Band Lines. *Zeit f. Physik*, vol. 33, 1925, p. 803.
18. Whiting, Ellis E.: Rotational Line Intensity Factors for Dipole Transitions in Diatomic Molecules. Ph.D. Thesis, York University, Toronto, Ontario, Aug. 1972.
19. Whiting, Ellis E.: Computer Program for Determining Rotational Line Intensity Factors for Diatomic Molecules. NASA TN D-7268, Sept. 1973.
20. Hougen, J. T.: The Calculation of Rotational Energy Levels and Rotational Line Intensities in Diatomic Molecules. NBS Monograph 115, June 1970.
21. Prasad, C. V. V.; and Bernath, P. F.: Fourier Transform Spectroscopy of the Swan ( $d^3P_g - a^3P_u$ ) System of the Jet-Cooled  $C_2$  Molecule. *Astrophysical J.*, vol. 426, 1994, p. 812.
22. Albritton, D. L.; Schmeltekoph, A. L.; Tellinghuisen, J.; and Zare, R. N.: Least-Squares Equivalence of Different Representations of Rotational Constants. *J. Mol. Spectrosc.*, vol. 53, 1994, p. 311.
23. Zare, R. N.; Schmeltekoph, A. L.; Harrop, W. J.; and Albritton, D. L.: Direct Approach for the Reduction of Diatomic Spectra to Molecular Constants for the Construction of RKR (Rydberg-Klein-Rees) Potentials. *J. Mol. Spectrosc.*, vol. 41, 1973, p. 37.
24. Schadee, Aert: Theory of First Rotational Lines in Transitions of Diatomic Molecules. *Astron. and Astro. Phys.*, vol. 41, no. 2, 1975, p. 203.
25. Hartung-Chambers, Lin: Predicting Radiative Heat Transfer in Thermochemical Nonequilibrium Flow Fields, Theory and User's Manual for the LORAN code. NASA TM-4564, Sept. 1994.
26. Park, Chul: Nonequilibrium Hypersonic Aerothermodynamics. John Wiley & Sons, New York, 1990.

27. Moreau, S.; Laux, C. O.; Chapman, D. R.; and MacCormack, R. W.: A More Accurate Nonequilibrium Air Radiation Code: NEQAIR Second Generation. AIAA 92-2968, July 1992.
28. Laux, C. O.; and Kruger, C. H.: Arrays of Radiative Transition Probabilities for the N<sub>2</sub> First and Second Positive, NO Beta and Gamma, N<sub>2</sub><sup>+</sup> First Negative, and O<sub>2</sub> Schumann-Runge Band Systems. *J. Quant. Spectrosc. Radiat. Transfer*, vol. 48, no. 1, 1992, pp. 9–24.
29. Laux, C. O.; Moreau, S.; and Kruger, C. H.: Experimental Study and Improved Modeling of High-Temperature Air Radiation. AIAA 92-2969, July 1992.
30. Laux, C. O.; Gessman, R. J.; and Kruger, C. H.: Modeling the UV and VUV Radiative Emission of High-Temperature Air. AIAA 93-2802, July 1993.
31. Laux, C. O.: Optical Diagnostics and Radiative Emission of Air Plasmas. Ph.D. Thesis, Stanford University, Aug. 1993.
32. Levin, D. A.; Laux, C. O.; and Kruger, C. H.: A General Model for the Spectral Calculation of OH Radiation in the Ultraviolet. AIAA Paper 95-1990, June 1995.
33. Levin, D. A.; Candler, G. V.; Howlett, L. C.; and Whiting, E. E.: Comparison of Theory with Atomic Oxygen Radiance Data from a Rocket Flight. *J. Thermophysics and Heat Transfer*, vol. 9, 1995, p. 629.
34. Hartung-Chambers, Lin: Nonequilibrium Radiative Heating Prediction Method for Aeroassist Flowfield Solvers. Ph.D. Thesis, North Carolina State University, 1991.
35. Meyer, S. A.; Sharma, S. P.; Bershader, D.; Whiting, E. E.; Exberger, R. J.; and Gilmore, J. O.: Absorption Line Shape Measurement of Atomic Oxygen at 130 nm Using a Raman-Shifted Excimer Laser. AIAA Paper 95-0290, Jan. 1995.
36. Meyer, S. A.; Sharma, S. P.; Bershader, D.; Whiting, E. E.; Exberger, R. J.; and Gilmore, J. O.: Atomic Oxygen Line Shape Measurement at 130 nm with Raman-Shifted Laser. *AIAA J.*, vol. 34, March 1996, p. 508.
37. Bershader, D.; and Park, C. S.: Nonequilibrium Shock Layer Radiation in a Simulated Titan Atmosphere. International Workshop on Strong Shock Waves, Chiba, Japan 1991.
38. Strawa, A. W.; Park, C.; Davy, W. C.; Craig, R. A.; Babikian, D. S.; Prabhu, D. K.; and Venkatapathy, E.: Proposed Radiometric Measurement of the Wake of a Blunt Aerobrake. *J. Spacecraft and Rockets*, vol. 29, 1992, p. 765.
39. Hornkohl, J. O.; Parigger, C.; and Lewis, J. W. L.: On the Use of Line Strengths in Applied Diatomic Spectroscopy. LACEA Conference, OSA, March 1996.

40. Parigger, C.; Lewis, J. W. L.; Plemmons, D. H.; Guan, G.; and Hornkohl, J. O.: Hydroxyl Measurements in Air-Breakdown Microplasmas. LACEA Conference, OSA, March 1996.
41. Parigger, C.; Lewis, J. W. L.; Plemmons, D. H.; and Hornkohl, J. O.: Nitric Oxide Optical Breakdown Spectra and Analysis by the Use of the Program NEQAIR. LACEA Conference, OSA, March 1996.
42. Rachelle, William C.: Simplified Engineering User's Guide for NONEQB and NEQAIR5 Nonequilibrium Flow/Radiation Codes. J. O. No. 060-EG-A3E Corr. No. AS-112-94, NASA JSFC, Dec. 1994.
43. Einstein, Albert: Zur Quantentheorie der Strahlung. Phys. Zeits., vol. 18, 1917, p. 121.
44. Vincenti, W. G.; and Kruger, C. H., Jr.: Introduction to Physical Gas Dynamics. Robert E. Kreiger Pub. Co., Malabar, FL, Reprint 1982, Original 1965.
45. Peach, G.: Continuous Absorption Coefficients for Non-Hydrogenic Atoms. Mem. R. Astr. Soc., vol. 73, 1970, p. 1.
46. Saha, M. N.: Ionization in the Solar Chromosphere. Phil. Mag. vol. 40, 1920, p. 472.
47. Bates, D. R.; and Dalgarno, A.: Electronic Recombination. page 245, Atomic and Molecular Processes. Edited by D. R. Bates, Academic Press, New York, 1961.
48. Levin, D. A.; Chandler, G. V.; Collins, R. J.; Howlett, C. L.; Epsy, P.; Whiting, E. E.; and Park, C.: Comparison of Theory with Atomic Oxygen 130.4 nm Radiation Data from the Bow Shock Ultraviolet 2 Rocket Flight. AIAA Paper 93-2811, July 1993.
49. Bouguer, M. (Pierre): Traite d'Optique. 1760. Translation, Optical Treatise on the Graduation of Light; with Introduction by W. E. Knowles Middleton, University of Toronto Press, Ontario, 1961.
50. Beer, A. V.: Poggendorff's Annalen der Physik., vol. 86, 1852, p. 78.
51. Nielsen, J. Rud: The Absorption Laws for Gases in the Infra-Red. Rev. Mod. Phys., vol. 16. 1944, p. 307.
52. Kirchhoff, G.; Monatsber. Berl. Akad. Wiss., 1859, p. 662.
53. Zel'dovich, Y. B.; and Raizer, Y. P.: Physics of Shock Waves and High-Temperature Hydrodynamic Phenomena, Vol. I. Translated by Scripta Technica, Inc., Academic Press, New York 1966.
54. Whiting, Ellis E.: An Empirical Approximation to the Voigt Profile. JQSRT, vol. 8, 1968, p. 1379.

55. Olivero, J. J.; and Longbothum, R. L.: Empirical Fits to the Voigt Line Width: A Brief Review. *JQSRT*, vol. 17, 1977, p. 233.
56. Levin, D. A.; Loda, R. T.; Candler, G. V.; and Park, C.: Theory of Radiation from Low Velocity Shock Heated Air. *J. Thermophysics and Heat Transfer*, vol. 7, 1993, p. 269.
57. Park, Chul: Assessment of Two-Temperature Kinetic Model for Ionizing Air. *J. Thermophysics and Heat Transfer*, vol. 3, 1980, p. 233.
58. Deiwert, G. S.; Strawa, A. W.; Sharma, S. P.; and Park, C.: Experimental Program for Real Gas Flow Code Validation at NASA Ames Research Center. AGARD CP-437. Symposium on Validation of Computational Fluid Dynamics, Lisbon, Portugal, May 1988.
59. Athay, Grant: Radiation Transport in Spectral Lines. D. Reidel Pub. Co., Dordrecht-Holland, 1972.
60. Morse, P. M.: Diatomic Molecules According to the Wave Mechanics. II. Vibrational Levels. *Physic. Rev.*, vol. 34, 1929, p. 57.
61. Liu, Y.; and Vinokur, M.: Equilibrium Gas Flow Computations. I. Accurate and Effective Calculation of Equilibrium Gas Properties. AIAA Paper 89-1738, June 1989.
62. Liu, Y.; and Shakib, F.: A Comparison of Internal Energy Calculation Methods for Diatomic Molecules. *Phys. Fluids. A*, vol. 2, 1990, p. 1884.
63. Steele, D.; and Lippincott, E. R.: Construction of Reliable Internuclear Potential Curves from Equilibrium Bond Lengths and Vibrational Frequencies. *J. Chem. Phys.*, vol. 35, 1961, p. 2065.
64. Hulburt, H. M.; and Hirschfelder, J. O.: Potential Energy Functions for Diatomic Molecules. *J. Chem. Phys.*, vol. 9, 1941, p. 61 (also, Erratum: *J. Chem. Phys.*, vol. 35, 1961, p. 1901).
65. Dabrowski, I.: The Lyman and Werner Bands of H<sub>2</sub>. *Can. J. Phys.*, vol. 62, 1984, p. 1639.
66. Dieke, G. H.: The Molecular Spectrum of Hydrogen and Its Isotopes. *J. Mol. Spec.*, vol. 2, 1958, p. 494.
67. Schwenke, D. W.: Program entitled edio.f.
68. Wolniewicz, L.: Relativistic Energies of the Ground State of the Hydrogen Molecule. *J. Chem. Phys.*, vol. 99, 1993, p. 1851.
69. Wolniewicz, L.; and Dressler, K.: The B <sup>1</sup>Σ<sub>u</sub><sup>+</sup>, B' <sup>1</sup>Σ<sub>u</sub><sup>+</sup>, C <sup>1</sup>Π<sub>u</sub> and D <sup>1</sup>Π<sub>u</sub> States of the H<sub>2</sub> Molecule. Matrix Elements of Angular and Radial Nonadiabatic Coupling and Improved *ab initio* Potential Energy Curves. *J. Chem. Phys.*, vol. 88, 1988, p. 3861.

70. Wolniewicz, L.; and Dressler, K.: Nonadiabatic Energy Corrections for the Vibrational Levels of the B and B'  $^1\Sigma_u^+$  states of the H<sub>2</sub> and D<sub>2</sub> molecules. J. Chem. Phys., vol. 96, 1992, p. 6053.
71. Wolniewicz, L.: Nonadiabatic Energies of the Ground State of the Hydrogen Molecule. J. Chem. Phys., vol. 103, 1995, p. 1792.



REPORT DOCUMENTATION PAGE			Form Approved OMB No. 0704-0188	
Public reporting burden for this collection of information is estimated to average 1 hour per response, including the time for reviewing instructions, searching existing data sources, gathering and maintaining the data needed, and completing and reviewing the collection of information. Send comments regarding this burden estimate or any other aspect of this collection of information, including suggestions for reducing this burden, to Washington Headquarters Services, Directorate for Information Operations and Reports, 1215 Jefferson Davis Highway, Suite 1204, Arlington, VA 22202-4302, and to the Office of Management and Budget, Paperwork Reduction Project (0704-0188), Washington, DC 20503.				
1. AGENCY USE ONLY (Leave blank)		2. REPORT DATE December 1996		3. REPORT TYPE AND DATES COVERED Reference Publication
4. TITLE AND SUBTITLE NEQAIR96, Nonequilibrium and Equilibrium Radiative Transport and Spectra Program: User's Manual			5. FUNDING NUMBERS  242-80-01	
6. AUTHOR(S) Ellis E. Whiting,* Chul Park,† Yen Liu, James O. Arnold, and John A. Paterson				
7. PERFORMING ORGANIZATION NAME(S) AND ADDRESS(ES) Ames Research Center Moffett Field, CA 94035-1000			8. PERFORMING ORGANIZATION REPORT NUMBER  A-962456	
9. SPONSORING/MONITORING AGENCY NAME(S) AND ADDRESS(ES) National Aeronautics and Space Administration Washington, DC 20546-0001			10. SPONSORING/MONITORING AGENCY REPORT NUMBER  NASA RP-1389	
11. SUPPLEMENTARY NOTES Point of Contact: Ellis E. Whiting, Ames Research Center, MS 229-3, Moffett Field, CA 94035-1000 (415) 604-3473 *Thermosciences Inst., Ames Research Center, Moffett Field, Calif. †Dept. of Aeronaut. and Space Engng., Faculty of Engng., Tohoku Univ., Aramaki, Aoba-Ku, Sendai, 980 Japan.				
12a. DISTRIBUTION/AVAILABILITY STATEMENT  Unclassified — Unlimited Subject Category 72			12b. DISTRIBUTION CODE	
13. ABSTRACT (Maximum 200 words)  This document is the User's Manual for a new version of the NEQAIR computer program, NEQAIR96. The program is a line-by-line and a line-of-sight code. It calculates the emission and absorption spectra for atomic and diatomic molecules and the transport of radiation through a nonuniform gas mixture to a surface. The program has been rewritten to make it easy to use, run faster, and include many run-time options that tailor a calculation to the User's requirements. The accuracy and capability have also been improved by including the rotational Hamiltonian matrix formalism for calculating rotational energy levels and Hönl-London factors for dipole and spin-allowed singlet, doublet, triplet, and quartet transitions.  Three sample cases are also included to help the User become familiar with the steps taken to produce a spectrum. A new User interface is included that uses check location, to select run-time options and to enter selected run data, making NEQAIR96 easier to use than the older versions of the code. The ease of its use and the speed of its algorithms make NEQAIR96 a valuable educational code as well as a practical spectroscopic prediction and diagnostic code.				
14. SUBJECT TERMS Spectra, Radiation, Transport, Equilibrium, Nonequilibrium, Entry, Shock tube			15. NUMBER OF PAGES 154	
			16. PRICE CODE A08	
17. SECURITY CLASSIFICATION OF REPORT Unclassified	18. SECURITY CLASSIFICATION OF THIS PAGE Unclassified	19. SECURITY CLASSIFICATION OF ABSTRACT	20. LIMITATION OF ABSTRACT	